FoxO3a signaling promotes the inflammatory response during *Salmonella* Typhimurium infection

Sandra Emmanuelle Ametepe

A thesis submitted to the
Faculty of Graduate and Postdoctoral Studies
in partial fulfillment of the requirements for the
MSc degree in Microbiology and Immunology

Department of Biochemistry, Microbiology and Immunology
Faculty of Medicine
University of Ottawa

PREFACE

CONTRIBUTION OF COLLABORATORS

Dr. Mary-Ellen Harper and Dr. Seung-Hwan Lee's laboratories (University of Ottawa) provided all the reagents used for the Seahorse assay, and the assay was performed using the Seahorse Bioscience XF24 Extracellular Flux Analyzer from Dr. Harper's laboratory.

APPROVALS

The experimental protocols used were approved by the University of Ottawa Animal Care Committee and include the protocols BMI1638 and BMI1639. A Biohazardous Materials Use Certificate was obtained from the University of Ottawa Office of Risk Management, Environmental Health and Safety.

ABSTRACT

FoxO3a is a transcription factor that regulates various cellular functions such as cell cycle or cell death. However, its role in the innate immune response is not clear. I investigated the impact of FoxO3a signaling on the immune response during infection with *Salmonella* Typhimurium (ST). My results revealed that FoxO3a regulated the homeostasis of myeloid cells in the spleen and blood of mice during steady-state. Following infection of macrophages with ST, FoxO3a signaling promoted the expression of pro-inflammatory cytokines such as IL12 and TNFα, but inhibited the expression of the anti-inflammatory cytokine IL10. Phenotypic analysis revealed that FoxO3a signaling had no effect on classical macrophage polarization into M1 vs M2 phenotypes, although it appeared to regulate mitochondrial function during infection with ST. Inflammatory responses are critical during infection with virulent intracellular pathogens, and these results provide new insights into the role of FoxO3a signaling in inflammatory responses.

ACKNOWLEDGEMENTS

To Jesus be the glory, for I completed this thesis by the grace of the Almighty.

I would like to thank my supervisor, Dr. Subash Sad, who gave me the opportunity to complete my master's degree research in his laboratory. Under your supervision, helped by your patience and trust, I have acquired indispensable skills not only in research but also in everyday life. I would like to extend my gratitude to my thesis advisory committee members, Dr. Lee, Dr. Makrigiannis, and Dr. Fullerton, for their advice and support. I also thank Dr. Harper, Dr. Lee, and Dr. Langlois' laboratories for their technical help with some of my experiments. I am sincerely grateful to Dr. Wright and Andrew Wight for having dedicated their time to the revision of my thesis. Dr. Julie Joseph, thank you for having demonstrated so much patience towards me during my Master's degree, as well as for your teachings in science and in life. Kwangsin Kim, thank you ever so much for your precious help with my experiments and for your encouragement throughout my journey in the laboratory. Many thanks to all the members of the BMI department and a special thank you to the members of the Subash Sad laboratory I have crossed paths with. You helped morph the trying times into pleasant ones, through your encouragements, discussions, and advice. Finally, I would like to thank my parents and siblings Inès, Carl, and Estelle for their prayers and moral support and for having shared my joys and tribulations during this season.

My work was supported by a scholarship from the University of Ottawa, and research funds were provided by grants awarded by the Canadian Institute of Health Research (CIHR) to Dr. Subash Sad.

TABLE OF CONTENTS

LIST OF ABBREVIATIONS

2-DG	2-Deoxy-D-Glucose
AMPKα1	5'-AMP-Activated Protein Kinase catalytic subunit alpha-1
APC	Antigen-Presenting Cell
ASC	Apoptosis-associated Speck-like protein containing a CARD
Atg12l	Autophagy related 12
ATP	Adenosine Triphosphate
Bcl-6	B cell Leukemia/Lymphoma 6
BCR	B-Cell Receptor
BFA	Brefeldin A
BHI	Brain-Heart Infusion Medium
BMDM	Bone Marrow-Derived Macrophage
Bnip3	BCL2/adenovirus E1B interacting protein
CARD	Caspase Activation and Recruitment Domain
CCCP	Carbonyl cyanide *m*-chlorophenyl hydrazone
CD	Cluster of Differentiation
cDNA	Complementary DNA
CFU	Colony-Forming Unit
CLP	Common Lymphoid Progenitor
CMP	Common Myeloid Progenitor
COI	Cytochrome c Oxidase I
DAMP	Danger-Associated Molecular Pattern
DMEM	Dulbecco's Modified Eagle's Medium
DNA	Deoxyribonucleic Acid
eIF2α	Eukaryotic translation Initiation Factor 2 subunit alpha
ELISA	Enzyme-Linked Immunosorbant Assay
EPO	Erythropoietin
ER	Endoplasmic Reticulum
ERK	Extracellular signal-Regulated Kinase
FADD	Fas-Associated protein with Death Domain
$FADH_2$	Flavin Adenine Dinucleotide
Fasl	Fas ligand
FBS	Fetal Bovine Serum
FKHRL1	Forkhead in Rhabdomyosarcoma-like 1
FoxO	Forkhead Box O
GADD45	Growth Arrest and DNA Damage-inducible 45
GLUT1	Glucose Transporter 1
GMP	Granulocyte-Monocyte Progenitor
HIF-1α	Hypoxia-inducible factor-1α
HIV	Human Immunodeficiency Virus
HRP	Horseradish Peroxidase
HSC	Hematopoietic Stem Cell
IFN	Interferon
IgA	Immunoglobulin A
IL	Interleukin
IMDM	Iscove's Modified Dulbecco's Medium

iNOS	Inducible Nitric Oxide Synthase
IRF	Interferon Regulatory Factor
ISRE	Interferon-Stimulated Response Elements
JNK	c-Jun N-terminal Kinase
LCMV	Lymphocytic Choriomeningitis Virus
LDL	Low-Density Lipoprotein
LPS	Lipopolysaccharide
LT-HSC	Long-Term Hematopoietic Stem Cell
M cells	Microfold cells
M-CSF	Macrophage Colony-Stimulating Factor
MAPK	Mitogen-Activated Protein Kinase
MEP	Megakaryocyte-Erythrocyte Progenitor
MFI	Mean Fluorescence Intensity
MHC	Major Histocompatibility Complex
MLKL	Mixed Lineage Kinase domain-Like protein
MOI	Multiplicity of Infection
M_{reg}	Regulatory Macrophage
mRNA	Messenger RNA
MtDNA	Mitochondrial DNA
MTT	3-(4,5-dimethylthiazol-2-yl)-2,5-diphenyltetrazolium bromide
NADH	Nicotinamide Adenine Dinucleotide
NADPH	Nicotinamide Adenine Dinucleotide Phosphate
Nec-1	Necrostatin-1
NFκB	Nuclear Factor Kappa-light-chain-enhancer of activated B cells
NK cells	Natural Killer cells
NLR	Nod-Like Receptor
NLRC4	NOD-LRR-CARD-containing 4
NLRP3	NOD-LRR-Pyrin domain-containing protein 3
NO	Nitric Oxide
NR	Neutral Red
O.D.	Optical Density
OCR	Oxygen Consumption Rate
PAMP	Pathogen-Associated Molecular Pattern
PBS	Phosphate-Buffered Saline
PCR	Polymerase Chain Reaction
PDK1	3-Phosphoinositide-Dependent protein Kinase-1
PI3K	Phosphatidylinositol 3-kinase
PKB	Protein Kinase B
PMN	Polymorphonuclear
PRR	Pattern Recognition Receptor
PtdIns3P	Phosphatidylinositol-3-Phosphate
PUMA	P53-Upregulated Modulator of Apoptosis
qPCR	Quantitative PCR
RBC	Red Blood Cell
RIP(1/3)K	Receptor-Interacting Protein Kinase 1/3
RLU	Relative Light Units
ROS	Reactive Oxygen Species
RPMI	Roswell Park Memorial Institute Medium

rRNA	Ribosomal RNA
RT-PCR	Real-Time PCR
S1P	Sphingosine-1-Phosphate
SCF	Stem Cell Factor
SCV	*Salmonella*-containing vacuole
SEM	Standard Error of the Mean
SET9	SET domain-containing protein 7
SOD1/2	Superoxide Dismutase 1/2
SPHK1	Sphingosine Kinase 1
SPI	Salmonella Pathogenicity Island
ST	*Salmonella* Typhimurium
ST-HSC	Short-Term Hematopoietic Stem Cell
T3SS	Type 3-Secretion System
TCR	T-Cell Receptor
TGFβ	Transforming growth Factor Beta
TLR	Toll-Like Receptor
TMB	Tetramethylbenzidine
TMRE	Tetramethylrhodamine Ethyl Ester
TNFα	Tumor Necrosis Factor α
WT	Wild Type
zVAD	Benzyloxycarbonyl-Val-Ala-Asp-Fluoromethylketone Pan-Caspase inhibitor

LIST OF FIGURES AND TABLES

1. INTRODUCTION

1.1. The immune system

The immune system is a network of cells and soluble mediators that protect the host from infectious disease and contribute to the maintenance of tissue homeostasis. When the skin and mucosal barriers fail to prevent pathogen entry into the host, cells and soluble mediators of the immune system intervene to halt their spread. The immune system can be divided into two main axes, termed innate and adaptive immunity. The innate immune system is the first to respond to breaches of physical barriers. It is not specific to pathogens and the strength of the response remains unchanged regardless of the number of encounters with a given pathogen (Delves et al., 2000). Adaptive immunity on the other hand develops more slowly, is pathogen-specific, and displays immunological memory. In other words, upon repeated exposure to the same pathogen or antigen, the adaptive immune response is faster and amplifies incrementally (Parkin and Cohen, 2001). These two branches of the immune system do not act independently, but instead interact to mediate efficient pathogen clearance (Parkin and Cohen, 2001).

1.1.1. Innate immune system

The innate immune system is the first to respond to infection. It is composed of cells and soluble mediators that participate in the clearance of pathogens from the host. Innate immune cells include neutrophils, eosinophils, basophils, mast cells, natural killer (NK) cells, monocytes, macrophages and dendritic cells. Soluble factors include complement proteins, which function in a cascade of reactions that result in attraction of phagocytes and enhancement of the adaptive immune response (Parkin and Cohen, 2001). Cytokines, reactive oxygen species

(ROS) and antimicrobial peptides are also soluble mediators of the innate immune system that are described in more detail in subsequent paragraphs.

Granulocytes include neutrophils, eosinophils, basophils and mast cells. These cells contain cytoplasmic granules of inflammatory mediators and antimicrobial peptides that degrade extracellular antigens, or phagocytosed antigens in the case of neutrophils. Eosinophils play a key role in the elimination of parasites such as helminths. NK cells are cytotoxic lymphocytes that destroy infected cells and tumor cells using perforin and granzyme. Perforin creates pores in the plasma membrane of target cells, whereas granzymes cause the cells to undergo a non-inflammatory form of cell death termed apoptosis (Parkin and Cohen, 2001).

Phagocytes are cells that can engulf foreign antigens and particulate matter by a process termed phagocytosis. It begins with cells first extending their plasma membrane around the antigen to form a vesicle. The resulting antigen-containing vesicle, also known as a phagosome, is next internalized into the cytosol where it fuses with a lysosome to form a phagolysosome (Parkin and Cohen, 2001). Lysosomes are organelles that are rich in hydrolytic enzymes, which promote degradation of the engulfed matter contained in the phagolysosome (Lim and Zoncu, 2016). Neutrophils, monocytes and macrophages also have the ability to degrade pathogens using ROS (Parkin and Cohen, 2001). ROS are generated from oxygen by a process called the respiratory burst. Neutrophils, monocytes, macrophages, and naïve dendritic cells are all phagocytes. Neutrophils are among the first cells to reach a site of infection but they are short-lived. Monocytes differentiate into highly phagocytic macrophages upon integration of various signals emanating from infection sites. Dendritic cells are also phagocytic in peripheral tissues and constantly sample the surrounding microenvironment to detect pathogens and antigenic material. Once activated – usually upon infection – they migrate to the lymph nodes where they

present antigens to T cells of the adaptive immune system, leading to their activation (Abbas and Janeway, 2000). Dendritic cells thus act as a bridge between the innate and adaptive immunity.

1.1.2. Adaptive immune system

Cells of the adaptive immune system include T and B lymphocytes. Each of these cells bears unique antigen-specific receptors from a diverse repertoire generated through random receptor gene rearrangements. T lymphocytes are activated when they recognize antigen-derived peptides presented by professional antigen-presenting cells (APCs) such as dendritic cells. Antigens can also be presented to T cells by macrophages and B cells. More precisely, T cells are activated upon binding of their T-cell receptor (TCR) to a specific peptide presented in the major histocompatibility complex (MHC) molecules, in association with other signals from the APCs, namely co-stimulation and cytokines (Delves et al., 2004). Activated T cells proliferate and differentiate into effector T cells. There are two types of effector T cells: $CD8^+$ T cells are cytotoxic cells that kill infected cells presenting their specific antigen on MHC class I molecules. $CD8^+$ T cells also express various cytokines such as IFNγ or TNFα upon recognition of infected target cells. In contrast, $CD4^+$ T cells recognize antigenic peptides presented by MHC class II molecules, and express a diverse array of inflammatory and anti-inflammatory cytokines.

B lymphocytes can recognize antigens in their environment through their B cell receptor (BCR). With the help of $CD4^+$ T cell cytokines, activated B cells undergo clonal expansion and mature into plasma cells, a differentiated type of B cell that secretes antibodies (Delves et al., 2000). An antibody is in fact a secreted form of the BCR that binds to specific extracellular antigens such as bacteria and toxins, neutralizing them and promoting their phagocytosis by innate immune cells. The onset of adaptive immunity is slower in comparison to innate immunity, as T cell activation requires antigen presentation from innate immune cells and is

completed by 2-3 days post-infection (Parkin and Cohen, 2001). Upon resolution of infection, the majority of activated T and B lymphocytes die by apoptosis, but some of the activated cells survive as long-lived cells termed memory cells. These memory cells can then quickly recognize their specific antigen upon secondary exposure, and induce an immune response that is faster and of greater efficacy than the first (Parkin and Cohen, 2001).

1.1.3. Generation of hematopoietic cells

Hematopoiesis is the process of generation of hematopoietic cells that takes place mainly in the bone marrow, although there are extra-medullary sites of minor hematopoiesis such as the spleen or the liver (Zhu and Emerson, 2002). More than 10^9 hematopoietic cells are produced each day in the homeostatic bone marrow to maintain blood cell counts in the human body (Petvises and O'Neill, 2012). All blood cells originate from a common precursor cell, the hematopoietic stem cell or HSC. Long-term HSCs (LT-HSCs) are capable of lifelong self-renewal and can differentiate into different cell lineages (Rosenbauer and Tenen, 2007). They give rise to short-term HSCs (ST-HSCs), which have gained expression of the CD34 marker. ST-HSCs can also differentiate into any blood cell type, but unlike LT-HSCs, they exhibit a significantly reduced self-renewal capacity (Rosenbauer and Tenen, 2007). ST-HSCs can give rise to both common myeloid progenitors (CMPs) and the common lymphoid progenitors (CLPs). CMPs are the precursors of all myeloid and erythroid cells, whereas CLPs are the precursors of all lymphoid cells. Common lymphoid progenitors express the IL7 receptor (Kondo et al., 1997). They give rise to all lymphoid cells, including B cells, T cells, and NK cells. They can also give rise to dendritic cells. B cells and NK cells mature in the bone marrow, whereas CLPs or early T cells migrate to the thymus to develop into mature T cells (Zhu and Emerson, 2002). After maturation, lymphoid cells home to the secondary lymphoid organs such as the spleen and

lymph nodes or to lymphoid tissues, and await their eventual encounter with their specific antigen.

Common myeloid progenitors can give rise to two types of progenitors: granulocyte-monocyte progenitors (GMPs) and megakaryocyte-erythrocyte progenitors or MEPs. All three types of progenitors can be distinguished based on their expression of two markers (Rosenbauer and Tenen, 2007). In fact, CMPs express CD34 but not CD16/32, also known as FcγRII/FcγRIII. GMPs express both CD34 and CD16/32, and MEPs express neither CD34, nor CD16/32. As their name implies, MEPs differentiate into erythrocytes or megakaryocytes. CMPs give rise to dendritic cells, granulocytes and monocytes, which migrate to the tissues via the bloodstream. Monocytes receive various signals from cells and tissues —such as the cytokine M-CSF— in homeostasis and during infection that cause them to differentiate into macrophages (Ushach and Zlotnik, 2016).

1.2. *Salmonella* infection

Bacteria of the *Salmonella enterica* species can infect a wide range of hosts and cause different types of diseases in them, including typhoid fever. The gram-negative species comprises over 2500 different serovars distinguished by the structure of their flagellar and lipopolysaccharide antigens (Coburn et al., 2007). Non-typhoidal serovars – which do not cause typhoid fever – such as *Salmonella* Typhimurium and Enteritidis can infect humans, cattle, poultry and swine (LaRock et al., 2015). They usually cause a self-limiting gastroenteritis in humans, characterized by vomiting, intestinal inflammation, and diarrhea (Haraga et al., 2008). However, immune-compromised individuals as well as infants and the elderly are at risk of developing septicemia (Gilchrist et al., 2015; Feasey et al., 2012). On the other hand, *Salmonella* serovars Typhi and Paratyphi are human-restricted pathogens that cause a systemic disease

called typhoid fever or enteric fever. The estimated number of typhoid fever cases worldwide is of around 13.5 million per year (Buckle et al., 2012). Symptoms include constipation or diarrhea, fever, abdominal pain, and septicemia (Haraga et al., 2008). There are a few genomic differences between typhoidal and non-typhoidal strains that can account for the differential symptoms observed during infection. For instance, unlike *Salmonella* Typhimurium, the *Salmonella* Typhi genome encodes a capsular polysaccharide – termed Vi capsular polysaccharide – that covers the bacterial surface, hindering complement activation and thus neutrophil recruitment (Keestra-Gounder et al., 2015). That way, the immune response to *Salmonella* Typhi is impaired, allowing the bacteria to disseminate into the bloodstream and infect other organs including the spleen (Keestra-Gounder et al., 2015).

Most studies on the pathogenesis of *Salmonella* infections have been performed in mice (Coburn et al., 2007). Murine *Salmonella* Typhimurium is in fact used as a model for human typhoidal infection. That is because mice are not susceptible to *Salmonella* Typhi, and *Salmonella* Typhimurium causes a systemic disease in susceptible mice, including the C57BL/6 strain, that resembles human typhoid fever (Santos et al., 2001). However, there are certain limitations to the murine typhoid model (Santos et al., 2001). First of all, *Salmonella* Typhimurium causes a different disease in mice and in humans, namely typhoid fever and gastroenteritis respectively. Furthermore, *Salmonella* Typhimurium has many active genes that are only pseudogenes in *Salmonella* Typhi and Paratyphi (McClelland et al., 2004). Thus, extrapolating mouse data to humans has to be exercised with caution. Nevertheless, the many strengths of this model outweigh its weaknesses. For instance, the functions of many effectors encoded by the *Salmonella* pathogenicity islands (SPIs) were discovered using mouse models (Santos et al., 2001; LaRock et al., 2015). SPIs are groups of genes that are essential for *Salmonella* virulence. Plus, live

attenuated vaccines against typhoid fever were designed based on mouse studies (Santos et al., 2001). Overall, the mouse model has given us new insights into the host-pathogen interactions involved in *Salmonella*-induced disease.

1.2.1. Mechanism of infection

Salmonella infections are common in areas of the world that lack adequate sanitation, and in developed countries due to increased dependence on food storage. Infection is acquired through ingestion of contaminated food or water. The bacteria survive the acidic pH of the stomach and the many adverse conditions of the small intestine, including digestive enzymes, bile salts, or IgA antibodies to reach the intestinal mucosa (Haraga et al., 2008). There, they can infect epithelial cells, and are usually taken up by microfold or M cells, which are specialized epithelial cells that take up antigen from the intestinal lumen to present them to the underlying lymphoid Peyer's patches (Figure 1). Thus, *Salmonella* are transported to immune cells including macrophages and dendritic cells in the Peyer's patches. They can also access these lymphoid tissues through dendritic cells that extend pseudopods between epithelial cells to sample antigens in the intestinal lumen. Upon exposure to *Salmonella*, local epithelial cells secrete small chemo-attractant proteins called chemokines, such as IL8, that recruit polymorphonuclear (PMN) leukocytes such as neutrophils to the site of infection (Eckmann et al., 1993). PMNs are efficient at clearing bacteria from the gut, but in typhoid fever, *Salmonella* is able to significantly alter recruitment of neutrophils (Jansen et al., 2011), thus evading a local immune response (Keestra-Gounder et al., 2015). In this case, the bacteria then travel to the blood, either directly or through the mesenteric lymph nodes when carried there by immune cells, causing a systemic infection (Mastroeni et al., 2009).

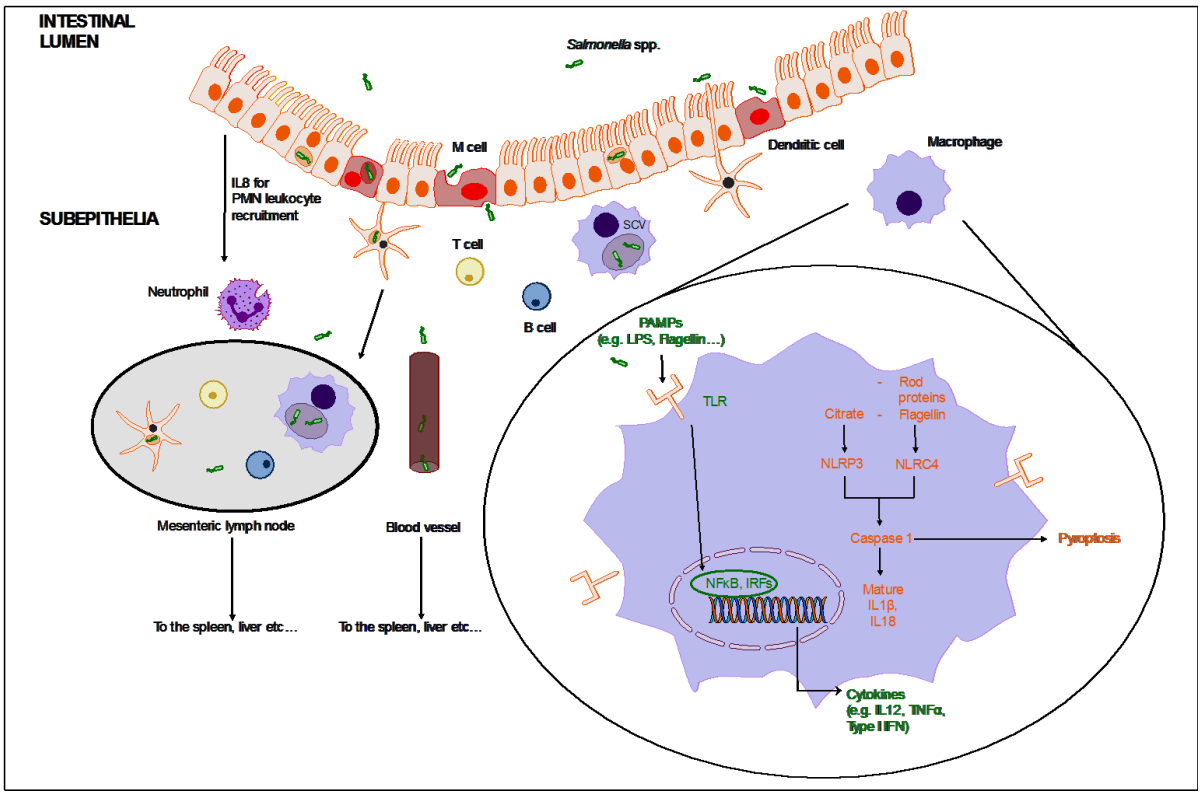
INTESTINAL LUMEN
Salmonella spp.
M cell
Dendritic cell
Macrophage
IL8 for PMN leukocyte recruitment
SUBEPITHELIA
SCV
T cell
Neutrophil
B cell
PAMPs (e.g. LPS, Flagellin…)
TLR
- Rod proteins
Citrate - Flagellin
NLRP3
NLRC4
Caspase 1
Pyroptosis
NFκB, IRFs
Mature IL1β, IL18
Cytokines (e.g. IL12, TNFα, Type I IFN)
Mesenteric lymph node
Blood vessel
To the spleen, liver etc…
To the spleen, liver etc…

Figure 1. Mechanism of *Salmonella* infection

Salmonella are preferentially taken up by M cells in the small intestine. Dendritic cells that sample the lumen can also take up the bacteria and transport them to the sub-mucosal space. *Salmonella* can also infect epithelial cells, which then secrete the chemokine IL8 to recruit polymorphonuclear leukocytes (PMNs) such as neutrophils to control the infection. In invasive infections, *Salmonella* impair neutrophil recruitment. In the sub-mucosa, *Salmonella* infect cells of the reticulo-endothelial system such as macrophages, and reside inside a spacious vacuole in the cells termed a *Salmonella*-containing vacuole (SCV). Recognition of bacterial pathogen-associated molecular patterns (PAMPs) such as lipopolysaccharide (LPS) or flagellin by macrophage toll-like receptors (TLRs) activates NFκB and interferon regulatory factors (IRFs). These transcription factors respectively induce expression of pro-inflammatory cytokines such as IL12 or TNFα and of type I IFNs. Recognition of citrate by NLRP3 or of bacterial rod proteins and flagellin by NRLC4 induces formation of the inflammasome and activates caspase 1 to produce the mature pro-inflammatory cytokines IL1β and IL18. Caspase 1 activation also leads to an inflammatory form of cell death termed pyroptosis. Activated macrophages and dendritic cells migrate to the lymph nodes to present antigen to lymphocytes, but failure to control the bacteria leads to systemic dissemination through the lymphatics and blood. *Salmonella* then go on to infect other organs such as the spleen or liver.

From the bloodstream, *Salmonella* enters the spleen or the liver (Dunlap et al., 1991) and infects and replicates preferentially within phagocytes of the reticulo-endothelial system, specifically macrophages (Richter-Dahlfors et al., 1997; Santos et al., 2001).

1.2.2. Intracellular lifestyle of *Salmonella*

Salmonella usually enters macrophages by macropinocytosis, a process by which cells engulf large volumes of fluid or particles (Alpuche-Aranda et al., 1994). The large vesicle – or phagosome – that contains the bacteria then fuses with a lysosome, acidifies and shrinks to form a *Salmonella*-containing vacuole (SCV) (Alpuche-Aranda et al., 1994; Haraga et al., 2008). Inside the SCV, the bacteria must thrive under numerous constraints including a pH of 5.5 or less, antimicrobial peptides, and reactive oxygen and nitrogen species (Haraga et al., 2008). Multiple virulence factors contribute to the intracellular survival of *Salmonella* (Alpuche-Aranda et al., 1992).

Salmonella can become virulent by injecting effectors into the host cell cytoplasm using the molecular machinery encoded by the Type 3-Secretion System (T3SS). The various effector proteins secreted through the T3SS are segregated into various *Salmonella* pathogenicity islands. These effectors have a wide range of roles in affecting host processes, from cytoskeletal organization to cell death (Hansen-Wester et al., 2001). Indeed, knowledge of the specific interaction of some *Salmonella* effectors with host processes is still scarce, and a better understanding of those would be useful to modulate the deleterious effects of the bacteria in infected hosts.

1.2.3. *Salmonella*-induced inflammation

Salmonella express various pathogen-associated molecular patterns (PAMPs) such as lipopolysaccharide (LPS) or flagellin, which are conserved structures on pathogens such as fungi, viruses, or bacteria in this case, and that can be recognized by the innate immune system. Innate immune cells recognize these bacterial components as well as host danger-associated molecular patterns (DAMPs) using pattern recognition receptors (PRRs) such as Toll-like receptors (TLRs) and Nod-like receptors (NLRs) (LaRock et al., 2015). These innate immune receptors are germline-encoded and thus are not pathogen-specific, unlike T and B cell receptors.

Pattern recognition receptors in *Salmonella* infection

TLR signaling

Upon binding of PAMPs or DAMPs, TLR engagement leads to downstream signal transduction that ultimately leads to the activation of the NFκB and IRF transcription factors (Gilchrist et al., 2015). Two major PAMPs involved in *Salmonella*-induced inflammation are LPS —a component of the outer membrane of gram-negative bacteria— and flagellin, recognized by TLR4 and TLR5 respectively (Gilchrist et al., 2015). In fact, mice lacking TLR4 show increased susceptibility to *Salmonella* infection (Weiss et al., 2014). TLRs such as TLR4 are not only expressed on the cell surface, but can also be recruited to phagosomes or endosomes (Gilchrist et al., 2015). Activation of transcription factors of the IRF family induces secretion of type I IFNs (IFNα and IFNβ). NFκB activation upon TLR signaling induces transcription and secretion of various pro-inflammatory cytokines, including IL12 and TNFα, which play a key role in controlling *Salmonella* (Gilchrist et al., 2015). IL12 is secreted by phagocytes such as macrophages, and induces the production of IFNγ by NK cells and helper T cells (Gilchrist et

al., 2015). IFNγ in turn augments the IL12 production (Gilchrist et al., 2015) and along with TNFα, increases the microbicidal activity of macrophages (Coburn et al., 2007). Anti-inflammatory cytokines such as IL10 act as dampeners of the immune response to prevent host tissue damage. Thus, they can also have a negative impact on host defense if high levels are secreted.

NLR signaling

NLRC4 (NOD-LRR-CARD-containing 4) and NLRP3 (NOD-LRR-Pyrin domain-containing protein 3) are two types of Nod-like receptors involved in the innate immune response to *Salmonella*. NLRP3 recognizes a diverse array of molecules such as citrate and possibly bacterial cardiolipin, whereas NLRC4 recognizes bacterial virulence mediators such as flagellin —a monomeric unit of the bacterial flagellum—, and T3SS rod proteins (LaRock et al., 2015). These NLRs are parts of multi-protein complexes found in myeloid cells and called inflammasomes. Upon binding of one of their ligands, NLRs associate with the apoptosis-associated speck-like protein containing a CARD (ASC) protein and activate caspase 1 (LaRock et al., 2015). Caspase 1 in turn cleaves the pro-forms of IL1β and IL18 – induced by TLR signaling – into the mature pro-inflammatory cytokines. Caspase 1 activation also leads to an inflammatory form of programmed cell death termed pyroptosis. Activation of another caspase, namely caspase 11, can also cause pyroptotic cell death upon detection of cytosolic LPS (Kayagaki et al., 2013). Pyroptosis releases *Salmonella* in the extracellular environment, allowing them to infect other cells, but also to potentially be eliminated by neutrophils or opsonized by antibodies and complement proteins for subsequent phagocytosis.

Pyroptosis shares characteristics of two other forms of cell death, apoptosis and necroptosis (Coburn et al., 2008), as it relies on caspases but also results in release of cellular contents, including newly produced IL1β and IL18, in the extracellular milieu.

Apoptosis is a programmed form of cell death occurring upon external or internal signals and dependent on cysteine aspartic proteases (caspases) 8 or 9 respectively (Galluzzi et al., 2016). Phenotypically, apoptotic cells are characterized by membrane blebbing followed by the formation of apoptotic bodies containing cellular contents (Blander, 2014). These are then phagocytosed by innate immune cells without induction of inflammation (Galluzzi et al., 2016). Necroptosis however is an inflammatory form of cell death that is independent of caspases. Instead, the kinase RIP1K gets activated initially, which phosphorylates RIP3K, which interacts with FADD, inactive caspase 8 and the pseudo-kinase MLKL. Activated RIP3K phosphorylates MLKL, which leads to trimerization of MLKL. As a result, MLKL relocates to the cell membrane, which results in impairment of membrane integrity, and cell rupture (Galluzzi et al., 2016). Cellular contents are thus released in the extracellular milieu and these DAMPs are recognized by innate immune cell PRRs to initiate inflammation (Blander, 2014).

1.2.4. Macrophage polarization

Macrophage function can be modulated by extracellular signals (Galván-Peña and O'Neill, 2014). Indeed, microbial products such as LPS, in association with the cytokines produced during infection such as IFNγ, cause macrophages to become pro-inflammatory. In this case, the cells become more phagocytic and produce higher amounts of antimicrobial peptides and pro-inflammatory cytokines such as IL12 or TNFα. These macrophages are called classically-activated or M1 macrophages. On the other hand, parasitic products associated with the cytokines produced in parasitic infections, namely IL4 or IL13, cause macrophages to

become more anti-inflammatory. In this case, they acquire functions that promote wound healing and control of parasites; they also secrete anti-inflammatory cytokines such as IL10. These cells are called alternatively-activated or M2 macrophages. There are no discrete subsets associated with macrophage polarization. Rather, polarized macrophages reflect a continuous spectrum of different states of activation. Thus, there are many macrophage phenotypes that resemble M1 or M2 cells but that also have distinctive characteristics (Mosser and Edwards, 2008). These include regulatory macrophages also called "M_{regs}", which are anti-inflammatory cells that secrete particularly high amounts of IL10 among other characteristics. Unlike M2 macrophages, they do not promote tissue repair (Mosser and Edwards, 2008). Differentiation towards this phenotype appears to be induced by TLR signaling associated with another stimulus such as binding of apoptotic bodies or immune complexes (Mosser and Edwards, 2008).

Modulation of metabolism is a direct consequence of macrophage polarization. M1 macrophages become highly glycolytic, which allows them to quickly produce the energy required for the cell growth and proliferation needed during inflammation (Galván-Peña and O'Neill, 2014). Glycolysis rapidly provides metabolic intermediates that are needed for the biosynthesis of cell constituents such as fatty acids for membrane growth (O'Neill et al., 2016). There is also a noted increase in the pentose phosphate pathway activity, for the generation of NADPH among other functions (O'Neill et al., 2016). NADPH is a co-factor used by NADPH oxidase to generate ROS used for bacterial killing. At the same time, M1 cells downregulate oxidative respiration by disrupting the Krebs cycle (O'Neill et al., 2016). This leads to the accumulation of citrate and succinate in the cell (O'Neill et al., 2016). Citrate is then used by the M1 macrophage to generate fatty acids (O'Neill et al., 2016). It is also used to produce itaconic

acid (Michelucci et al., 2013), as well as nitric oxide (NO) (Infantino et al., 2011), which are antimicrobials. NO in turn can inhibit the electron transport chain (Clementi et al., 1998), further contributing to the shutting down of oxidative respiration by M1 cells. Succinate is known to increase the stability of the transcription factor hypoxia-inducible factor (HIF)-1α (Tannahill et al., 2013). HIF-1α can be activated by LPS to increase the transcription of glycolytic enzymes and pro-inflammatory cytokines including IL1β (Tannahill et al., 2013).

M2 macrophages, because of their role in tissue injury repair, need a sustained energy supply. Thus, they rely on oxidative respiration and β-oxidation of fatty acids, which result in the slow generation of energy (O'Neill et al., 2016). Both oxidative respiration and β-oxidation take place in the mitochondria, so mitochondrial biogenesis is required in M2 macrophages. Catabolism of fatty acids provides the cells with the Krebs cycle intermediate acetyl CoA and with the reducing equivalents NADH and $FADH_2$, which are used by the electron transport chain to generate ATP (O'Neill et al., 2016). A key difference between M1 and M2 macrophages is how they make use of the amino acid arginine (O'Neill et al., 2016). In M1 macrophages, arginine is used by the enzyme inducible nitric oxide synthase (iNOS) to generate NO. In M2 macrophages however, arginine is used by the enzyme arginase to produce urea, ornithine and polyamines, which are used in the production of the extracellular matrix, in accordance with the role of M2 cells in tissue repair.

Thus, macrophage polarization can be assessed by measuring metabolic rates, as well as the transcription of the various genes involved in cell-specific functions. Molecular contributors to macrophage polarization still remain to be discovered.

1.3. FoxO3a transcription factor

Forkhead box O (FoxO) transcription factors are a subclass of the Forkead family of transcription factors. They were discovered in the fly *Drosophila melanogaster*, and mutations in the gene encoding their homolog dFoxO resulted in flies with ectopic head structures that resembled a fork (Jürgens and Weigel, 1988). Another well-studied homolog is the worm *Caenorhabditis elegans*' Daf-16. In mammals, there are four FoxO transcription factors, namely FoxO1, 3, 4, and 6, with FoxO6 being expressed mostly in the brain (Eijkelenboom and Burgering, 2013). In humans, FoxO transcription factors were discovered at chromosomal translocations in rhabdomyosarcomas and acute myeloid leukemias (Eijkelenboom and Burgering, 2013). FoxO3a phosphorylation, which is associated with its inactivation, was found to have a negative effect on survival to acute myeloid leukemia in humans (Kornblau et al., 2010). Overall, FoxO transcription factors function as sensors of cellular stress. Thus, upon disruption of cellular homeostasis, they undergo a wide variety of post-translational modifications such as phosphorylation, acetylation, or methylation that regulate their activity by affecting their cellular localization or their DNA binding ability (Eijkelenboom and Burgering, 2013). Depending on the context, FoxO transcription factors regulate the transcription of genes involved in important cellular processes including cell cycle, cell survival/cell death, and cell metabolism (van der Horst and Burgering, 2007). FoxO transcription factors all recognize the same consensus sequence 5'-TTGTTTAC-3' via their DNA binding domain (Furuyama et al., 2000). Thus, they act redundantly, although many specific functions have been attributed to each FoxO family member, especially as they are expressed differently throughout cell types and can be regulated differently (Furuyama et al., 2000).

Many FoxO transcription factor functions have been studied using mouse knockout models. FoxO3a-deficient mice are viable, but females display age-dependent infertility due to early exhaustion of their oocyte pool (Castrillon et al., 2003).

1.3.1. Regulation of FoxO3a by post-translational modifications

FoxO function is regulated by two main factors: insulin and growth factor signaling, and oxidative stress (Eijkelenboom and Burgering, 2013) (Figure 2). Insulin or growth factor signaling activates PI3K, which produces phosphatidylinositol-3-phosphate. This lipid activates PDK1, which phosphorylates Akt (also called PKB). Phosphorylation of Akt induces its nuclear localization, where it phosphorylates FoxO on three amino acid residues. In the case of FoxO3a, also known as FKHRL1, phosphorylation occurs on Threonine 32, Serine 253, and Serine 315 (van der Horst and Burgering, 2007). Phosphorylated FoxO displays increased binding to 14-3-3 proteins, which shuttle it out of the nucleus into the cytoplasm, where it can be degraded (van der Horst and Burgering, 2007).

Upon oxidative stress, JNK activates FoxO3a by phosphorylation on residues that are not known yet, to promote its nuclear localization (Greer and Brunet, 2005). Additionally, a host of other post-translational modifications affect FoxO3a function. For instance, the kinases Akt and ERK can promote FoxO3a ubiquitination and subsequent degradation (Eijkelenboom and Burgering, 2013). Moreover, the SET9 methyltransferase can inhibit the transcriptional activity of FoxO3a by methylation of its DNA binding domain (Eijkelenboom and Burgering, 2013).

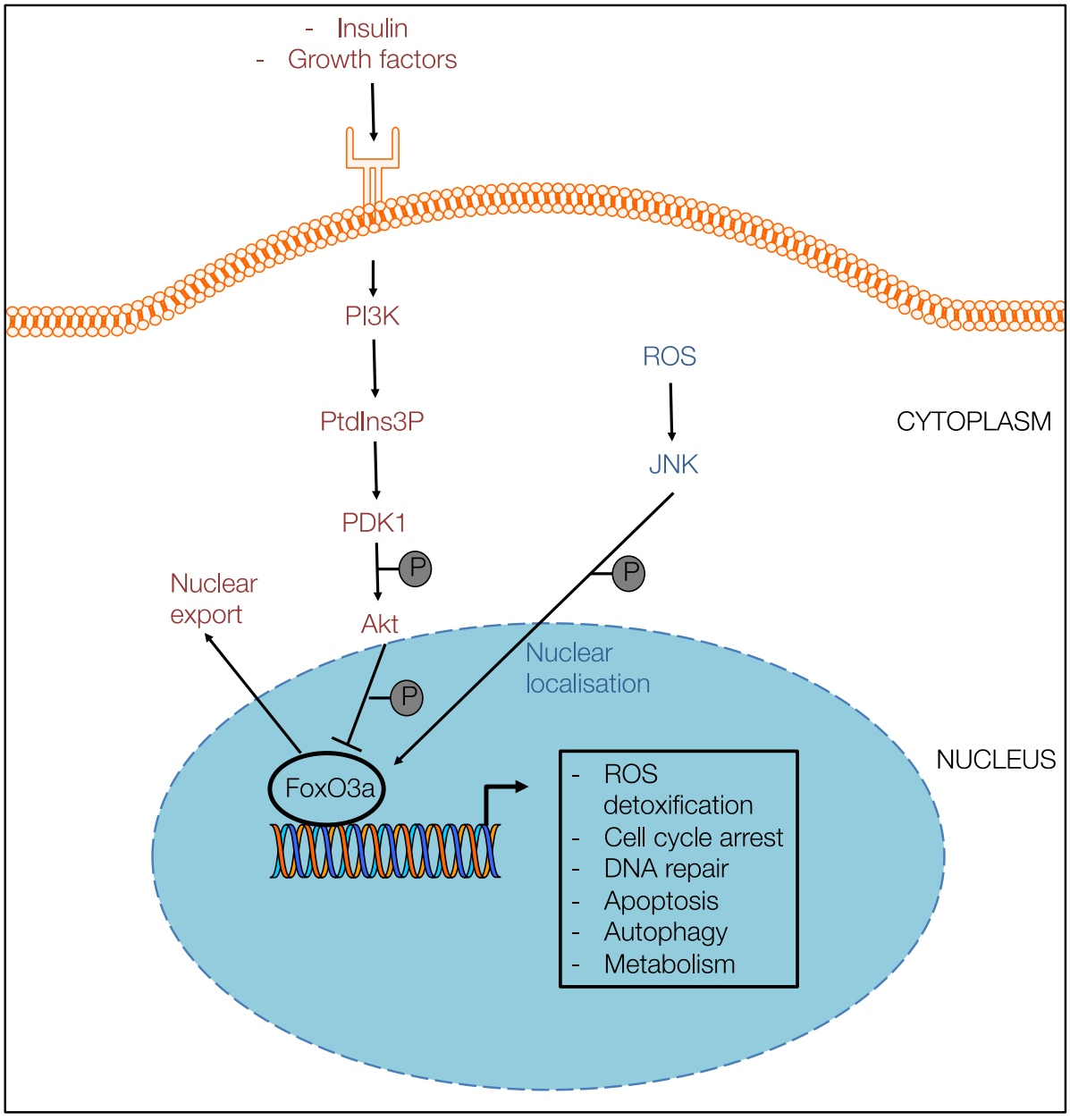
- Insulin
- Growth factors
PI3K
PtdIns3P
PDK1
P
Akt
P
Nuclear export
ROS
JNK
P
Nuclear localisation
CYTOPLASM
NUCLEUS
FoxO3a
- ROS detoxification
- Cell cycle arrest
- DNA repair
- Apoptosis
- Autophagy
- Metabolism

Figure 2. Regulation of FoxO3a
Insulin and growth factor signaling inhibit FoxO3a whereas oxidative stress activates the transcription factor. Insulin and growth factors signal through the PI3K/Akt pathway to phosphorylate FoxO3a on three residues (Thr 32, Ser 253 and Ser 315). Akt phosphorylation of FoxO3a induces shuttling of the transcription factor out of the nucleus into the cytoplasm where it can be degraded. Excess of reactive oxygen species (ROS) activates JNK, which phosphorylates FoxO3a on unknown residues, but in a manner that promotes its nuclear localization. In the nucleus, FoxO3a can regulate the transcription of genes involved in various cellular processes such as cell cycle arrest or cell apoptosis.
PtdIns3P = Phosphatidylinositol-3-phosphate. P=phosphorylation.

1.3.2. Regulation of FoxO3a target gene expression

The role of FoxO transcription factors becomes apparent when cellular homeostasis is disturbed, for example during nutrient deprivation or oxidative stress (Eijkelenboom and Burgering, 2013). FoxO transcription factors upregulate the transcription of genes involved in various functions including ROS detoxification, cell cycle arrest, autophagy, DNA repair or cell death. In fact, some FoxO3a single nucleotide polymorphisms have been associated with increased longevity in humans (Morris et al., 2015). The precise ways in which FoxO3a regulates lifespan are not known. Possible mechanisms include the control of cellular health by FoxO3a, through the promotion of DNA repair and oxidative stress resistance for example, which would increase host longevity (Morris et al., 2015). The different stimuli that cause FoxO factors to activate one type of genes or the other remain to be clarified.

Upon excessive ROS production, FoxO transcription factors can upregulate expression of ROS detoxifying genes such as catalase and manganese superoxide dismutase (Greer and Brunet, 2005). Indeed, FoxO3a was shown to promote the transcription of antioxidant enzymes such as catalase, SOD1, and SOD2 in mouse erythroid precursors (Marinkovic et al., 2007). In addition, Miyamoto et al. (2007) demonstrated that FoxO3a is required for hematopoietic stem cell self-renewal in adult mice. Since FoxO3a-deficient mice displayed increased ROS, it is possible that FoxO3a maintains HSCs by reducing oxidative stress (Miyamoto et al., 2007). Another possible mechanism they underlined is through the observed modulation of negative cell cycle regulators by FoxO3a such as p27, which would maintain HSC quiescence.

FoxO transcription factors are known to mediate cell cycle arrest by upregulating genes such as $p27^{kip1}$ or cyclin G2. Martínez-Gac et al. (2007), for instance, demonstrated that cyclin G2 can be upregulated in fibroblasts in a FoxO3a-dependent manner.

Another role of FoxO3a is the positive regulation of autophagy-related genes. In 2007, Mammucari et al. showed that FoxO3a could induce autophagy through Bnip3 when muscle cells were starved. Results from Zhao et al. (2007) also indicate that FoxO3a signaling can lead to muscle autophagy during nutrient deprivation, through modulation of genes such as Atg12l or LC3b.

FoxO3a is directly implicated in cell metabolism as it is inhibited by insulin signaling through PI3K/Akt phosphorylation. A recent study by Jensen et al. (2011) showed that FoxO3a can be activated by HIF-1α during hypoxia to repress various mitochondrial genes in HeLa cells.

During DNA damage, FoxO transcription factors can increase transcription of DNA repair genes. Upon DNA damage, FoxO3a induced cell cycle arrest at the G2-M phase and mediated DNA repair in a GADD45-dependent manner (Tran et al., 2002).

Finally, FoxO transcription factors can induce cell death by apoptosis through up-regulation of genes including BIM and FasL (Greer and Brunet, 2005). In fact, Cui et al. (2008) demonstrated that FoxO3a signaling could cause macrophage cell death by apoptosis during HIV-1 infection of human monocyte-derived macrophages. Cell death in this case was mediated by up-regulation of the apoptosis modulator PUMA.

1.4. Rationale

Salmonella infections still cause thousands of deaths worldwide (Buckle et al., 2012); this finding can be attributed to poor efficacy of vaccines and increased resistance of *Salmonella* to antibiotics (Gilchrist et al., 2015). Understanding the pathogenesis of these bacteria could therefore be key to the design of better vaccines for prevention and new treatment alternatives in the advent of antibiotic resistance. Given the importance of innate immunity in controlling infection early on – especially of macrophages in *Salmonella* infections both as host weapon and

Salmonella reservoir –, we decided to investigate the host-pathogen interactions in this cell type. Previous research in our laboratory has demonstrated that FoxO3a-deficient mice were more susceptible to systemic infection with *Salmonella* Typhimurium (ST) as they displayed a median survival of 16 days after infection compared with 32 days for WT mice (Joseph et al., 2016). Given the role of FoxO3a in sensing cellular stress, which occurs during *Salmonella* infection, and in maintenance of homeostasis, as well as the importance of inflammation in mediating pathogen clearance (see previous sections), I here investigate the potential inflammatory mechanisms through which FoxO3a promotes survival of *S*T infected mice.

1.5. Hypothesis

I hypothesize that chronic infection of mice with *Salmonella* Typhimurium results in excessive inflammation which is deleterious to host survival, and FoxO3a regulates excessive inflammation to promote host survival.

1.6. Objectives

1. To determine the role of FoxO3a in the regulation of immune cells during homeostasis and infection with *Salmonella* Typhimurium.

2. To investigate the impact of FoxO3a signaling on macrophage function during homeostasis and infection with *Salmonella* Typhimurium.

2. MATERIALS AND METHODS

2.1. Animals

Mice were housed at the University of Ottawa Animal Facility. They were maintained in accordance with Canadian Council on Animal Care (CCAC) guidelines. Wild type (WT) C57BL/6J mice were obtained from The Jackson Laboratory (Bar Harbor, Maine, USA). FoxO3a-deficient mice were generated as previously described (Tzelepis et al., 2013). Briefly, a gene-trap targeting strategy was used to disable the FoxO3a allele and thus generate FoxO3a-deficient mice (Lin et al., 2004). These were maintained by mating male homozygous knockouts with female heterozygous knockouts. Genomic polymerase chain reaction (PCR) on mouse ear clips was used for genotype determination. All mice were age and sex-matched for experiments. Protocols and procedures were approved by the University of Ottawa Animal Care Committee and Ethics Board.

2.2. Bacterial strains

Two bacterial strains were used for experiments:

1. SL1344 strain *Salmonella enterica* serovar Typhimurium (ST WT)
2. OVA-expressing SL1344 *Salmonella* (ST-OVA), engineered as previously described (Tzelepis et al., 2012).

2.3. *In vivo* infection model

Animals were infected by intravenous (i.v.) injections. ST-OVA bacteria were re-suspended at 10^5 CFU/mL in cold phosphate-buffered saline (PBS) and 100 µl were injected into each mouse. Mice were sacrificed 7 days following infection. The bacterial burden in the spleens was assessed upon euthanasia. Briefly, spleens were homogenized using frosted glass slides (Fisher Scientific #12-550-343) and re-suspended in 10 mL of R8 medium (RPMI-1640 (Thermo Fisher Scientific #31800089) supplemented with 8% fetal bovine serum (FBS) (NorthBio #NBSF-701) and 55µM 2-mercaptoethanol (Thermo Fisher Scientific #21985-023)). Ten-fold serial dilutions of the spleen suspensions were made and 100 µl aliquots were plated onto BHI-Agar plates. Plates were incubated at 37°C overnight and colony-forming units (CFU) were then counted.

2.4. Flow cytometry

Uninfected and infected mouse spleen, blood, and bone marrow immune cells were analyzed by flow cytometry. Specifically, spleens were removed and placed in R8 medium on ice. The R8 medium for uninfected samples also contained 50 µg/ml gentamicin (Thermo Fisher Scientific #15750-060). The R8 medium for infected samples did not contain any gentamicin. Whole spleens were homogenized using frosted glass slides and filtered through a 70 µm cell strainer (Fisher Scientific #22363548). The resulting single-cell suspension was used for flow cytometry. Blood was collected via saphenous bleeding in lithium-heparin anti-coagulant tubes (BD Biosciences #365965) to prevent clotting. Red blood cells were lysed using RBC lysis buffer (Sigma-Aldrich #R7757) according to manufacturer's instructions, then cells were washed with ice cold PBS and re-suspended in R8 medium for flow cytometric analysis. To collect bone marrow cells, mice were sacrificed and hind limbs were excised and placed in R8 medium, on

ice. Fur and muscles were removed from the bones using scissors and forceps. Bones were then flushed with a 26-gauge needle (BD Biosciences #309625) through a 100 μm strainer (Fisher Scientific #22363549). The resulting single cell suspension was used for flow cytometry.

For live cell staining, up to 3×10^6 cells (or 50 μl of blood) were transferred to 5 ml tubes (Fisher Scientific #14-961-10) and washed with staining buffer (1% Bovine serum albumin (Sigma-Aldrich #A7906) in PBS). To prevent non-specific binding of antibodies, FcBlock (anti-CD16/32) (BD Biosciences #553142) was added to the cells in staining buffer followed by a 10-minute incubation period at 4°C. Then, fluorophore-conjugated antibodies against various cell surface receptors were added in staining buffer. Cells were protected from light and incubated for 30 minutes at 4°C. A list of the antibodies used can be found in table 1.

Table 1. Flow cytometry staining antibodies

Antibody	Conjugated fluorophore	Source	Catalog number
CD11c	eFluor 450	eBioscience	48-0114-80
CD11b	PE/Cy7	eBioscience	2500112-81
Ly6G	FITC	eBioscience	11-5931-82
Ly6C	PE	eBioscience	12-5932-82
F4/80	APC-eFluor 780	eBioscience	47-4801-80
TCRβ	PE	eBioscience	12-5961-82
B220	BV510	BioLegend	103247
DX5	FITC	eBioscience	11-5971-82
Ter119	APC	eBioscience	17-5921-81
Lin*	FITC	eBioscience	22-7770-72
c-kit	PE/Cy7	eBioscience	25-1171-81
Sca-1	PerCP-Cy5.5	eBioscience	45-5981-80
CD34	eFluor 450	eBioscience	48-0341-80
IL7R	APC	eBioscience	17-1271-82
CD16/32	PE	eBioscience	12-0161-81

*Lin cocktail contains antibodies against the following markers: CD11b, Ly6G, CD3, B220, Ter119.

Cells were then washed with staining buffer to remove excess unbound antibodies. Cells were re-suspended in flow fixative (PBS containing 1% paraformaldehyde and 0.02% sodium azide)

and acquired immediately on the flow cytometer (CyAn ADP analyzer, Beckman Coulter). Data were analyzed using Kaluza software (Version 1.2, Beckman Coulter).

2.5. Bone marrow myeloid precursor colony-forming assay

Murine bones were extracted and flushed as detailed above. Bone marrow cells were resuspended in Iscove's IMDM supplemented with 2% FBS (STEMCELL #07700) and added to 3 ml of Methocult methylcellulose medium (STEMCELL # M3534) at a concentration of 2×10^4 cells/ml. Then, 2×10^4 cells in Methocult medium were plated in duplicates in low cell adherence 35 mm dishes (STEMCELL #27100). Dishes were then placed inside a loosely covered 100 mm petri dish (Fisher Scientific #FB0875713). An uncovered supplementary 35 mm dish filled with sterile water was added to the 100mm petri dish to maintain humidity. Cells were incubated in a 5% CO_2 incubator at 37°C for 12 days. Myeloid colony assessment was performed according to colony morphology as per manufacturer's instructions using a Nikon TMS inverted microscope. Methods of colony identification are described in more details in the Results section. Colony numbers of three myeloid sub-populations were obtained – namely CFU-G, CFU-M and CFU-GM (Colony-forming unit – Granulocyte, Macrophage and Granulocyte/Macrophage respectively).

2.6. Generation of Bone Marrow-Derived Macrophages

Mouse hind limbs were extracted and flushed as mentioned above. One hundred millimeter plastic petri dishes were coated with macrophage colony-stimulating factor (M-CSF) (R&D Systems #416-ML-010) at 5 ng/ml using an L-stick (Sigma-Aldrich #SPR-L-S10). Thirteen million bone marrow cells were re-suspended in 10 ml R8 media with gentamicin and

were added to each petri dish. Roughly, bone marrow cells from both hind limbs of a mouse yielded 8-10 petri dishes. Cells were incubated at 37°C for 12 days to allow macrophage differentiation to occur. In some cases, they were harvested 6 days post-incubation. On average, 3-6 million live macrophages could be collected from each petri dish. Macrophage purity was confirmed by flow cytometry ($CD11b^+$, $F4/80^+$).

2.7. *In vitro* ST infection

Bone marrow-derived macrophages (BMDMs) were plated after differentiation in M-CSF-coated dishes. Cells were seeded in a 24-well flat bottom tissue culture plate (Fisher Scientific #353047) at 3×10^5 cells/well in R8 medium without gentamicin. Macrophages were incubated overnight at 37°C to prevent the effects of plating-derived cellular stress from impacting the experiment. The following day, cells were infected with ST WT. Higher multiplicity of infection (100 MOI) was used for cell death measurements. Lower multiplicity of infection (10 MOI) was used for cytokine measurements. Upon addition of the bacteria, cells were centrifuged at 1500 RPM for 10 minutes, followed by a 30-minute incubation at 37°C to allow infection to occur. Gentamicin was then added to eliminate extracellular bacteria. This was followed by a 6-hour incubation period for RNA extractions, or a 24-hour incubation period for cell death and cytokine measurements.

In some experiments, cells were also treated with various inhibitors while being infected with ST. For 2-deoxy-D-Glucose (2-DG) treatment, 1 mM 2-DG was added to macrophages 3 hours prior to infection. Then, cells were treated with the same concentration of 2-DG concurrently with ST. For the anti-IL10 treatment, macrophages were treated with 10 μg/ml anti-IL10 antibody concurrently with ST. A list of the inhibitors used can be found in table 2.

Table 2. Inhibitors and agonists used for experiments

Inhibitor/Agonist	Source	Catalog number	Concentration
Ultra-pure lipopolysaccharide (LPS)	Sigma-Aldrich	L3024	100 ng/ml
2-Deoxy-D-glucose (2-DG)	Sigma-Aldrich	D6134	1 mM
Anti-IL10 Antibody	BD Biosciences	554421	10 μg/ml
zVAD	ApexBio	A1902	50 μM
Necrostatin-1 (nec-1)	Sigma-Aldrich	N9037	25 μM
Brefeldin A (BFA)	eBioscience	00-4506-51	3 μg/ml
Salubrinal	Sigma-Aldrich	SML0951	20 μM

2.8. Cell viability assays

Two methods were used to determine cell viability in my experiments. To determine cell death after ST infection, a Neutral Red assay was performed 24 hours after infection. A 5% Neutral Red solution (Sigma-Aldrich #N2889) was prepared in R8 medium. To minimize the possibility of crystal formation, the solution was then filtered with a 0.22 μm filter (EMD Millipore #SLG033SS) before addition to the cells. Macrophages were incubated with the Neutral Red solution for 15 minutes. The stain was then removed by aspiration and the cells washed with PBS. Next, the dye was solubilized with a solution of ethanol and acetic acid in sterile water. The absorbance of the dye was immediately measured at 570 nm using a FilterMax™ F5 plate reader (Molecular Devices). Absorbance measured was normalized to the unstimulated control (i.e. cells with R8 medium only).

To determine cell death after LPS and inhibitor treatments, a 3-(4,5-dimethylthiazol-2-yl)-2,5-diphenyltetrazolium bromide (MTT) assay was performed 24 hours after treatment. A 5% MTT solution (Sigma-Aldrich #M5655) was prepared in R8 medium and 100 μl were added to the cells. Macrophages were incubated for 2 hours at 37°C. Cells were then lysed by adding

100 µl of a solution of 37% HCl diluted in isopropanol. To solubilize the MTT crystals, the solution was mixed as vigorously as possible inside the wells. The absorbance of the solubilized dye was immediately measured at 570 nm using a FilterMax™ F5 plate reader (Molecular Devices). Absorbance values were normalized to the unstimulated control (i.e. cells with R8 medium only).

2.9. *In vitro* LPS treatment and inhibitor assays

BMDMs were plated after differentiation in M-CSF-coated dishes. Cells were seeded in a 96-well flat bottom tissue culture plate at 10^5 cells/well in R8 medium. Macrophages were incubated overnight at 37°C to prevent cellular stress. The following day, cells were treated with lipopolysaccharide (LPS) concurrently with various small molecule inhibitors listed in table 2. Techniques varied for some experiments and details are provided in the text. Cells were treated for 24 hours, before cell death or viability was measured by MTT assay.

2.10. TMRE staining

Mitochondrial membrane potential in macrophages was assessed using tetramethylrhodamine ethyl ester (TMRE) staining. Cells were seeded in a 24-well tissue culture plate, on circular cover slips. The cover slips allowed for easy macrophage detachment when transferring the cells to 5 ml tubes for TMRE staining. Cells were infected with ST or treated with LPS for 24 hours, and then macrophages were detached with a cell scraper. Cells were transferred into a 5 mL tube and washed with warm R8 medium lacking phenol. FcBlock was then added to the macrophages to prevent any non-specific binding, and cells were incubated for 10 minutes at 37°C. Next, 485 nM TMRE (Thermo Fisher Scientific #T669) was added to

the cells, followed by 30 minutes of incubation at 37°C. Cells were washed twice with R8 medium lacking phenol and immediately acquired on the flow cytometer.

2.11. Quantitative RT-PCR

RNA was extracted from macrophages 6 hours after ST infection using TRIzol (Thermo Fisher Scientific #15596026). DNA was extracted from cells 24h post-infection, using a QIAamp DNA mini kit (Qiagen #51304). RNA was converted to cDNA using Superscript III Reverse Transcriptase (Thermo Fisher Scientific #56575). DNA or cDNA relative amounts were then obtained by the SYBR green method using an Applied Biosystems 7500-Fast qRT-PCR System. Specific primers for mRNA or DNA sequences of interest were generated using the NCBI primer tool and are listed in table 3.

Table 3. List of primers used for qPCR

Gene of interest	Forward primer sequence (5'-3')	Reverse primer sequence (3'-5')
β-actin	GATCAAGATCATTGCTCCTCCTG	AGGGTGTAAAACGCAGCTCA
AMPKα1	GCCATGCGCAGACTCAGTTC	ACTCGTGCTTGCCCACCTT
Arginase 1	TTTTAGGGTTACGGCCGGTG	CCTCGAGGCTGTCCTTTTGA
Cytochrome c oxidase 1	GCCCCAGATATAGCATTCCC	GTTCATCCTGTTCCTGCTCC
GLUT1	ACGATCTGAGCTACGGGGTC	GTCACCTTCTTGCTGCTGGGAT
HIF-1α	TGACGGCGACATGGTTTACA	ACTGGGCCATTTCTGTGTGT
IL1β	TGCCACCTTTTGACAGTGATG	TGATGTGCTGCTGCGAGATT
IL10	GGTTGCCAAGCCTTATCGGA	GGGGAGAAATCGATGACAGC
IL12a	ATGTGTCAATCACGCTACCTCC	TCAGGCGGAGCTCAGATAGCC
iNOS	GCCACCAACAATGGCAACAT	TCGATGCACAACTGGGTGAA

LIGHT	CTGCATCAACGTCTTGGAGA	GATACGTCAAGCCCCTCAAG
Mannose receptor	GGCTGATTACGAGCAGTGGA	ATGCCAGGGTCACCTTTCAG
SPHK1	ACAGCAGTGTGCAGTTGATGA	GGCAGTCATGTCCGGTGATG
18S rRNA	TAGAGGGACAAGTGGCGTTC	CGCTGAGCCAGTCAGTGT
TGFβ1	TGACGTCACTGGAGTTGTACGG	GGTTCATGTCATGGATGGTGC
TNFα	ACGTCGTAGCAAACCACCAA	ATAGCAAATCGGCTGACGGT

2.12. Mitochondrial bioenergetics assay

Cell adhesive Cell-Tak™ (Corning #354240) was used to coat the wells of a 24-well Seahorse tissue culture plate (Seahorse Bioscience #100777-004) to ensure macrophage adherence. Macrophages were then seeded into the wells at a density of 3×10^5 cells/well and incubated overnight at 37°C. The following day, cells were infected with ST as described above, for 24 hours. The R8 medium was then removed and cells were washed twice with warm Seahorse assay medium (Bicarbonate-free DMEM supplemented with D-glucose, L-Glutamine and sodium pyruvate, pH 7.4). Cells were then allowed to equilibrate at 37°C for 1 hour without CO_2. Next, oxygen consumption rates (OCR, in pmol/min) were recorded on a Seahorse Bioscience XF24 Extracellular Flux Analyzer, to assess mitochondrial respiration. Basal OCR was recorded, as well as OCR fluctuations in response to sequential addition of mitochondrial inhibitors in the following order: Oligomycin, CCCP, and Antimycin A (Sigma-Aldrich). Once the experiment was over, cells were lysed with 50 µl 0.5N NaOH and their protein contents measured using a Bradford assay (Bio-Rad #500-0006). OCR values were normalized to protein contents.

2.13. Cytokine Analysis

Enzyme-linked immunosorbant assays (ELISAs) were used to measure the concentrations of cytokines in the supernatants of ST-infected macrophages, as well as macrophages treated with various inhibitors and agonists *in vitro*. Murine TNF-α, IL12, IL1β, IL6, and IL10 were measured using kits purchased from BD Biosciences. Specifically, extra-high binding 96-well plates (Fisher Scientific #14245153) were coated with 50 µl/well of diluted capture antibody and incubated overnight at 4°C. The following day, plates were washed 3 times with PBST washing buffer (1X PBS and Tween 20 in H_2O). They were then blocked with 200 µl of assay diluent (10% FBS in PBS) for 1 hour at room temperature. Plates were subsequently washed 3 times with PBST and 50 µl of standards and samples were added. Sample and standard incubation lasted 2 hours, at room temperature. After washing 5 times, a mix of detection antibody + Streptavidin-HRP in assay diluent was made and 50 µl were added for 1 hour. Finally, after washing 7 times, 50 µl of a 1:1 mix ratio of tetramethylbenzidine (TMB) substrate solution (R&D systems #DY999) was added. Plates were incubated in the dark for up to 30 minutes, depending on the development of standards. Lastly, the reaction was stopped by adding 25 µl of stop solution (96% H_2SO_4 diluted in H_2O). Absorbance was read at 450 nm on the plate reader. Data were analyzed using SoftMax Pro software.

2.14. Type I IFN assay

Type I IFN concentration in cell culture supernatants was assessed using an L929 cell line obtained from Dr. Bruce Beutler (University of Texas, USA). The cell line contains a luciferase reporter gene cloned under the regulation of an ISRE promoter. A frozen stock of ISRE-L929 cells was thawed in DMEM media (Sigma-Aldrich #D5796) supplemented with 10% FBS and

2-mercaptoethanol. Cells were incubated at 37°C for several days to allow proliferation. ISRE-L929 cells were seeded at 5×10^4 cells/well in a 96-well flat bottom plate and incubated with 50 µl of ST-infected macrophage culture supernatant for 4h. Cells were washed with PBS then lysed with 30 µl of 1.5X lysis buffer supplied in the luciferase assay system kit (Promega #E1500). 100 µl of luciferase assay reagent were added to the wells and luminescence was measured using the plate reader.

2.15. Griess assay

The Griess diazotization assay was used to estimate nitrite concentrations as a measure of nitric oxide (NO), in ST-infected macrophage supernatants. The kit used for this assay was purchased from Thermo Fisher Scientific (#G7921). The Griess reagent was prepared by mixing equal volumes of N-(1-Naphtyl)ethylenediamine and sulfanilic acid. Twenty µl of Griess reagent were added to wells of a 96-well plate, along with 130 µl of deionized water and 150 µl of samples or standards. The mixture was incubated at room temperature for 30 minutes. Absorbance was measured at 570 nm using the plate reader.

2.16. Statistics

All error bars show standard error of the mean. Unpaired two-tailed student's t-test was used to determine statistical significance. All statistical analyses were performed using GraphPad Prism Software.

2.17. Technical acknowledgment

The following technical procedures were performed with my assistance by: (1) Kwangsin Kim – intravenous injections and some CFU assays after *in vivo* ST infections, (2) Ardeshir Ariana – Type I IFN assay.

3. RESULTS

3.1. Impact of FoxO3a signaling on immune cell homeostasis before and during ST infection

3.1.1. FoxO3a regulates cell numbers in the spleen

FoxO3a has been shown to regulate genes involved in various cellular functions such as cell cycle or cell death (Eijkelenboom and Burgering, 2013). Thus, the first aim of this thesis was to determine the impact of FoxO3a on the numbers of various immune cell types in mice before and upon infection with *Salmonella* Typhimurium (ST). First, total cell numbers were analyzed in primary and secondary immune tissues in naïve mice. WT mice and mice lacking the FoxO3a gene, herein referred to as FoxO3a-deficient mice, were used. Blood was collected by saphenous bleed, and then mice were euthanized as described in the materials and methods section. Spleens and hind leg bones were extracted for isolation of cells and single cell suspensions were prepared. Blood, spleen, and bone marrow cells were stained with Trypan blue. Trypan blue is a dye that is taken up by dead cells but not by live cells. Hence, live cells were counted. As indicated in Figure 3, there were no differences in total bone marrow cell counts between WT and FoxO3a-deficient mice. FoxO3a-deficient mice displayed a trend towards an increase in blood cell counts and a significant increase in splenocyte numbers compared with WT mice. Collectively, these results indicate that FoxO3a prevents abnormal expansion of splenocytes.

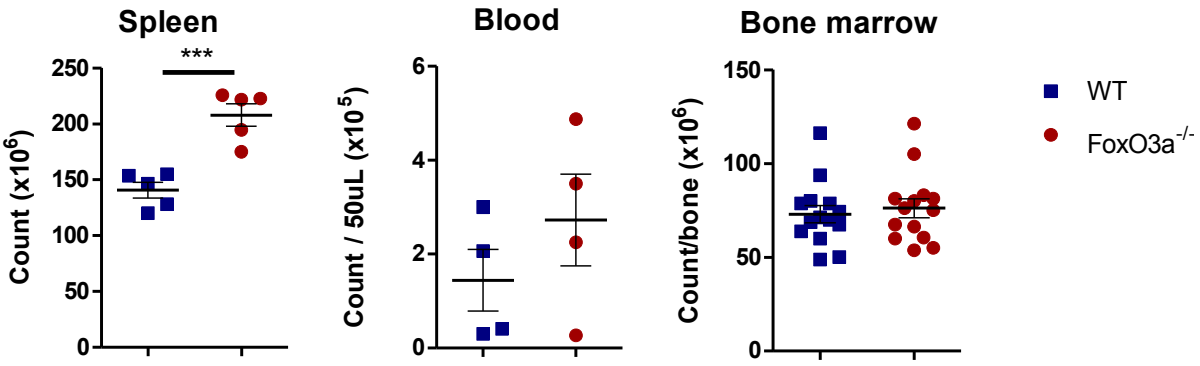
Spleen
***
Count (x10^6)
250
200
150
100
50
0
Blood
Count / 50uL (x10^5)
6
4
2
0
Bone marrow
Count/bone (x10^6)
150
100
50
0
WT
FoxO3a-/-

Figure 3. FoxO3a signaling controls immune cell numbers in the spleen

Blood, spleen, and hind leg bones (hip bone, femur, and tibia) were collected from naïve WT and FoxO3a-deficient mice. Blood, spleen, and bone marrow single cell suspensions were obtained as described in the experimental methods. Live cells were counted with a hemocytometer, using trypan blue stain.

Graphs show total live cell counts, excluding red blood cells. Blood cell counts are indicated per 50 μl of blood collected. Bone marrow cell counts are indicated per bone flushed. Data are pooled from at least 4 independent experiments, and presented as mean ± SEM. Statistical significance was calculated by unpaired two-tailed Student's t-test: ***$p<0.0001$.

3.1.2. FoxO3a limits T cell numbers in the spleen but not in the bone marrow

To further investigate the impact of FoxO3a on specific immune cell subsets, flow cytometry was used to analyze lymphoid cells in the spleens of WT and FoxO3a-deficient mice. Spleen suspensions were stained with fluorophore-conjugated antibodies against the various lymphoid markers listed in Figure 4B. Cells were immediately acquired on a flow cytometer, and cell subsets were analyzed using the gating strategy indicated in Figure 4A. Briefly, a gate was drawn around cells that were not debris, and then doublets were excluded and cell subsets were gated. FoxO3a-deficient spleens had increased numbers of T cells ($TCR\beta^+$) compared to WT mice (Figure 5). There were no differences in B cell ($B220^+$) and NK cell ($DX5^+$) numbers between WT and FoxO3a-deficient mice. The same protocol was used for blood and bone marrow cells. In the blood, there were no significant differences in any of the cell types studied, although there was a trend towards a decrease in B cell numbers in FoxO3a-deficient mice (Figure 6). In the bone marrow, there were fewer B cells in the absence of FoxO3a (Figure 6). Nevertheless, NK cell and T cell numbers were similar in the two groups. Taken together, these results indicate that FoxO3a controls T cell numbers in the spleen, and is required for bone marrow B cell homeostasis.

A

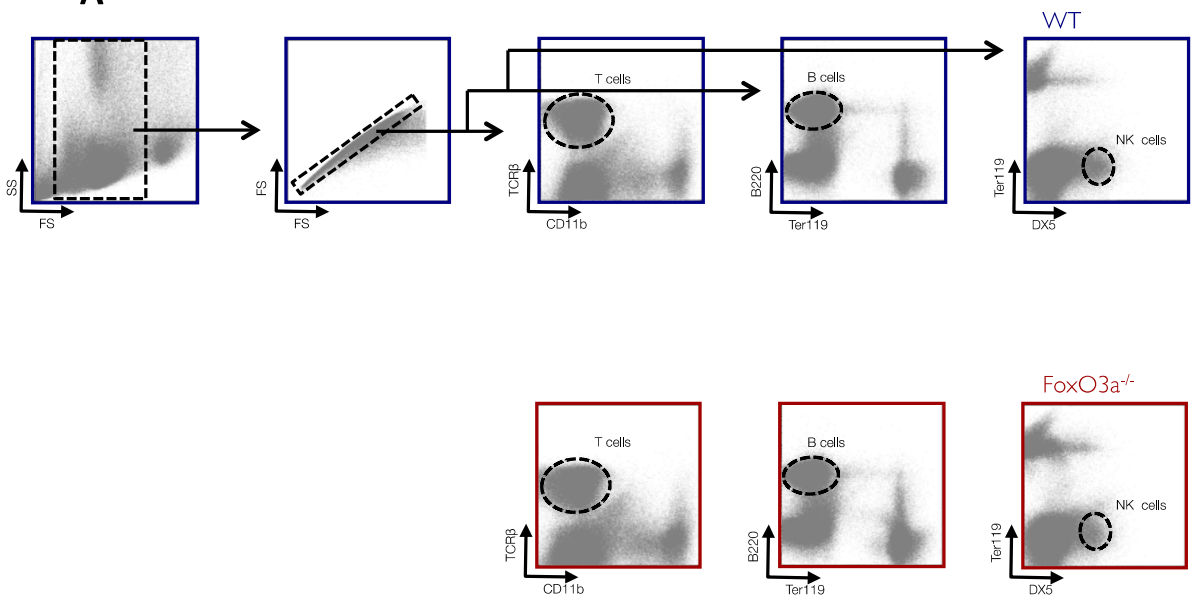

B

Cell type	Markers
T cells	TCRβ^{+}
B cells	B220^{+}
NK cells	DX5^{+}

Figure 4. Gating strategy employed to analyze lymphoid cells

Spleens were collected from naïve WT and FoxO3a-deficient mice and homogenized using frosted glass slides. Splenocytes were washed and resuspended in R8 medium, then counted and resuspended at 10^7 cells/ml. Cells were treated with FcBlock (anti-CD16/32) to prevent non-specific binding of antibodies and stained with various fluorophore-conjugated antibodies against lymphoid markers. Cells were acquired on a flow cytometer (CyAn ADP analyzer, Beckman Coulter).

(A) Representative gating strategy employed for lymphoid cells. Data were analyzed using Kaluza software (Version 1.2, Beckman Coulter). Data are representative of at least 3 independent experiments.
(B) List of markers used to identify lymphoid cell types.

Spleen

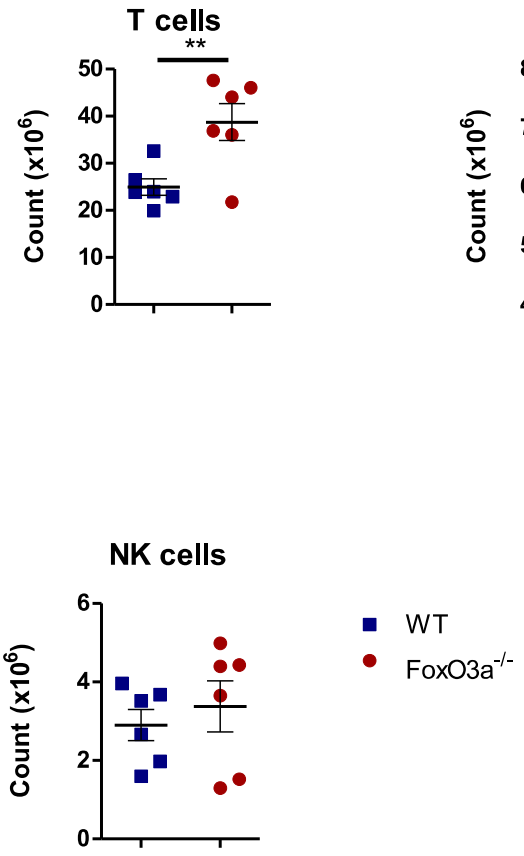
T cells
**
Count (x10^6)
50
40
30
20
10
0
B cells
Count (x10^6)
80
70
60
50
40
NK cells
Count (x10^6)
6
4
2
0
WT
FoxO3a-/-

Figure 5. FoxO3a controls T cell numbers in the spleen

Spleen cells were obtained from naïve WT and FoxO3a-deficient mice as mentioned above. Cells were stained for flow cytometry, acquired on a flow cytometer and data were analyzed using Kaluza software (Version 1.2, Beckman Coulter) as mentioned above.

Graphs display total numbers of the various lymphoid cell types indicated in graph titles. Data are pooled from at least 3 independent experiments, and presented as mean ± SEM. Statistical significance was calculated by unpaired two-tailed Student's t-test: $^{**}p<0.001$.

Blood

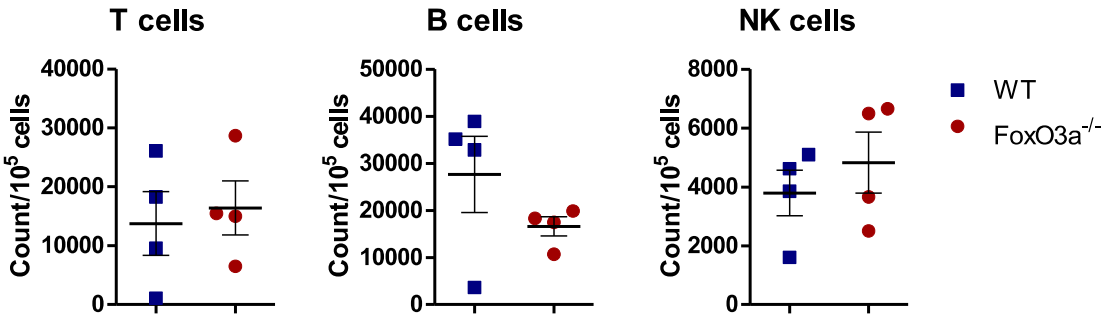

Bone marrow

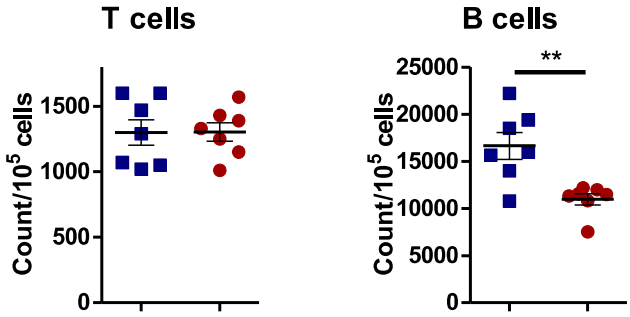

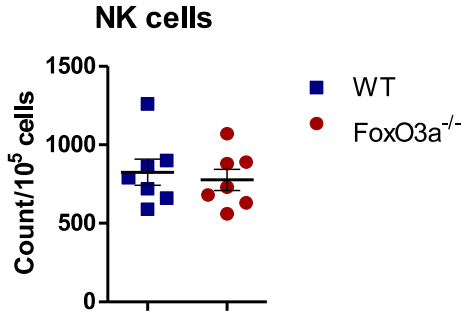

Figure 6. FoxO3a signaling does not impact T cell numbers in the bone marrow and blood

Blood was obtained by saphenous bleed and hind leg bones (hip bone, femur, and tibia) were extracted from naïve WT and FoxO3a-deficient mice. Bones were flushed with R8 medium to extract bone marrow cells. Blood and bone marrow cells were stained for flow cytometry, acquired on a flow cytometer and data were analyzed using Kaluza software (Version 1.2, Beckman Coulter) as mentioned above.

Graphs display counts/10^5 cells of the various lymphoid cell types indicated in graph titles. Data are pooled from at least 3 independent experiments, and presented as mean ± SEM. Statistical significance was calculated by unpaired two-tailed Student's t-test: **$p<0.001$.

3.1.3. FoxO3a signaling limits myeloid cell numbers in the spleen and blood but not in the bone marrow

Myeloid cell numbers in the spleen and blood of WT and FoxO3a-deficient mice were also analyzed using flow cytometry. The same protocol used for lymphoid cells was employed, only here, myeloid cell markers were used (Figure 7B).

Figure 7A describes the gating strategy employed in this case. In FoxO3a-deficient spleens compared with WT spleens, there was a significant increase in the counts of all myeloid cell subsets studied, namely dendritic cells ($CD11c^{+}$), neutrophils ($CD11b^{+}$ $Ly6G^{high}$ $Ly6C^{-/int}$), monocytes ($CD11b^{+}$ $Ly6G^{-/int}$ $Ly6C^{high}$) and macrophages ($CD11b^{+}$ $Ly6G^{-/int}$ $Ly6C^{low/int}$ $F4/80^{+}$) (Figure 8). The same trend was observed for blood dendritic cells and neutrophils. Although the difference was not significant, there was also an increase in FoxO3a-deficient monocyte counts. These results indicate that FoxO3a signaling thus contributes to homeostasis of myeloid cell numbers in spleen and blood, and in the absence of this transcription factor, the numbers of myeloid cells in these tissues increase.

The bone marrow is known to be the main site of generation of immune cells (Zhu and Emerson, 2002). I hypothesized that the increase in spleen and blood myeloid cells in the absence of FoxO3a could be due to an increase in the production of these cells in the bone marrow. To address this possibility, myeloid cell subsets in the bone marrow of WT and FoxO3a-deficient mice were compared by flow cytometry.

A

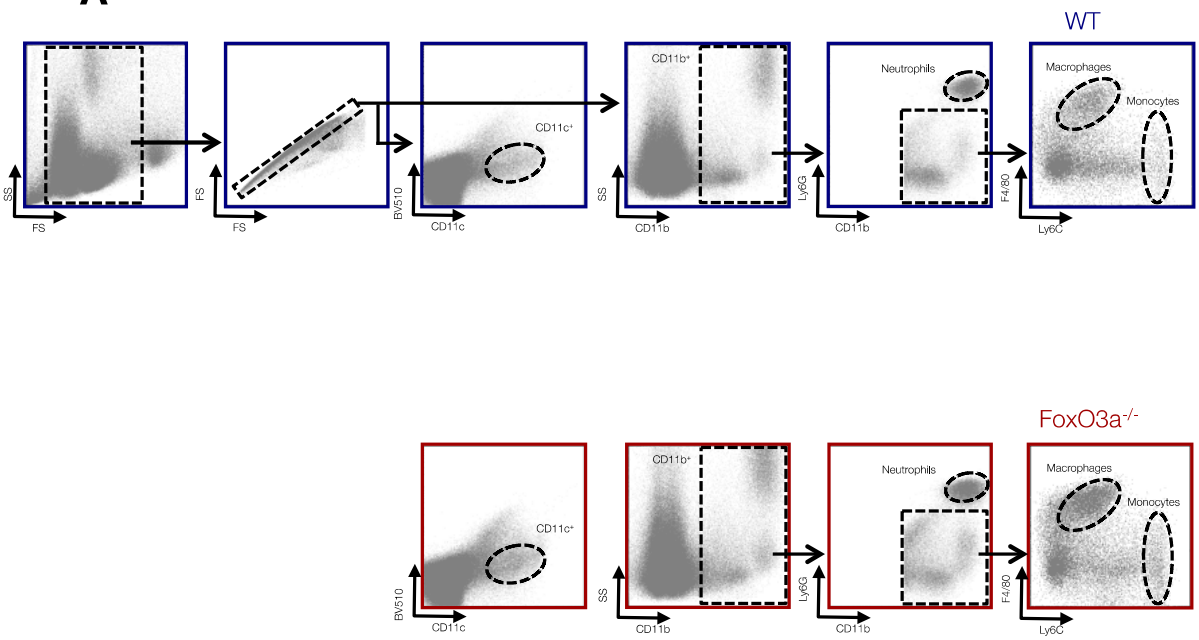

B

Cell type	Markers
Neutrophils	$CD11b^{+}$ $Ly6G^{high}$ $Ly6C^{-/int}$
Monocytes	$CD11b^{+}$ $Ly6G^{-/int}$ $Ly6C^{high}$
Macrophages	$CD11b^{+}$ $Ly6G^{-/int}$ $Ly6C^{low/int}$ $F4/80^{+}$

Figure 7. Gating strategy employed to analyze myeloid cells

Spleens were collected from naïve WT and FoxO3a-deficient mice and homogenized using frosted glass slides. Splenocytes were washed and resuspended in R8 medium, then counted and resuspended at 10^7 cells/ml. Cells were treated with FcBlock (anti-CD16/32) to prevent non-specific binding of antibodies and stained with various fluorophore-conjugated antibodies against myeloid markers. Cells were acquired on a flow cytometer (CyAn ADP analyzer, Beckman Coulter).

(A) Representative gating strategy employed for myeloid cells. Data were analyzed using Kaluza software (Version 1.2, Beckman Coulter). Data are representative of at least 3 independent experiments.

(B) List of markers used to identify myeloid cell types.

Spleen

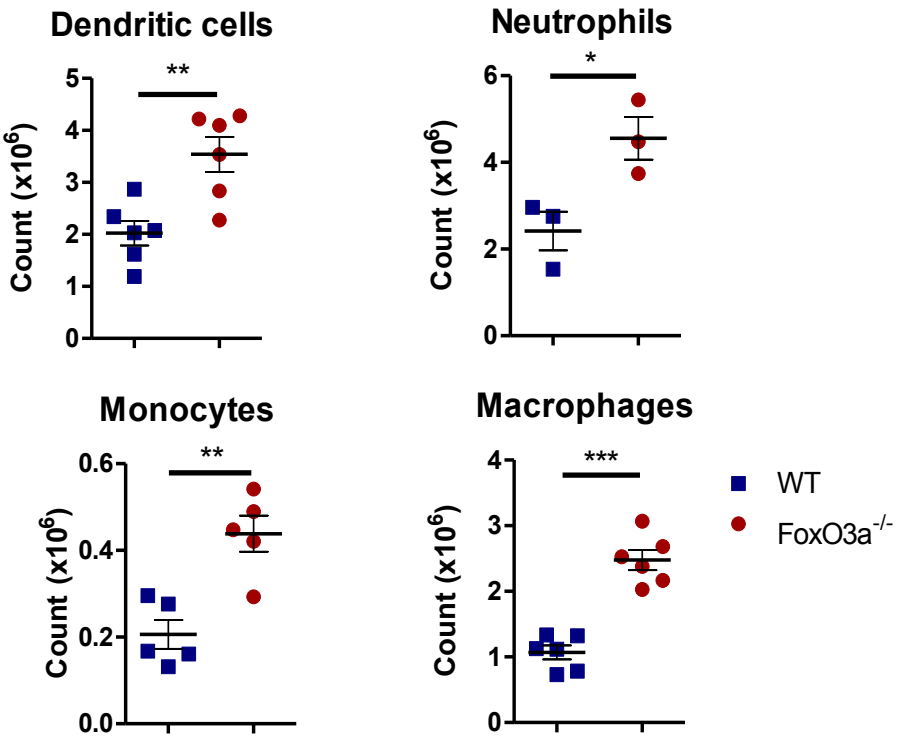

Blood

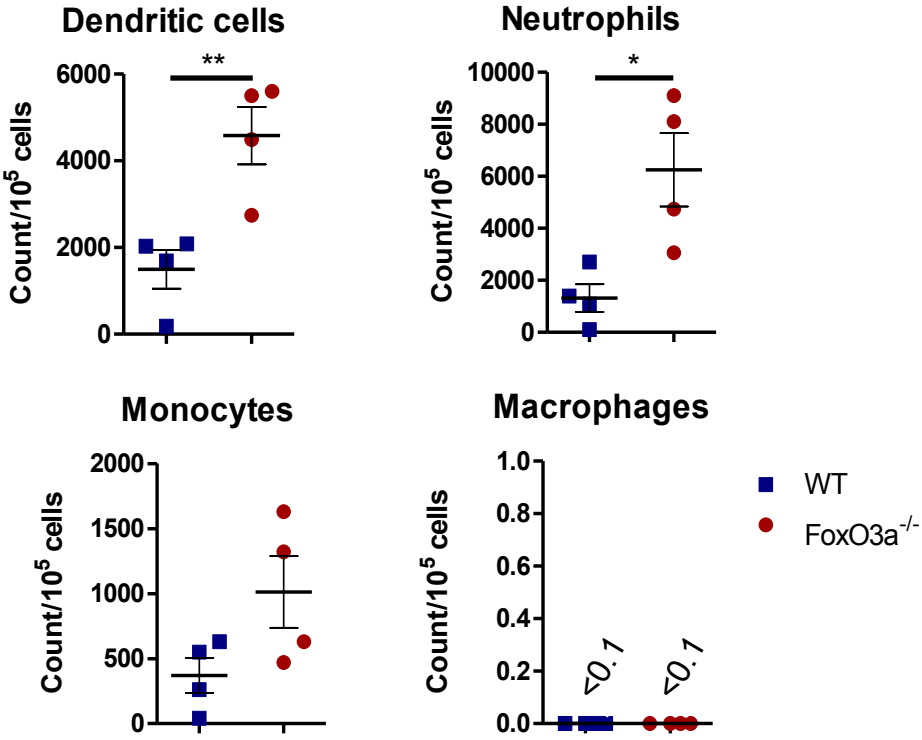

Figure 8. FoxO3a signaling prevents abnormal expansion of myeloid cells in the spleen and blood

Spleen and blood cells were obtained from naïve WT and FoxO3a-deficient mice as mentioned above. Cells were stained for flow cytometry, acquired on a flow cytometer and data were analyzed using Kaluza software (Version 1.2, Beckman Coulter) as mentioned above.

Graphs display the total numbers in the spleen and counts/10^5 cells in the blood of the myeloid cell types indicated in graph titles. Data are pooled from at least 3 independent experiments, and presented as mean ± SEM. Statistical significance was calculated by unpaired two-tailed Student's t-test: *$p<0.05$, **$p<0.001$, ***$p<0.0001$.

Bone Marrow

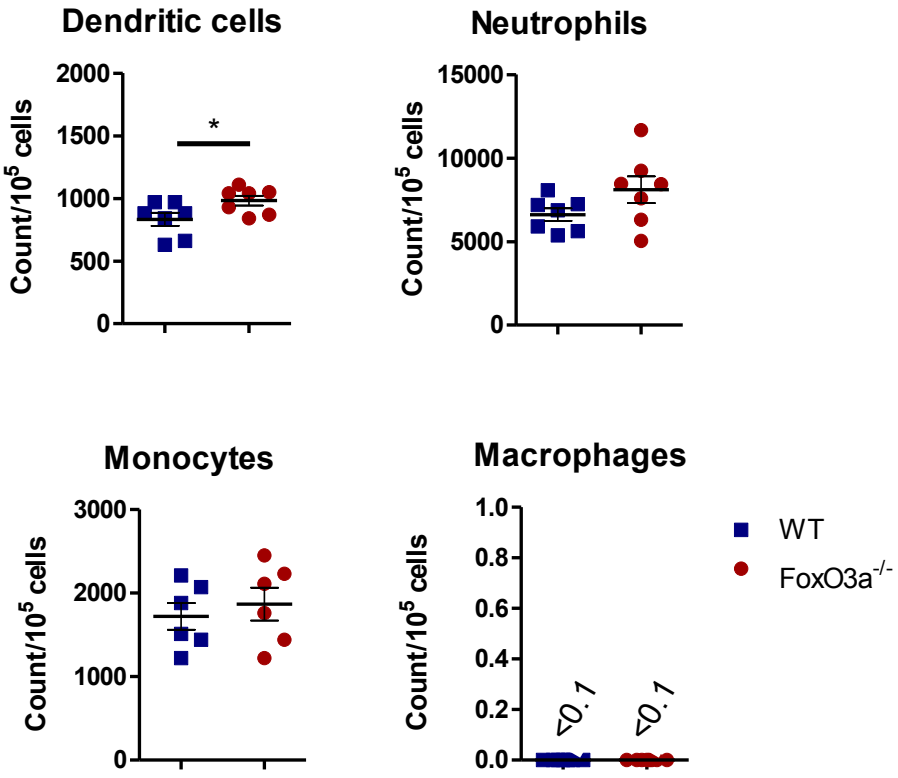
Dendritic cells
Count/10^5 cells
2000
1500
1000
500
0
*
Neutrophils
Count/10^5 cells
15000
10000
5000
0
Monocytes
Count/10^5 cells
3000
2000
1000
0
Macrophages
Count/10^5 cells
1.0
0.8
0.6
0.4
0.2
0.0
<0.1
<0.1
WT
FoxO3a-/-

Figure 9. FoxO3a does not regulate myeloid cell numbers in the bone marrow

Bone marrow cells were obtained from naïve WT and FoxO3a-deficient mice as mentioned above. Cells were stained for flow cytometry, acquired on a flow cytometer and data were analyzed using Kaluza software (Version 1.2, Beckman Coulter) as mentioned above.

Graphs display the counts/10^5 cells of the myeloid cell types indicated in graph titles. Data are pooled from at least 3 independent experiments, and presented as mean ± SEM. Statistical significance was calculated by unpaired two-tailed Student's t-test: *$p<0.05$.

A subtle but statistically significant increase was observed in dendritic cell numbers in the bone marrow of FoxO3a-deficient animals (Figure 9). Despite the high numbers in the spleen and blood of FoxO3a-deficient mice, there were no differences in bone marrow neutrophil and monocyte counts between the two groups. Collectively, these results demonstrate that loss of FoxO3a expression had no impact on bone marrow myeloid cell numbers, except for dendritic cells.

3.1.4. Loss of FoxO3a has no impact on bone marrow myeloid progenitor numbers

I wanted to further investigate why there was an increase in spleen and blood myeloid cell counts in the absence of FoxO3a, but no difference in cell numbers in the bone marrow of these mice. There could be more cells produced in the bone marrow of FoxO3a-deficient mice associated with more egress of these cells. This would explain why no differences were observed in bone marrow myeloid numbers. Myeloid cells mainly originate from differentiated bone marrow progenitors that arise from hematopoietic stem cells (HSCs) (Figure 10) (Zhu and Emerson, 2002). Thus, the numbers of HSCs in the bone marrow of WT and FoxO3a-deficient mice were assessed by flow cytometry, using the markers cited in Figure 11B and the gating strategy described in Figure 11A. There was no impact of loss of FoxO3a on the numbers of HSCs (c-kit^{+} Lin^{-} CD34^{-} Sca-1^{+}) (Figure 12).

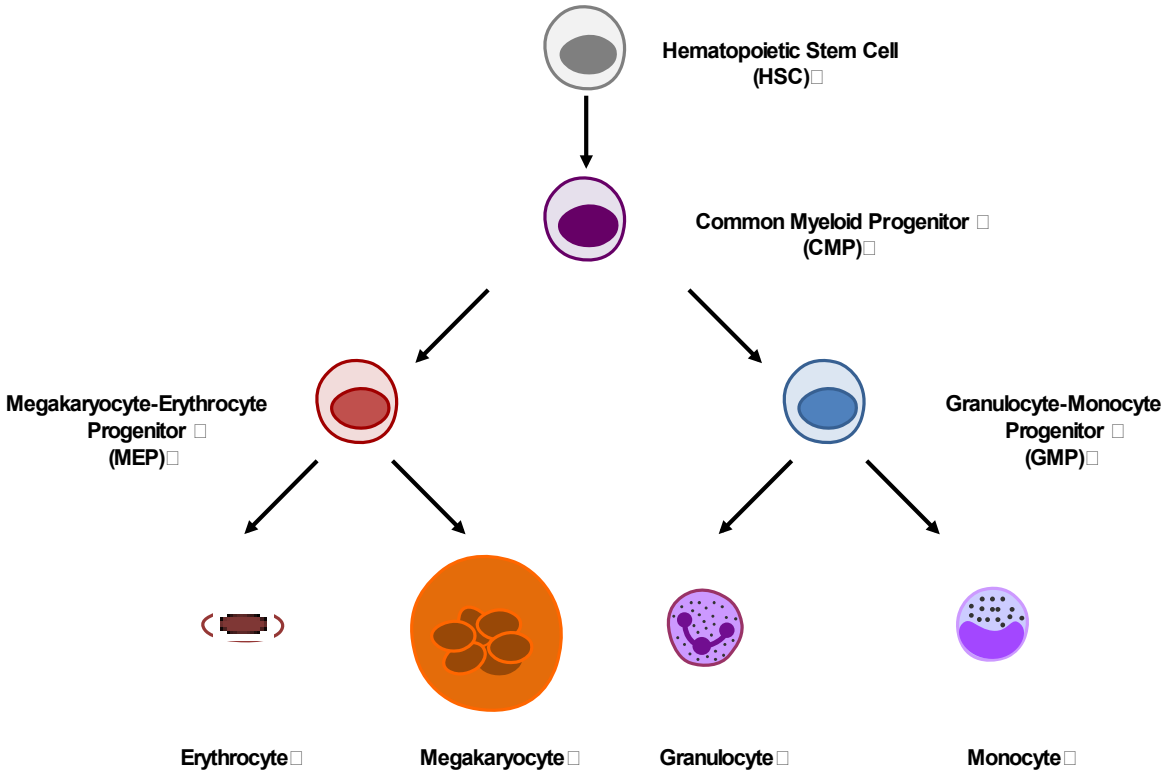
Hematopoietic Stem Cell
(HSC)
Common Myeloid Progenitor
(CMP)
Megakaryocyte-Erythrocyte
Progenitor
(MEP)
Granulocyte-Monocyte
Progenitor
(GMP)
Erythrocyte
Megakaryocyte
Granulocyte
Monocyte

Figure 10. Myeloid cells differentiate from progenitors in the bone marrow

Myeloid cells are produced in the bone marrow from progenitors. Hematopoietic stem cells (HSCs) in the bone marrow give rise to all immune cells. HSCs differentiate into common myeloid progenitors (CMPs), which in turn differentiate into granulocyte-monocyte progenitors (GMPs) and megakaryocyte-erythrocyte progenitors (MEPs). GMPs give rise to granulocytes (neutrophils, eosinophils, basophils, mast cells) and to monocytes, while MEPs give rise to erythrocytes (RBCs) and to megakaryocytes.

A

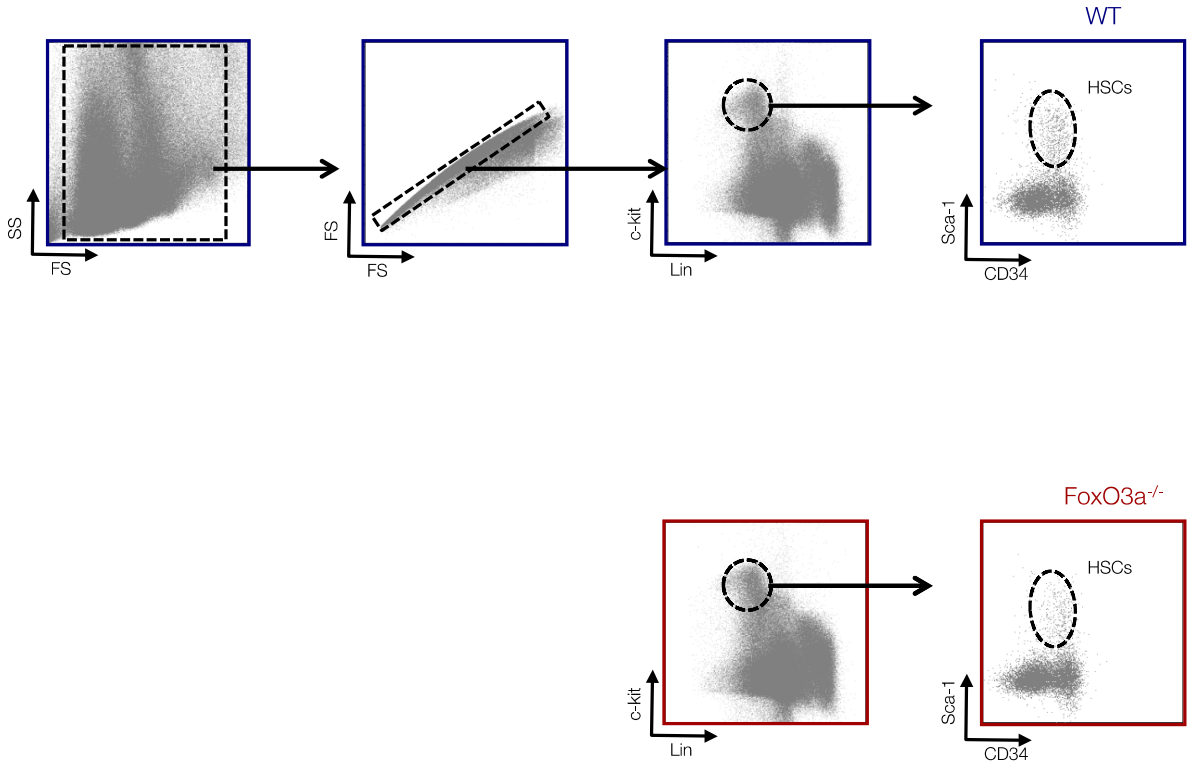

B

Cell type	Markers
Hematopoietic Stem Cells (HSCs)	c-kit^{+} Lin^{-} CD34^{-} Sca-1^{+}

Figure 11. Gating strategy employed to analyze hematopoietic stem cells (HSCs)

Bone marrow cells were obtained as mentioned above, from naïve WT and FoxO3a-deficient mice. Cells were treated with FcBlock (anti CD16/32) to prevent non-specific binding of antibodies and stained with fluorophore-conjugated antibodies against HSC markers. Cells were acquired on a flow cytometer (CyAn ADP analyzer, Beckman Coulter).

(A) Representative gating strategy employed for HSCs. Data were analyzed using Kaluza software (Version 1.2, Beckman Coulter). Data are representative of at least 3 independent experiments.

(B) Markers used to identify HSCs. Lin cocktail contains antibodies against the following markers: CD11b, Ly6G, CD3, B220, Ter119.

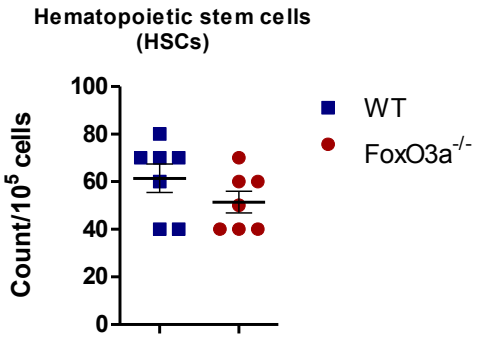
Hematopoietic stem cells
(HSCs)
Count/10^5 cells
100
80
60
40
20
0
WT
FoxO3a-/-

Figure 12. FoxO3a signaling does not affect HSC numbers in the bone marrow

Bone marrow cells were obtained from naïve WT and FoxO3a-deficient mice as mentioned above. Cells were stained for flow cytometry, acquired on a flow cytometer and data were analyzed using Kaluza software (Version 1.2, Beckman Coulter) as mentioned above.

Graph displays the numbers of HSCs/10^5 cells. Data are pooled from at least 3 independent experiments, and presented as mean ± SEM. Statistical significance was calculated by unpaired two-tailed Student's t-test.

HSCs differentiate into common myeloid progenitors (CMPs), which in turn differentiate into granulocyte monocyte-progenitors (GMPs) and megakaryocyte-erythrocyte progenitors (MEPs). Finally, GMPs give rise to granulocytes (neutrophils, eosinophils, basophils, mast cells) and to monocytes. MEPs give rise to erythrocytes (RBCs) and to megakaryocytes. Hence, the numbers of these three populations of progenitor cells were studied by flow cytometry, using the markers listed in Figure 13B and the gating strategy detailed in Figure 13A. There was no impact of the loss of FoxO3a signaling on the numbers of any of the progenitor cell subsets analyzed, namely CMPs (c-kit$^+$ Lin$^-$ IL7R$^-$ Sca-1$^-$ CD34$^+$ CD16/32$^-$), GMPs (c-kit$^+$ Lin$^-$ IL7R$^-$ Sca-1$^-$ CD34$^+$ CD16/32$^+$) and MEPs (c-kit$^+$ Lin$^-$ IL7R$^-$ Sca-1$^-$ CD34$^-$ CD16/32$^-$) (Figure 14).

The impact of FoxO3a on GMP numbers was further examined by using a colony-forming assay described in Figure 15. Briefly, bone marrow cells from WT and FoxO3a-deficient mice were plated in a semi-solid methylcellulose medium formulated for granulocyte and macrophage progenitor growth. After 12 days of incubation, GMP colonies (called CFU-GM) were counted using an inverted microscope. This technique also allowed us to identify specific colonies that would differentiate into granulocytes (CFU-G) or into macrophages (CFU-M). Colonies could be distinguished based on morphology (Figure 15). Upon enumeration of the colonies, no effect of FoxO3a was detected on the numbers of CFU-GM, CFU-G or CFU-M (Figure 16), providing further support to the previous data demonstrating that FoxO3a has no impact on bone marrow precursor numbers.

A

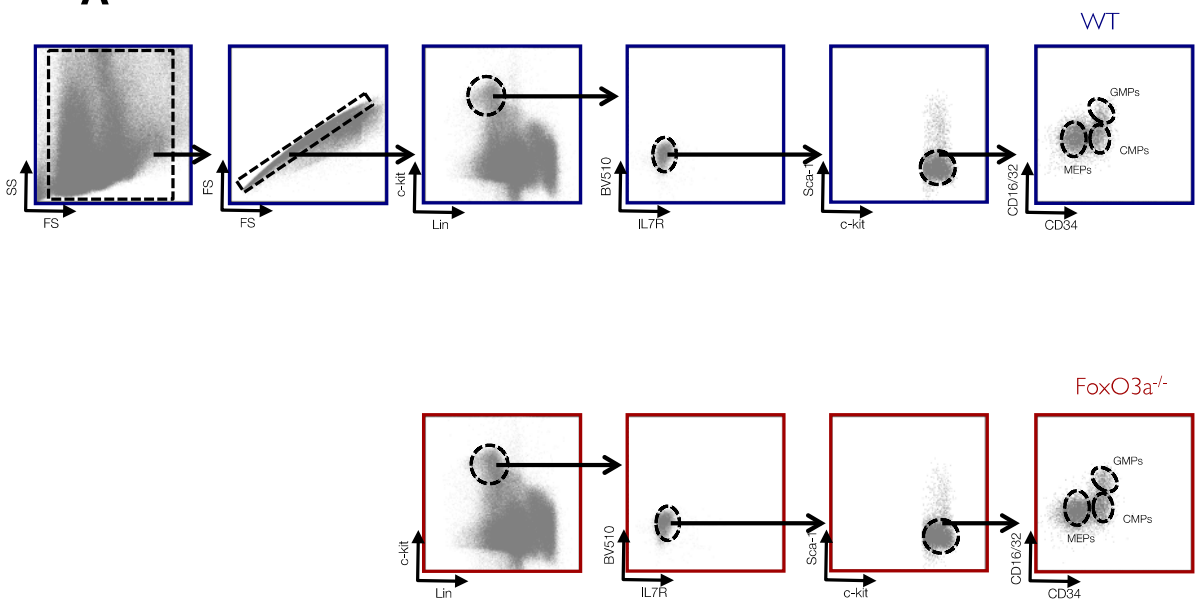

B

Cell type	Markers
Common Myeloid Progenitors (CMPs)	c-kit^{+} Lin^{-} IL7R^{-} Sca-1^{-} CD34^{+} CD16/32^{-}
Granulocyte-Monocyte Progenitors (GMPs)	c-kit^{+} Lin^{-} IL7R^{-} Sca-1^{-} CD34^{+} CD16/32^{+}
Megakaryocyte-Erythrocyte Progenitors (MEPs)	c-kit^{+} Lin^{-} IL7R^{-} Sca-1^{-} CD34^{-} CD16/32^{-}

Figure 13. Gating strategy employed to analyze myeloid progenitors

Bone marrow cells were obtained as mentioned above, from naïve WT and FoxO3a-deficient mice. Cells were stained with various fluorophore-conjugated antibodies against myeloid progenitor markers and acquired on a flow cytometer (CyAn ADP analyzer, Beckman Coulter).

(A) Representative gating strategy employed for myeloid progenitors. Data were analyzed using Kaluza software (Version 1.2, Beckman Coulter). Data are representative of at least 3 independent experiments.

(B) Markers used to identify myeloid progenitors. Lin cocktail contains antibodies against the following markers: CD11b, Ly6G, CD3, B220, Ter119.

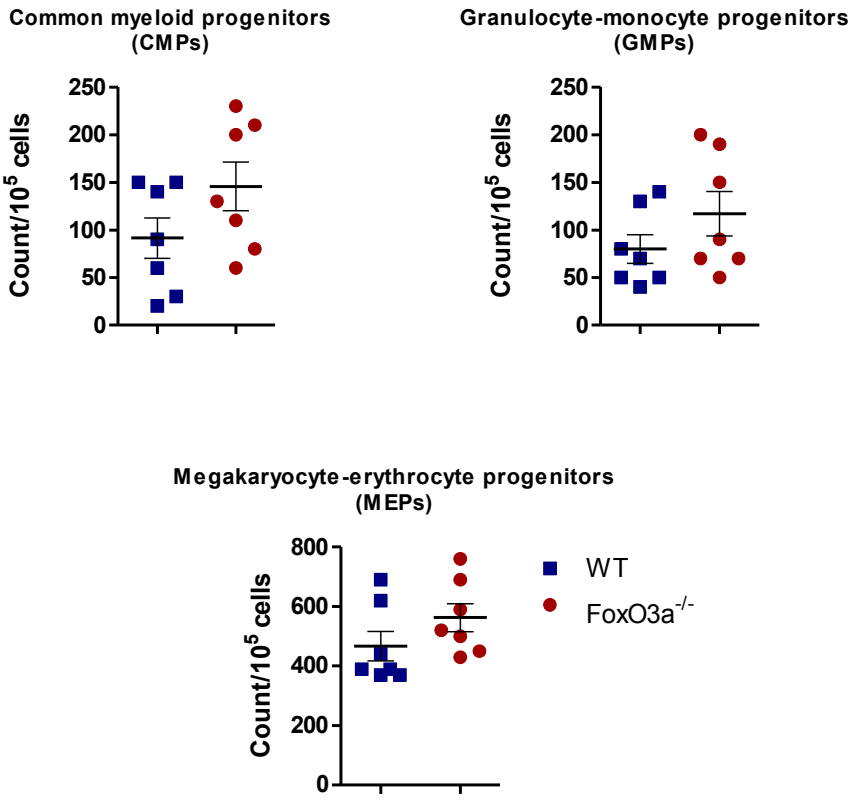
Common myeloid progenitors
(CMPs)
Count/10^5 cells
250
200
150
100
50
0
Granulocyte-monocyte progenitors
(GMPs)
Count/10^5 cells
250
200
150
100
50
0
Megakaryocyte-erythrocyte progenitors
(MEPs)
Count/10^5 cells
800
600
400
200
0
WT
FoxO3a-/-

Figure 14. FoxO3a does not impact myeloid progenitor numbers in the bone marrow

Bone marrow cells were obtained from naïve WT and FoxO3a-deficient mice as mentioned above. Cells were stained for flow cytometry, acquired on a flow cytometer and data were analyzed using Kaluza software (Version 1.2, Beckman Coulter) as mentioned above.

Graph displays the numbers of myeloid progenitors/10^5 cells. Cell types are indicated in graph titles. Data are pooled from at least 3 independent experiments, and presented as mean ± SEM. Statistical significance was calculated by unpaired two-tailed Student's t-test.

Methocult M3534
(for growth of myeloid precursors)

rm SCF
rm IL-3
rh IL-6
rh insulin
human transferrin (iron-saturated)

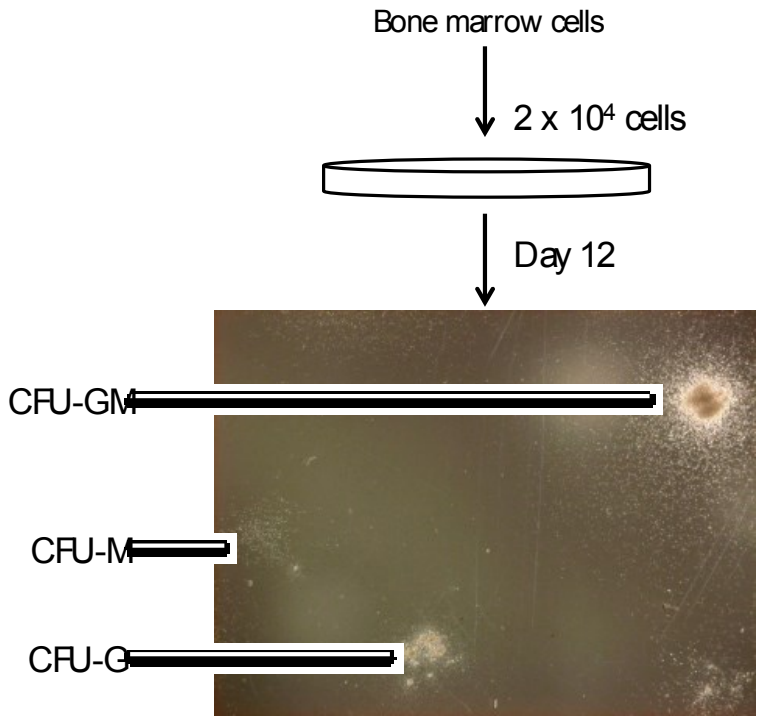

Figure 15. Myeloid progenitor CFU assay protocol

Bone marrow cells were obtained from naïve WT and FoxO3a-deficient mice as described above, and were plated in a semi-solid methylcellulose medium formulated for granulocyte and macrophage progenitor growth. Cells were incubated for 12 days in a CO_2 incubator at 37°C, then GMP colonies (called CFU-GM), granulocyte progenitor colonies (CFU-G) and macrophage progenitor colonies (CFU-M) were counted using an inverted microscope. Colonies could be distinguished based on morphology as indicated on the photograph.

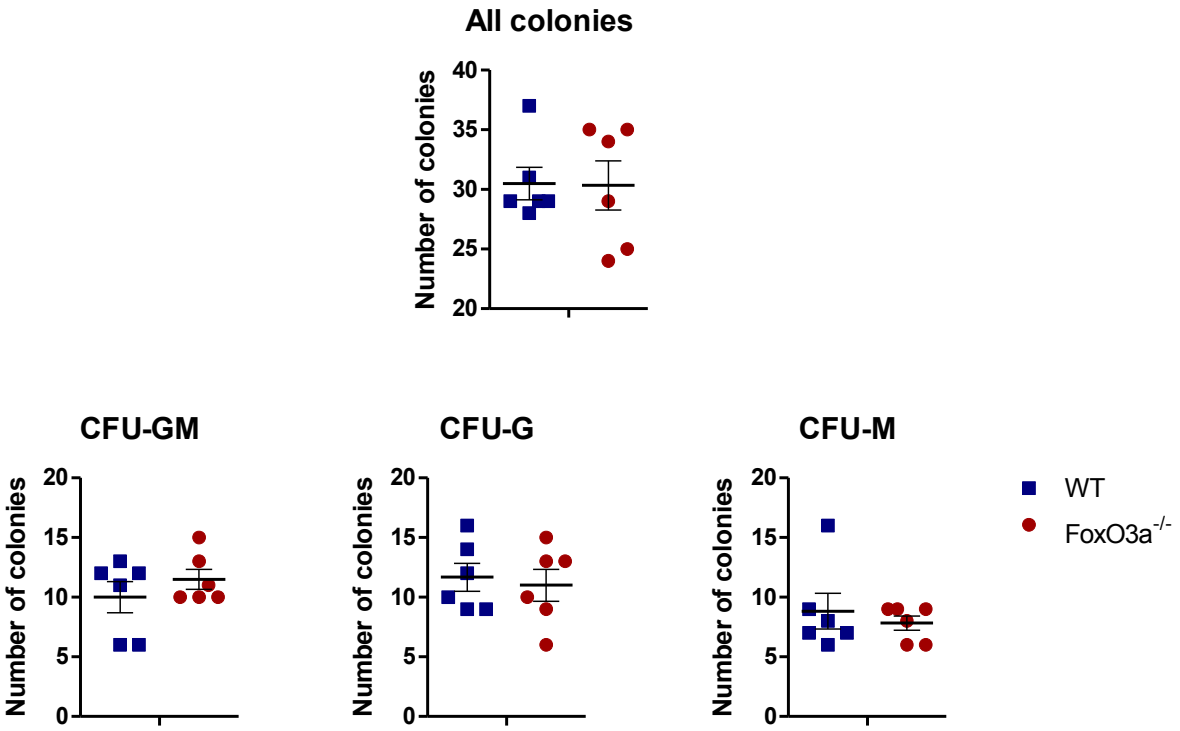
All colonies
Number of colonies
40
35
30
25
20
CFU-GM
CFU-G
CFU-M
Number of colonies
20
15
10
5
0
WT
FoxO3a-/-

Figure 16. FoxO3a signaling does not affect granulocyte or macrophage progenitor numbers in the bone marrow

Bone marrow cells were obtained from naïve WT and FoxO3a-deficient mice as mentioned above. A myeloid progenitor CFU assay was performed on cells as mentioned above and in the experimental methods.

Graphs display the numbers of colonies counted per myeloid progenitor cell type. Cell types are indicated in graph titles. Data are pooled from 3 independent experiments performed in duplicates, and presented as mean ± SEM. Statistical significance was calculated by unpaired two-tailed Student's t-test.

3.1.5. FoxO3a does not regulate immune cell numbers in the spleen and blood of mice infected with ST

After observing increased numbers of immune cells in the spleen and blood of naïve FoxO3a-deficient mice, the next aim was to determine the impact of FoxO3a on immune cell numbers during ST infection, especially as FoxO3a-deficient mice were more susceptible to ST (Joseph et al., 2016). Thus, WT and FoxO3a-deficient mice were infected intravenously with 10^4 CFU of bacteria in 100 µl of PBS. OVA-expressing *Salmonella* (ST-OVA) were used in this case, as they inject OVA peptide into the cytosol of host cells, allowing a strong immune response (Tzelepis et al., 2012). Since splenic CFUs are similar between WT and FoxO3a-deficient mice at day 7 post-infection (Figure 17), total cell counts were determined at this time point. Spleen cellularity increased during infection in both sets of mice (Figure 18). Blood counts increased very subtly in WT mice but slightly decreased in FoxO3a-deficient mice. Bone marrow cell numbers decreased in both groups. In contrast to the previous observations with naïve mice, there were no differences in blood or spleen cell numbers between the two groups of infected mice. Furthermore, there was a significant decrease in bone marrow cellularity in the absence of FoxO3a compared with WT mice during infection (Figure 18).

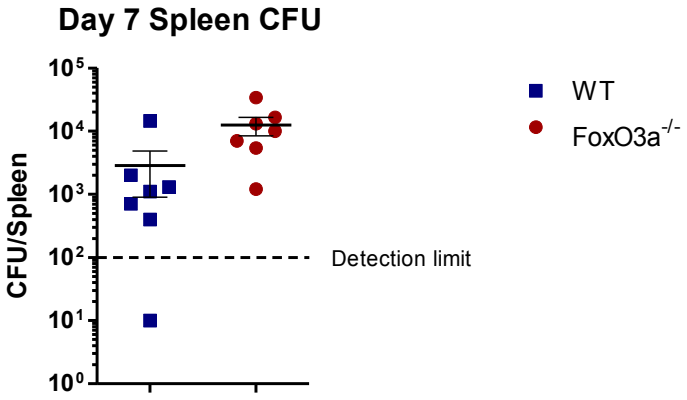
Day 7 Spleen CFU
CFU/Spleen
10^5
10^4
10^3
10^2
10^1
10^0
Detection limit
WT
FoxO3a-/-

Figure 17. Splenic CFUs are comparable in WT and FoxO3a-deficient mice 7 days after ST infection

WT and FoxO3a-deficient mice were infected with 10^4 CFU of ST-OVA as described in the experimental methods. Seven days after infection, spleens were collected and homogenized with frosted glass slides. Splenocytes were resuspended in 10 ml R8 medium and 100 µl aliquots of 10-fold serial dilutions were plated on BHI-Agar plates. Plates were incubated at 37°C overnight after which the colony-forming units (CFUs) were counted.

Graph displays CFU counts per spleen. Data are pooled from 2 independent experiments, each with 3-4 mice per group, and presented as mean ± SEM. Statistical significance was calculated by unpaired two-tailed Student's t-test.


Bone marrow
Count/bone (x10^6)
100
80
60
40
20
0
*
0
7
Time after infection (days)
Spleen
Count (x10^6)
400
300
200
100
0
***
0
7
Time after infection (days)
Blood
Count / 50uL (x10^5)
4
3
2
1
0
0
7
Time after infection (days)
WT
FoxO3a-/-

Figure 18. FoxO3a affects immune cell numbers in the bone marrow but not in the spleen and blood following ST infection

WT and FoxO3a-deficient mice were infected with 10^4 CFU of ST-OVA as described in the experimental methods. 7 days after infection, spleen, bone marrow, and blood cells were collected as mentioned above and live cells were counted with a hemocytometer using trypan blue.

Graphs show total cell counts, excluding red blood cells. Blood cell counts are indicated per 50 μl of blood collected. Bone marrow cell counts are indicated per bone flushed. Data are pooled from at least 4 mice per group, and presented as mean ± SEM. Statistical significance was calculated by unpaired two-tailed Student's t-test: *$p<0.05$, ***$p<0.0001$.

3.1.6. FoxO3a controls CMP and monocyte numbers in the bone marrow of ST-infected mice

I delved further into the impact of FoxO3a on specific immune cell populations in the bone marrow of ST-infected mice. After infection, the hind leg bones of infected mice were flushed and the isolated cells were stained for flow cytometry. First, precursor populations in the bone marrow were determined at 7 days post-infection with ST. HSC counts increased after infection in both sets of mice to a similar extent (Figure 19), which suggests that there was no effect of FoxO3a signaling on their numbers. The ST-induced increase in CMP numbers was significantly more marked in FoxO3a-deficient mice (Figure 19). Infection of WT mice with ST resulted in an increase in the GMP population and a reduction in MEP numbers in the bone marrow. In the FoxO3a-deficient mice, the change in numbers of these populations was the same as in the WT mice.

Subsequently, mature myeloid cell populations in the bone marrow were analyzed. Counts of all myeloid cells studied, namely dendritic cells, neutrophils, and monocytes, increased as a result of infection (Figure 20). There were no differences in bone marrow dendritic cell and neutrophil numbers between WT and FoxO3a-deficient mice after infection. However, bone marrow monocyte counts were significantly higher in the absence of FoxO3a (Figure 20). Collectively, these results reveal that FoxO3a controls CMP and monocyte expansion in the bone marrow during ST infection.

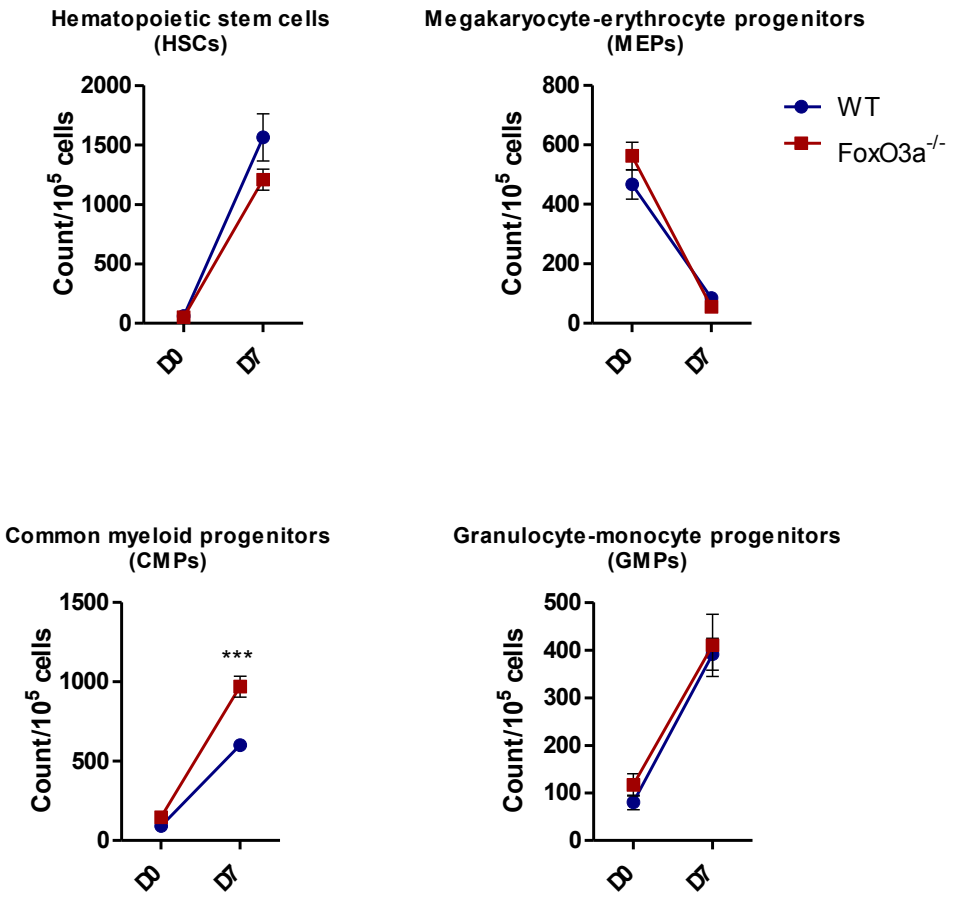
Hematopoietic stem cells
(HSCs)
Count/10^5 cells
2000
1500
1000
500
0
D0
D7
Megakaryocyte-erythrocyte progenitors
(MEPs)
800
600
400
200
WT
FoxO3a-/-
Common myeloid progenitors
(CMPs)
***
Granulocyte-monocyte progenitors
(GMPs)
100
300

Figure 19. FoxO3a signaling limits CMP but not GMP expansion in response to ST

WT and FoxO3a-deficient mice were infected with 10^4 CFU of ST-OVA as described in the experimental methods. Seven days after infection, bone marrow cells were obtained as mentioned above. Cells were stained for flow cytometry, acquired on a flow cytometer, and data were analyzed using Kaluza software (Version 1.2, Beckman Coulter) as mentioned above.

Graphs display the numbers of progenitors/10^5 cells. Cell types are indicated in graph titles. Data are pooled from at least 2 independent experiments with a total of 7 mice per group, and presented as mean ± SEM. Statistical significance was calculated by unpaired two-tailed Student's t-test: ***$p<0.0001$.

Bone Marrow

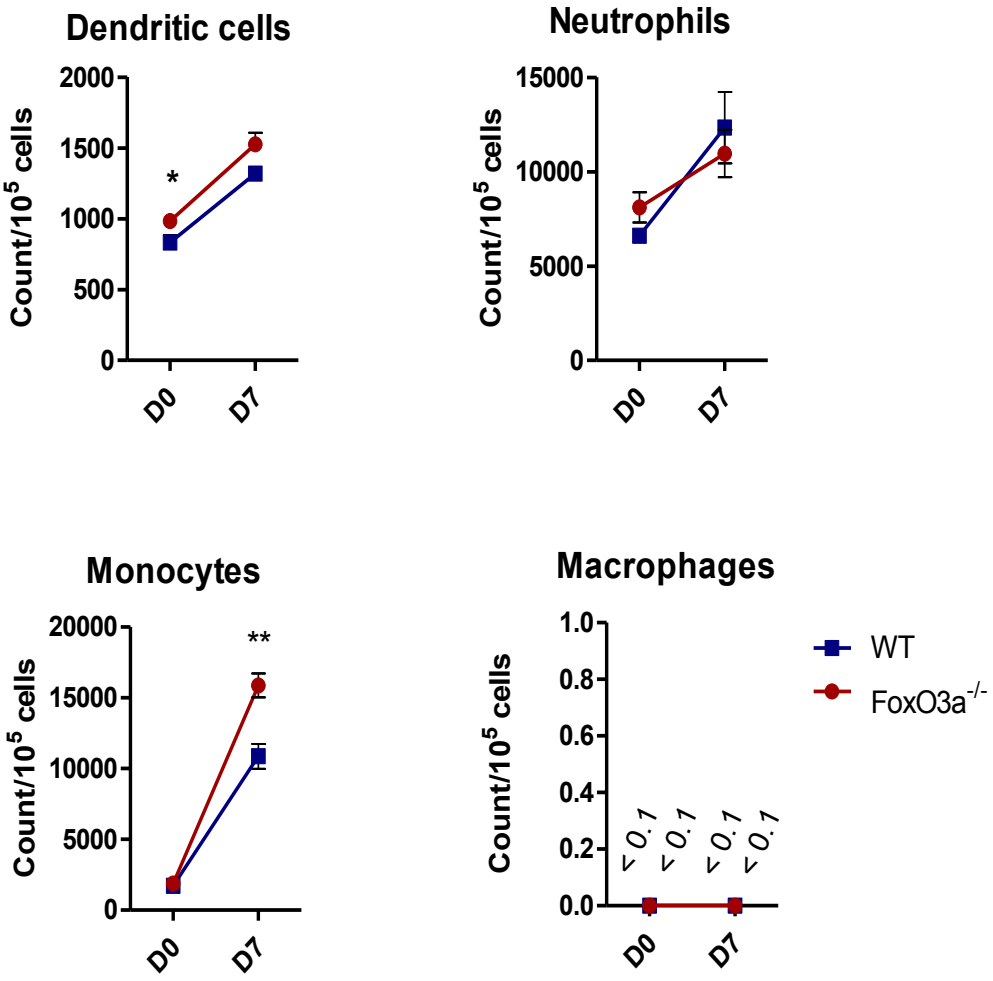
Dendritic cells
Count/10^5 cells
2000
1500
1000
500
0
*
D0
D7
Neutrophils
Count/10^5 cells
15000
10000
5000
0
D0
D7
Monocytes
Count/10^5 cells
20000
15000
10000
5000
0
**
D0
D7
Macrophages
Count/10^5 cells
1.0
0.8
0.6
0.4
0.2
0.0
< 0.1
< 0.1
< 0.1
< 0.1
D0
D7
WT
FoxO3a-/-

Figure 20. FoxO3a hinders the increase in monocyte numbers in the bone marrow in response to ST infection

WT and FoxO3a-deficient mice were infected with 10^4 CFU of ST-OVA as described in the experimental methods. Seven days after infection, bone marrow cells were obtained as mentioned above. Cells were stained for flow cytometry, acquired on a flow cytometer, and data were analyzed using Kaluza software (Version 1.2, Beckman Coulter) as mentioned above.

Graphs display the counts/10^5 cells of the myeloid cell types indicated in graph titles. Data are pooled from at least 2 independent experiments with a total of at least 6 mice per group, and presented as mean ± SEM. Statistical significance was calculated by unpaired two-tailed Student's t-test: *$p<0.05$, **$p<0.001$.

3.1.7. FoxO3a does not control myeloid cell numbers in the spleen and blood during ST infection

Having evaluated the impact of FoxO3a on bone marrow myeloid cells and observed that FoxO3a was important for preventing aberrant expansion of monocytes after infection, I next analyzed spleen and blood myeloid cell numbers. In the spleen, neutrophil numbers dropped after infection and the difference between WT and FoxO3a-deficient mice was no longer observable (Figure 21). Dendritic cells, monocytes, and macrophage counts all increased after infection in both sets of mice and in contrast with naïve mice, the effect of FoxO3a on their numbers was no longer present. In the blood, dendritic cell and neutrophil counts were reduced after infection in both groups of mice and unlike naïve mice, infected mice did not display any difference between WT and FoxO3a-deficient groups (Figure 21). Monocyte numbers increased in WT mice and decreased in FoxO3a-deficient mice after infection. There were no differences in monocyte counts between the two groups. These results demonstrate that FoxO3a signaling maintains spleen and blood myeloid cell numbers in naïve mice but does not affect changes in cell numbers associated with ST infection.

3.1.8. FoxO3a signaling limits T cell numbers in the bone marrow but not in the spleen and blood of ST-infected mice

Next, the effect of FoxO3a on lymphoid cell numbers during infection with ST was assessed. In the bone marrow, B cell numbers decreased after infection in both groups but compared with uninfected mice, there was no longer a difference between WT and FoxO3a-deficient mice after infection (Figure 22). The numbers of bone marrow NK cells did not change in WT mice after infection but were slightly increased in FoxO3a-deficient mice (Figure 22). There was no significant difference in NK cell numbers between the two groups.

T cell counts in the bone marrow increased in both groups after ST infection, although the increase was significantly higher in FoxO3a-deficient mice (Figure 22).

In the spleen, T cell numbers decreased as a result of infection but the differences observed before infection between the two groups were not present after infection (Figure 23). Splenic B cell and NK cell counts also decreased during infection but there were no differences between the two sets of mice. In the blood, T cell and B cell counts decreased upon infection and I did not note any difference between the two groups (Figure 23). Collectively, these results highlight the fact that even though there are differences in the bone marrow between infected WT and FoxO3a-deficient mice, FoxO3a has no impact on lymphoid cell numbers in the blood and in the spleen.

Spleen

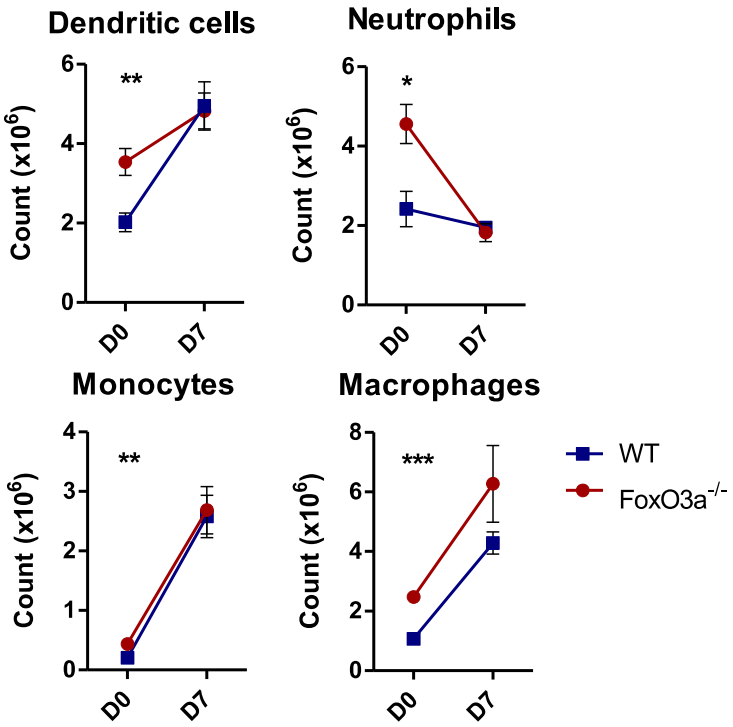

Blood

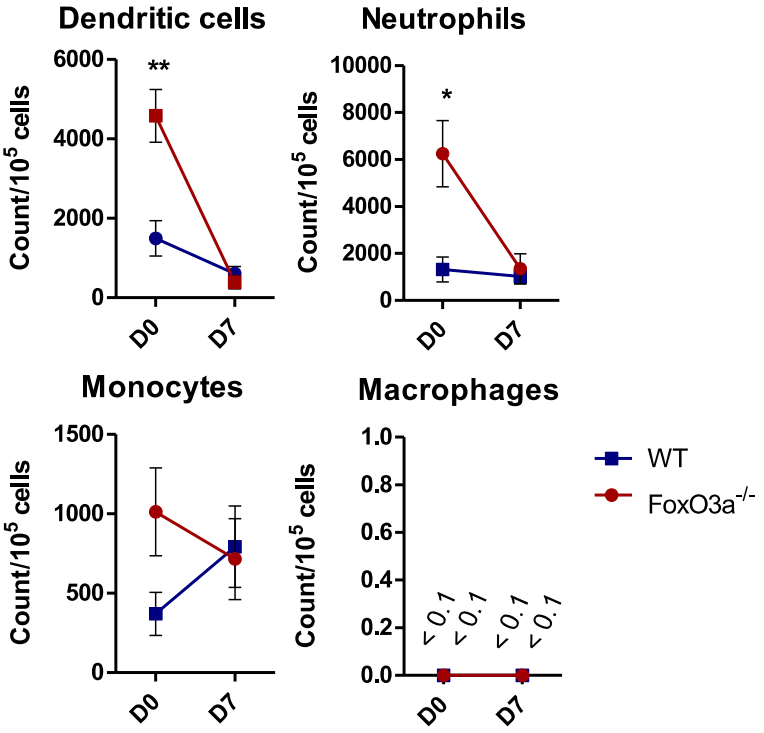

Figure 21. FoxO3a does not control myeloid cell numbers in the spleen and blood upon ST infection

WT and FoxO3a-deficient mice were infected with 10^4 CFU of ST-OVA as described in the experimental methods. Seven days after infection, spleen and blood cells were obtained as mentioned above. Cells were stained for flow cytometry, acquired on a flow cytometer, and data were analyzed using Kaluza software (Version 1.2, Beckman Coulter) as mentioned above.

Graphs display the total numbers in the spleen and counts/10^5 cells in the blood of the myeloid cell types indicated in graph titles. Data are pooled from at least 2 independent experiments with a total of at least 3 mice per group, and presented as mean ± SEM. Statistical significance was calculated by unpaired two-tailed Student's t-test: *$p<0.05$, **$p<0.001$, ***$p<0.0001$.

Bone marrow

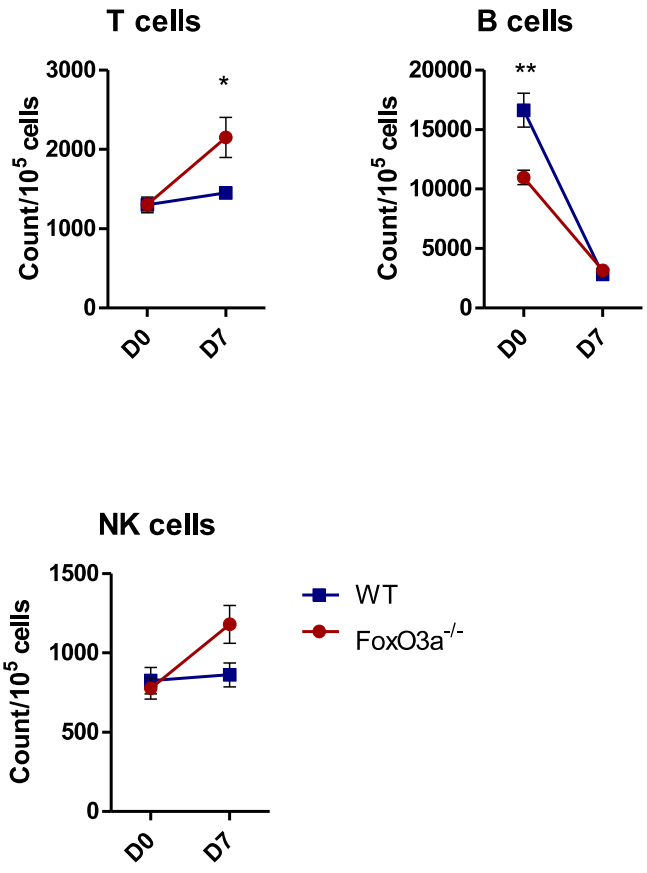
T cells
Count/10^5 cells
3000
2000
1000
0
*
D0
D7
B cells
Count/10^5 cells
20000
15000
10000
5000
0
**
D0
D7
NK cells
Count/10^5 cells
1500
1000
500
0
D0
D7
WT
FoxO3a-/-

Figure 22. FoxO3a limits the increase in T cell numbers in response to ST in the bone marrow

WT and FoxO3a-deficient mice were infected with 10^4 CFU of ST-OVA as described in the experimental methods. Seven days after infection, bone marrow cells were obtained as mentioned above. Cells were stained for flow cytometry, acquired on a flow cytometer, and data were analyzed using Kaluza software (Version 1.2, Beckman Coulter) as mentioned above.

Graphs display the counts/10^5 cells of the lymphoid cell types indicated in graph titles. Data are pooled from at least 2 independent experiments with a total of 7 mice per group, and presented as mean ± SEM. Statistical significance was calculated by unpaired two-tailed Student's t-test: *$p<0.05$, **$p<0.001$.

Spleen

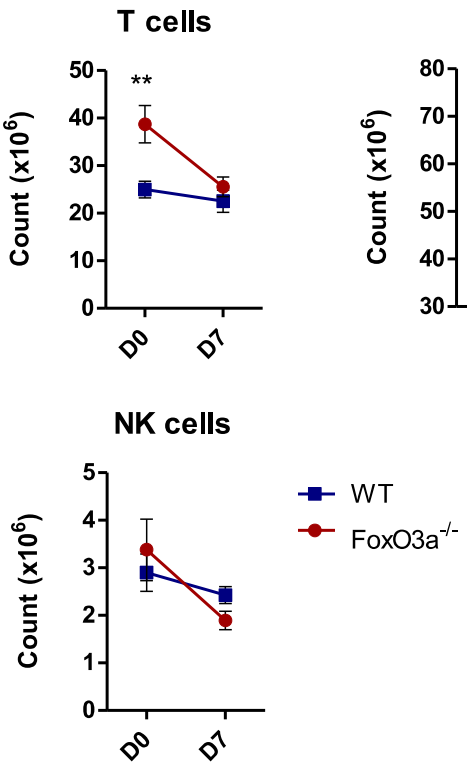

Blood

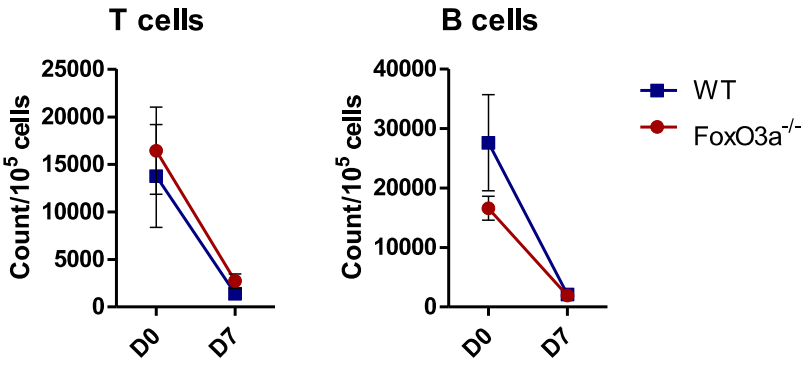

Figure 23. FoxO3a signaling does not affect lymphoid cell numbers in the spleen and blood upon ST infection

WT and FoxO3a-deficient mice were infected with 10^4 CFU of ST-OVA as described in the experimental methods. Seven days after infection, spleen and blood cells were obtained as mentioned above. Cells were stained for flow cytometry, acquired on a flow cytometer, and data were analyzed using Kaluza software (Version 1.2, Beckman Coulter) as mentioned above.

Graphs display the total numbers in the spleen and counts/10^5 cells in the blood, of the lymphoid cell types indicated in graph titles. Data are pooled from at least 2 independent experiments with a total of at least 4 mice per group, and presented as mean ± SEM. Statistical significance was calculated by unpaired two-tailed Student's t-test: **$p<0.001$.

3.2. FoxO3a signaling promotes the inflammatory response in ST-infected macrophages

3.2.1. FoxO3a signaling does not impact macrophage cell death

Because of the importance of macrophages during ST infection, the second aim of this thesis was to examine the impact of FoxO3a on macrophage function during ST infection. Inflammatory cell death following infection has been previously shown to be a protective mechanism to fight intracellular pathogens (Broz and Monack, 2011). Thus, the impact of FoxO3a on macrophage cell death after various stimuli was evaluated. Briefly, WT and FoxO3a-deficient mice were euthanized, hind legs were collected and bones were flushed to collect the bone marrow. Bone marrow cells were then counted and plated in petri dishes coated with recombinant M-CSF. M-CSF is a cytokine that differentiates myeloid precursors and monocytes into macrophages. Cells were then incubated for 12 days and in some cases 6 days at 37°C and 5% CO_2. The resulting bone marrow-derived macrophages (BMDMs) were harvested and plated for experiments. On both day 6 and 12 after incubation, there were more BMDMs from FoxO3a-deficient mice than WT mice (Figure 24). For the first cell death assay, macrophages were infected with ST for 24h, at a multiplicity of infection (MOI) of 100. At this MOI, cells died whereas lower MOIs did not kill the macrophages. After infection, a neutral red assay was performed on the cells to determine cell viability. Neutral red is a dye that is taken up by the lysosomes of live cells but not of dead cells. Cell survival was established by normalizing neutral red optical density (O.D.) of infected cells to that of control cells.

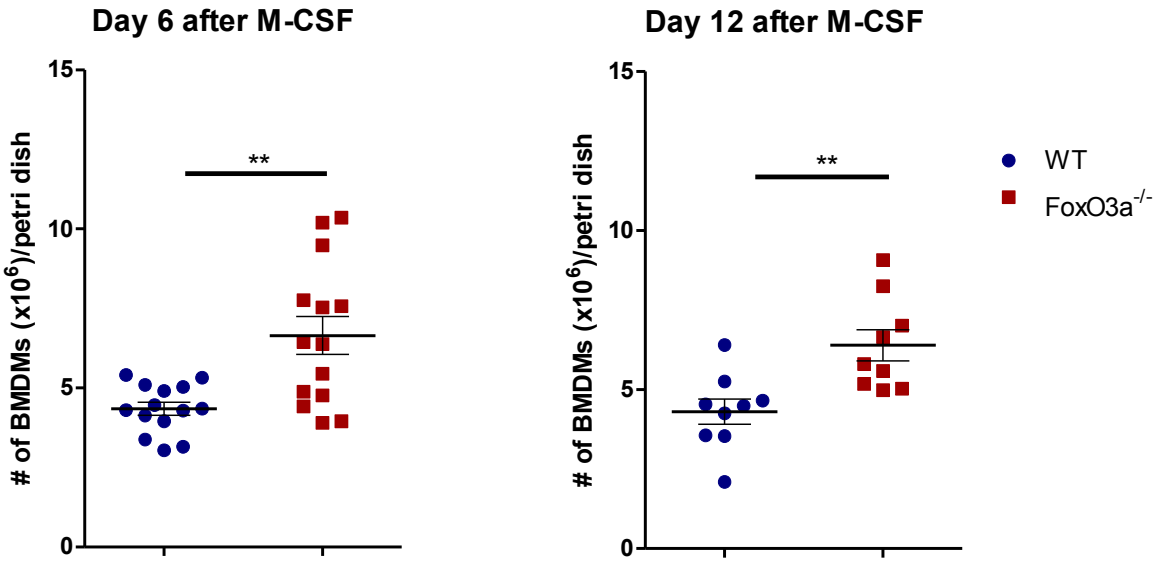
Day 6 after M-CSF
Day 12 after M-CSF
# of BMDMs (x10^6)/petri dish
15
10
5
0
**
WT
FoxO3a-/-

Figure 24. FoxO3a signaling controls bone marrow-derived macrophage numbers after M-CSF treatment

Bone marrow derived macrophages (BMDMs) were generated from WT and FoxO3a-deficient mice as described in the experimental methods. Live cells were counted with a hemocytometer, using trypan blue stain.
Graphs display the numbers of BMDMs harvested per petri dish. Data are pooled from at least 9 independent experiments and presented as mean ± SEM. Statistical significance was calculated by unpaired two-tailed Student's t-test: **$p<0.001$.

I did not note any difference in BMDM survival between WT and FoxO3a-deficient cells (Figure 25). The main form of cell death observed during ST infection of macrophages is called pyroptosis (Brennan and Cookson, 2000) and is an inflammatory form of cell death wherein cells are lysed, releasing their contents. The results obtained reveal that FoxO3a does not impact pyroptotic cell death.

The impact of the FoxO3a transcription factor on another form of cell death called necroptosis was also evaluated. Necroptosis can be induced by treating macrophages simultaneously with lipopolysaccharide (LPS) and zVAD (McComb, 2014). LPS is a portion of gram-negative bacteria that acts as a pro-inflammatory signal, and zVAD is a pan-caspase inhibitor. Inhibiting caspases while providing a pro-inflammatory stimulus induces necroptosis (McComb, 2014). Hence, macrophages were treated with LPS and zVAD for 24h. After treatment, cell viability was determined by MTT assay. This assay is based on the reduction of the dye 3-(4,5-dimethylthiazol-2-yl)-2,5-diphenyltetrazolium bromide into formazan crystals in live cells but not in dead cells. Cell survival was established by normalizing MTT optical density of infected cells to that of uninfected control cells. There were no differences in necroptotic cell death between WT and FoxO3a-deficient macrophages (Figure 26). Necroptosis can be inhibited by necrostatin-1 (nec-1) treatment (McComb, 2014). Thus, the cells were treated concomitantly with LPS, zVAD and nec-1 to verify that the cell death observed was indeed necroptosis. As expected, nec-1 treatment did rescue the BMDMs from death (Figure 26), thus confirming that necroptosis occurred upon LPS and zVAD treatment. There were still no differences between WT and FoxO3a-deficient macrophages.

The impact of FoxO3a on a third type of cell death induced upon endoplasmic reticulum (ER) stress was also studied. WT and FoxO3a-deficient macrophages were treated with brefeldin A for 24 hours before an MTT assay was performed on them to determine cell viability. Brefeldin A is an antibiotic that inhibits protein transport between the endoplasmic reticulum and the Golgi apparatus, leading to protein accumulation in the ER (Klausner et al., 1992). This causes ER stress, followed by cell death through apoptosis. There was no difference in ER-stress-induced cell death between WT and FoxO3a-deficient macrophages after brefeldin A treatment (Figure 27). ER stress can be inhibited by treating cells with salubrinal. Salubrinal is a small molecule that phosphorylates and prevents dephosphorylation of eukaryotic translation initiation factor 2 subunit alpha (eIF2α) (Boyce et al., 2005). eIF2α is a protein that, when phosphorylated, temporarily down-regulates global protein translation but up-regulates translation of stress-induced proteins (Celli and Tsolis, 2015). This leads to a reduction of ER-stress. Accordingly, co-treating macrophages with brefeldin A and salubrinal rescued them from death, but no differences could be noted between WT and FoxO3a-deficient cells in this case either. Together, these findings reveal that FoxO3a has no impact on macrophage cell death induced by various stimuli.

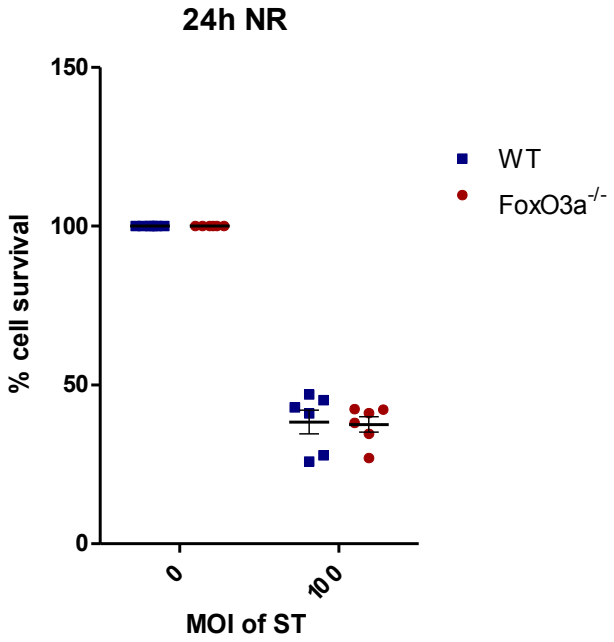
24h NR
150
100
50
0
% cell survival
0
100
MOI of ST
WT
FoxO3a-/-

Figure 25. FoxO3a signaling does not impact macrophage cell death upon ST infection

Bone marrow derived macrophages (BMDMs) were generated from WT and FoxO3a-deficient mice as described in the experimental methods. BMDMs were infected with ST at 100 MOI for 24 hours. Cell viability was then assessed by neutral red (NR) assay.

Graphs display % cell survival. NR optical densities (ODs) were normalized to the unstimulated control (i.e. cells with R8 medium only). Data are pooled from 2 independent experiments performed in triplicate and presented as mean ± SEM. Statistical significance was calculated by unpaired two-tailed Student's t-test.

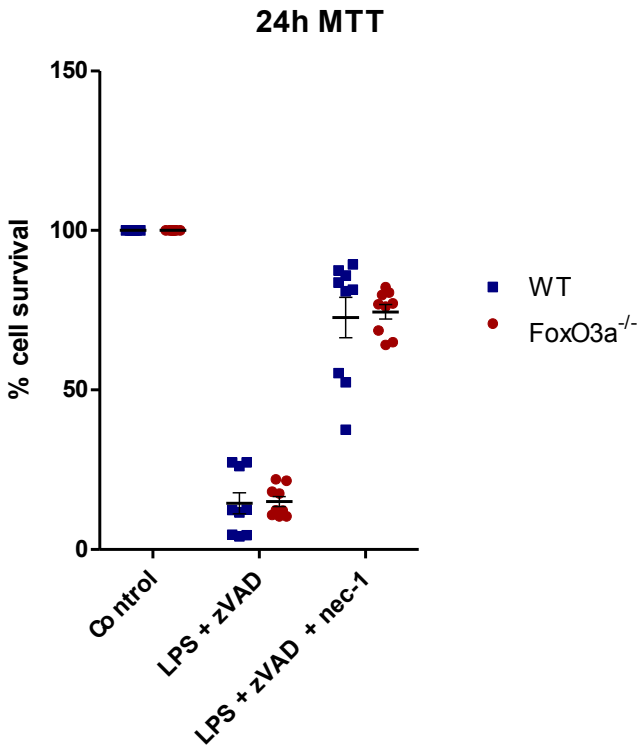
24h MTT
% cell survival
150
100
50
0
Co ntrol
LPS + zVAD
LPS + zVAD + nec-1
WT
FoxO3a-/-

Figure 26. FoxO3a signaling does not impact necroptotic cell death in macrophages

Bone marrow derived macrophages (BMDMs) were generated from WT and FoxO3a-deficient mice as described in the experimental methods. BMDMs were treated with LPS (100 ng/ml) and zVAD (50 μM) with or without nec-1 (25 μM) for 24 hours. Cell viability was then assessed by MTT assay.

Graphs display % cell survival. MTT ODs were normalized to the unstimulated control (i.e. cells with R8 medium only). Data are pooled from 3 independent experiments performed in triplicate and presented as mean ± SEM. Statistical significance was calculated by unpaired two-tailed Student's t-test.

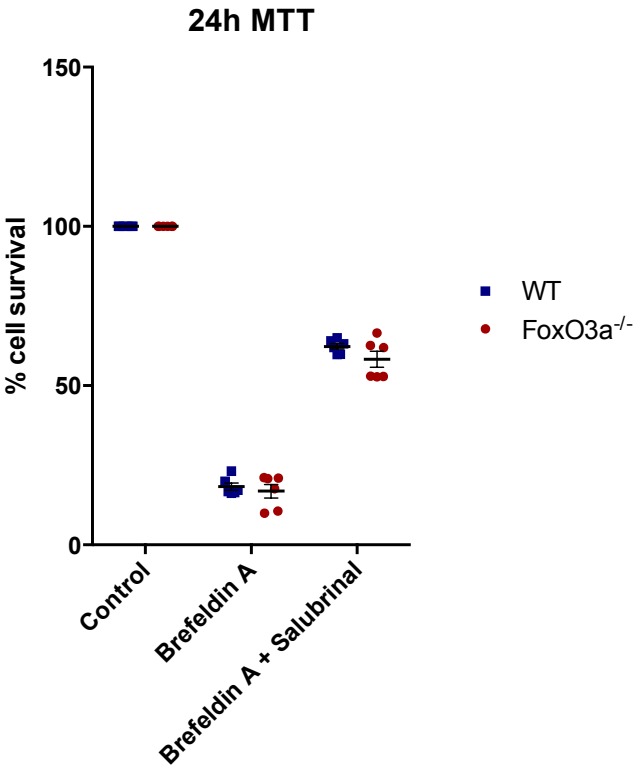
24h MTT
% cell survival
150
100
50
0
Control
Brefeldin A
Brefeldin A + Salubrinal
WT
FoxO3a-/-

Figure 27. FoxO3a signaling does not influence ER stress-induced cell death in macrophages

Bone marrow derived macrophages (BMDMs) were generated from WT and FoxO3a-deficient mice as described in the experimental methods. BMDMs were pre-treated with salubrinal (20 μM) for 1h. Cells were then treated with brefeldin A (3 μg/ml) with or without salubrinal for 24 hours. Cell viability was then assessed by MTT assay.

Graphs display % cell survival. MTT ODs were normalized to the unstimulated control (i.e. cells with R8 medium only). Data are pooled from 3 independent experiments performed in triplicate and presented as mean ± SEM. Statistical significance was calculated by unpaired two-tailed Student's t-test.

3.2.2. FoxO3a promotes macrophage inflammatory cytokine production upon ST infection

Next, I wanted to determine the effect of FoxO3a on macrophage function. For that purpose, I started by evaluating the impact of the transcription factor on macrophage cytokine production upon ST infection. Cytokines are proteins whose production is generally increased upon infection. Cytokines are secreted by various cell types including macrophages and can modulate macrophage function towards an anti-inflammatory or pro-inflammatory phenotype (Mosser and Edwards, 2008). Thus, they act as great indicators of macrophage function. To study the impact of FoxO3a on macrophage cytokine production, WT and FoxO3a-deficient macrophages were infected with ST at 10 MOI for 24h. Cell supernatants were then collected, and secreted cytokine concentrations were determined by ELISA. Pro-inflammatory cytokine (TNFα, IL12, IL1β and IL6) and the anti-inflammatory cytokine IL10 concentrations were assessed. Upon infection with ST, all cytokine concentrations increased in both WT and FoxO3a-deficient macrophage supernatants relative to uninfected controls (Figure 28). All pro-inflammatory cytokine concentrations were significantly lower in the absence of the transcription factor FoxO3a (Figure 28A). However, FoxO3a-deficient macrophages produced significantly higher amounts of the anti-inflammatory cytokine IL10.

Type I IFN has been shown to positively regulate IL10 production in macrophages infected with *Mycobacterium tuberculosis* (McNab et al., 2014). Hence, the amount of type I IFN, specifically IFNα and IFNβ, produced in cell supernatants after ST infection was measured. A mouse connective tissue cell line - namely the L929-ISRE cell line – which expresses luciferase under the control of interferon-stimulated response element (ISRE) sequences was used for that purpose. ISRE sequences are normally responsive to IFNα or IFNβ signaling. In the L929-

ISRE cell line, presence of type I IFN in cell supernatants thus activates the luciferase gene. The activated luciferase produces luminescence by cleaving the substrate luciferin contained in the luciferase assay reagent added. Quantifying this luminescence allows for an estimation of the amount of IFNα and IFNβ produced by the cells from which the supernatant was harvested. As expected, results indicated that there was significantly more type I IFN produced by FoxO3a-deficient macrophages compared with WT macrophages during infection, and surprisingly there were low but significant levels of type I IFN production in uninfected FoxO3a-deficient cells (Figure 28B).

ST infection activates many macrophage receptors including toll-like receptors (TLRs). TLR4 is known to bind to LPS, a common pathogen-associated molecular pattern (PAMP) found on gram-negative bacteria (de Jong et al., 2012). I investigated the impact of FoxO3a on cytokine production during TLR4 signaling. To do that, WT and FoxO3a-deficient macrophages were treated with LPS for 24h, and then cytokine concentrations were determined by ELISA. The results were similar to those obtained in the ST infection model, in that the quantities of pro-inflammatory cytokines produced were reduced compared to WT controls in the absence of FoxO3a, specifically IL12 and IL1β (Figure 29). Other pro-inflammatory cytokines, namely TNFα and IL6 were reduced in supernatants from FoxO3a-deficient cells compared with WT supernatants, although the differences did not reach statistical significance. A significant increase in IL10 concentrations was also noted in cells lacking FoxO3a. These results confirm that FoxO3a promotes pro-inflammatory cytokine production by macrophages in the context of ST infection.

In some cases, IL10 has been shown to inhibit IL12 production (Rahim et al., 2005). Since there was an increase in IL10 production during infection of FoxO3a-deficient macrophages I wanted to determine if this caused the concomitant reduction in IL12 concentrations. Hence, cells from both groups were treated with an antibody against IL10 during ST infection for 24h, and then cytokine concentrations were measured by ELISA. As expected, after neutralizing IL10, there was a decrease of about 100 fold in IL10 concentration in both sets of cells, although the difference between WT and FoxO3a-deficient macrophages was still present (Figure 30). IL10 neutralization caused an increase in IL12 concentrations but also in TNF concentrations in both groups. There were still significant differences between the two groups, indicating that IL10 was not the only factor causing the decrease in IL12 or TNF production in the absence of FoxO3a.

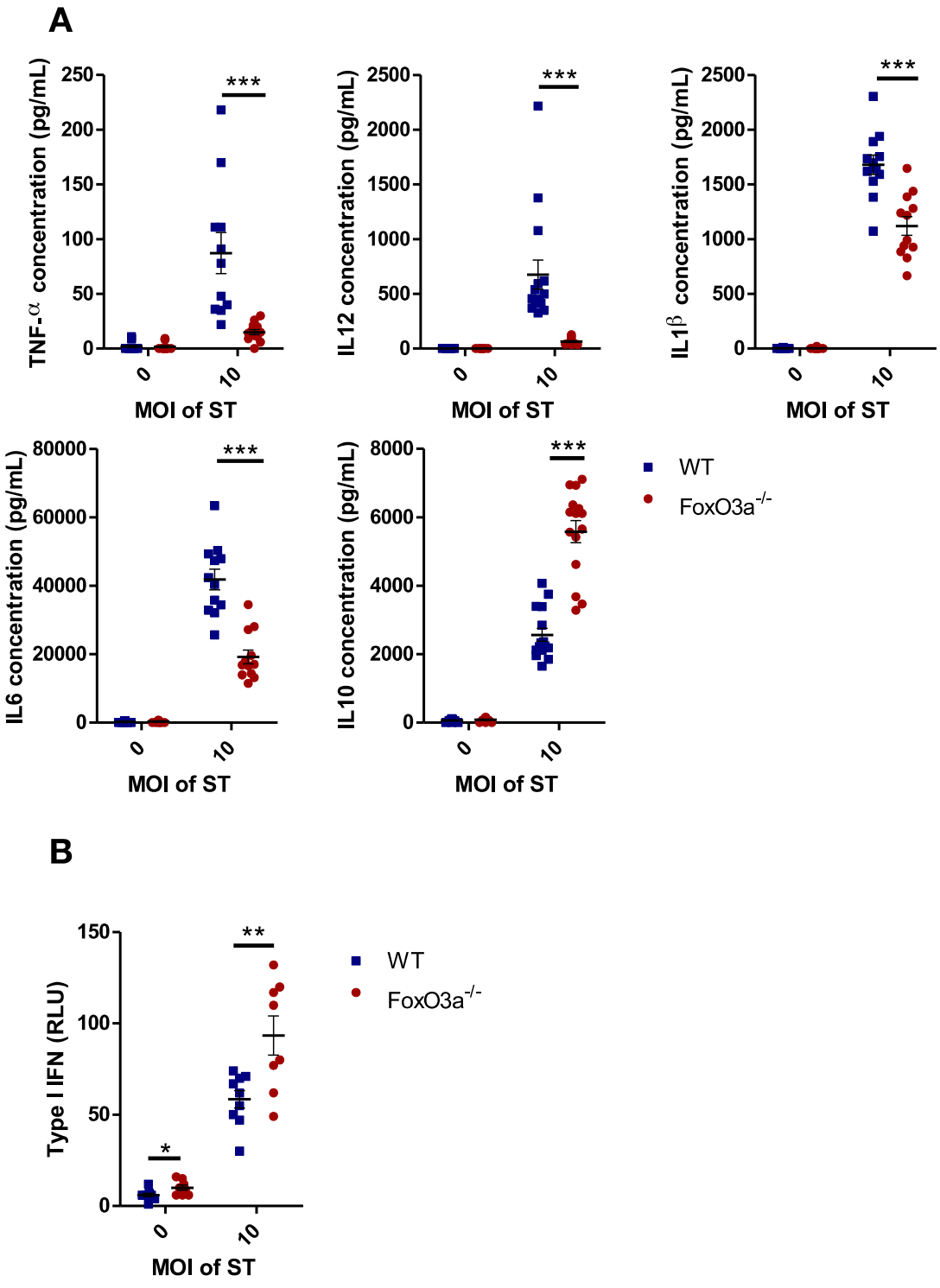
A
TNF-α concentration (pg/mL)
IL12 concentration (pg/mL)
IL1β concentration (pg/mL)
IL6 concentration (pg/mL)
IL10 concentration (pg/mL)
MOI of ST
***
WT
FoxO3a-/-
B
Type I IFN (RLU)
*
**

Figure 28. FoxO3a promotes pro-inflammatory cytokine production upon ST infection

Bone marrow derived macrophages (BMDMs) were generated from WT and FoxO3a-deficient mice as described in the experimental methods. Cells were infected with ST at 10 MOI for 24 hours. Cell supernatants were used for measurements of various cytokine concentrations.

(A) Graphs display cytokine concentrations determined by ELISA, in pg/ml. Cytokines measured are indicated on the y-axes. Data are pooled from at least 3 independent experiments performed in triplicate and presented as mean ± SEM. Statistical significance was calculated by unpaired two-tailed Student's t-test: ***$p<0.0001$.

(B) Graph shows type I IFN (IFNα and IFNβ) relative light units (RLU) determined by type I IFN bioassay, as described in the experimental methods. Data are pooled from 3 independent experiments performed in triplicate and presented as mean ± SEM. Statistical significance was calculated by unpaired two-tailed Student's t-test: *$p<0.05$, **$p<0.001$.

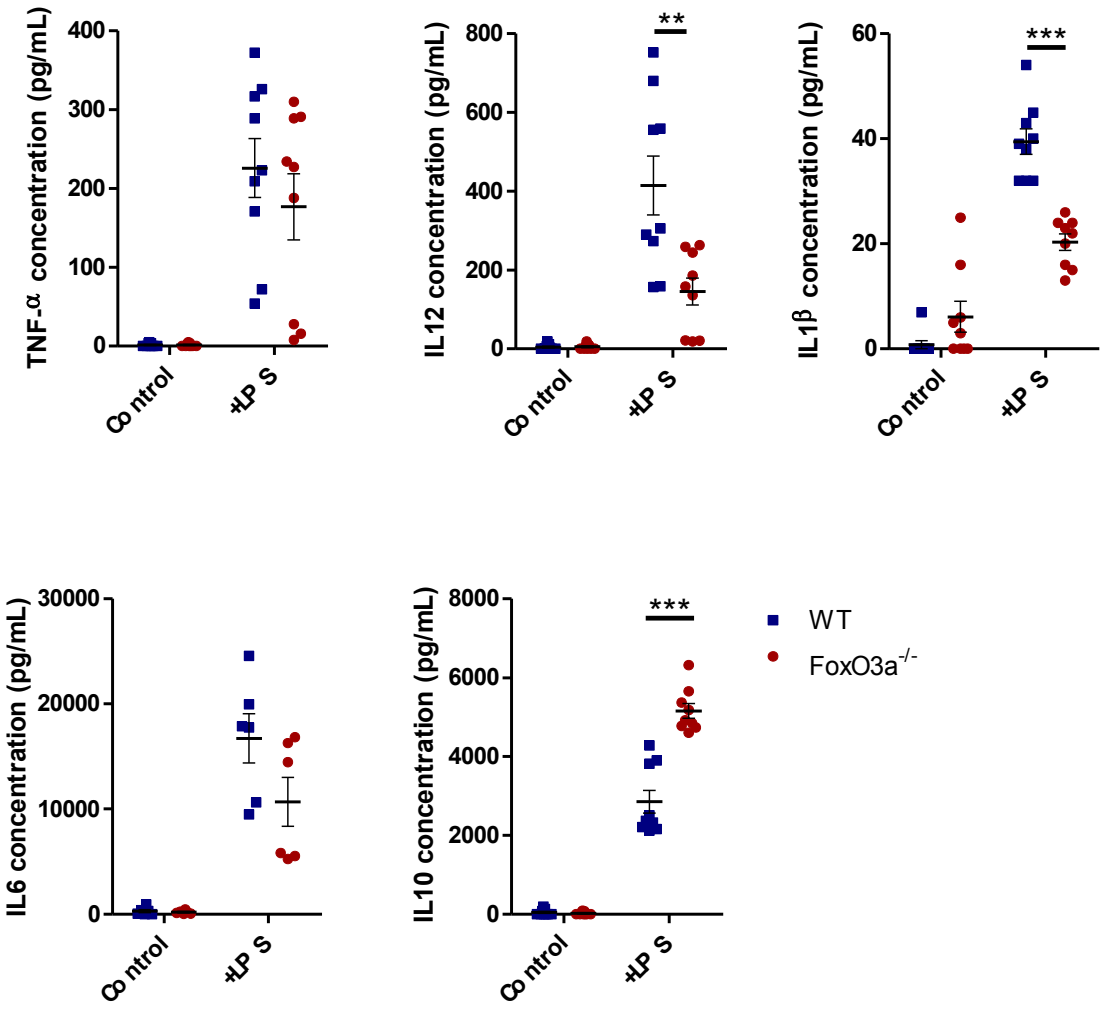
TNF-α concentration (pg/mL)
400
300
200
100
0
Control
+LPS
IL12 concentration (pg/mL)
800
600
400
200
0
**
IL1β concentration (pg/mL)
60
40
20
0
***
IL6 concentration (pg/mL)
30000
20000
10000
0
IL10 concentration (pg/mL)
8000
6000
4000
2000
0
***
WT
FoxO3a-/-

Figure 29. FoxO3a signaling promotes pro-inflammatory cytokine production upon LPS treatment

Bone marrow derived macrophages (BMDMs) were generated from WT and FoxO3a-deficient mice as described in the experimental methods. Cells were treated with LPS (100 ng/ml) for 24 hours. Cell supernatants were used for measurements of various cytokine concentrations.

Graphs display cytokine concentrations determined by ELISA, in pg/ml. Cytokines measured are indicated on the y-axes. Data are pooled from at least 2 independent experiments performed in triplicate and presented as mean ± SEM. Statistical significance was calculated by unpaired two-tailed Student's t-test: $^{**}p<0.001$, $^{***}p<0.0001$.

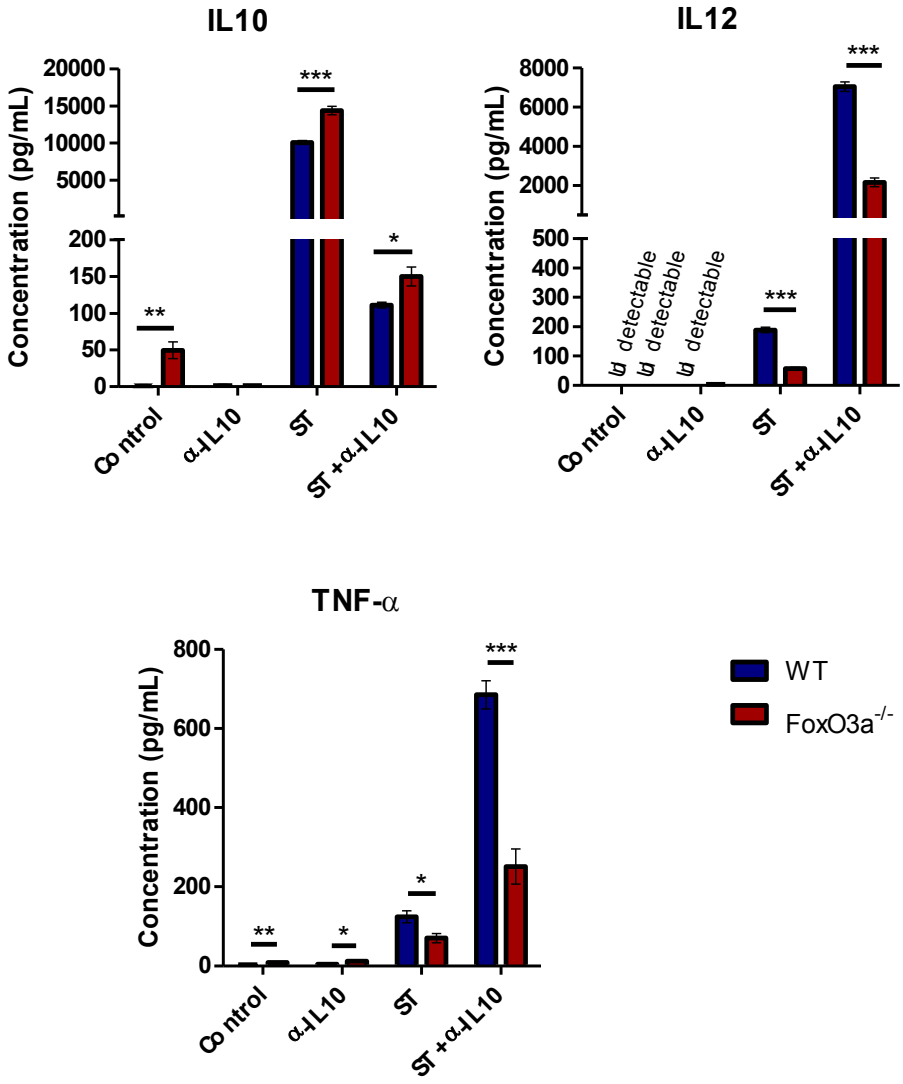
IL10
Concentration (pg/mL)
20000
15000
10000
5000
200
150
100
50
0
**
***
*
Control
α-IL10
ST
ST +α-IL10
IL12
Concentration (pg/mL)
8000
6000
4000
2000
500
400
300
200
100
0
Undetectable
Undetectable
Undetectable
***
***
Control
α-IL10
ST
ST +α-IL10
TNF-α
Concentration (pg/mL)
800
600
400
200
0
**
*
*
***
Control
α-IL10
ST
ST +α-IL10
WT
FoxO3a-/-

Figure 30. Reduction of IL12 and TNF expression in FoxO3a-deficient macrophages is not solely due to increased expression of IL10

Bone marrow derived macrophages (BMDMs) were generated from WT and FoxO3a-deficient mice as described in the experimental methods. Cells were infected with ST at 10 MOI and treated with anti-IL10 antibody (10 μg/ml) for 24 hours. Cell supernatants were used for measurements of various cytokine concentrations.

Graphs display cytokine concentrations determined by ELISA, in pg/ml. Cytokines measured are indicated in graph titles. Data are pooled from 2 independent experiments performed in triplicate and presented as mean ± SEM. Statistical significance was calculated by unpaired two-tailed Student's t-test: *$p<0.05$ **$p<0.001$, ***$p<0.0001$.

3.2.3. FoxO3a signaling does not impact macrophage polarization upon ST infection

Macrophage function can be modulated by a wide variety of extracellular signals (Mosser and Edwards, 2008). For instance, infection can induce macrophage differentiation towards a pro-inflammatory phenotype also called M1. These macrophages display an increased microbicidal activity and produce more pro-inflammatory cytokines such as IL12 or TNF. On the other hand, macrophages can also be polarized towards an anti-inflammatory phenotype, producing more IL10 and contributing to tissue repair. These macrophages are called M2 macrophages. Since FoxO3a signaling affected the production of pro-inflammatory and anti-inflammatory cytokines by macrophages during ST infection, I wanted to investigate the impact of FoxO3a on macrophage polarization. M1 and M2 macrophages can be recognized using specific markers. To examine polarization, the relative amounts of mRNA of some of these markers was assessed by qRT-PCR before infection and 6h after infection in WT and FoxO3a-deficient macrophages. Before ST infection, the M1 markers studied were metabolism genes GLUT1 and HIF-1α, as well as the pro-inflammatory cytokine IL1β. The M2 markers used were the metabolism regulator AMPKα, the cytokine TGFβ and the pathogen-sensitive mannose receptor (MannoseR). After infection, the same M1 markers were used, plus the cytokines TNFα, the p35 subunit of IL12, and the enzyme iNOS. The cytokine IL10 and the enzyme arginase-1 were added as M2 markers after infection. Results revealed relative transcript levels of M1 and M2 markers were similar when comparing WT and FoxO3a-deficient macrophages before infection (Figure 31). The same trends were obtained after infection.

Since macrophage polarization is a spectrum, some macrophage phenotypes are not fully M1 or M2 but instead have shared characteristics of both. One of these is the regulatory macrophage phenotype. These macrophages are polarized by TLR activation associated with

another signal such as IL10 or apoptotic bodies, and produce high levels of IL10 and low levels of IL12 for instance (Mosser and Edwards, 2008). Since these are characteristics observed in FoxO3a-deficient macrophages, I wanted to know if FoxO3a played a role in M_{reg} polarization. The markers used in this case were the TNF superfamily ligand LIGHT and the enzyme SPHK1. There was no difference in SPHK1 expression between WT and FoxO3a-deficient macrophages before infection. There was a slight increase in the transcription of these markers in the absence of FoxO3a after infection, although that increase was subtle. These results suggest that FoxO3a does not play a role in macrophage polarization.

To confirm that FoxO3a does not have any impact on M1 macrophage polarization, the production of nitric oxide (NO), an M1 marker, was determined. NO is a chemical compound that can have an antimicrobial function. Since NO has a very short half-life, the concentration of nitrites, a product of the breakdown of NO, can be used as a direct measure of NO concentrations using a Griess assay. Briefly, nitrites react with sulfanilic acid and N-(1-Naphtyl)ethylenediamine to form a colored product, the absorbance of which can be determined using a plate reader. Measurements of supernatants collected from WT and FoxO3a-deficient macrophages revealed an increase in nitrite concentrations in both groups at 24h but not 6h after ST infection, as compared with uninfected control cells (Figure 32). There were no differences between WT and FoxO3a-deficient macrophages. These results indicate that FoxO3a does not influence nitric oxide production upon ST infection.

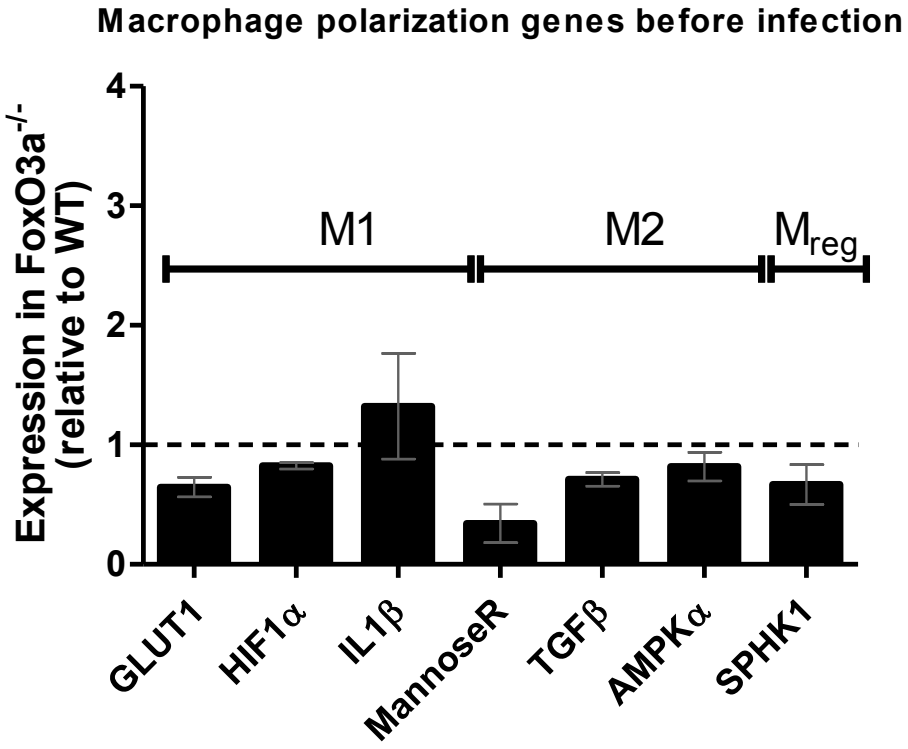
Macrophage polarization genes before infection
Expression in FoxO3a-/- (relative to WT)
0
1
2
3
4
M1
M2
Mreg
GLUT1
HIF1α
IL1β
MannoseR
TGFβ
AMPKα
SPHK1

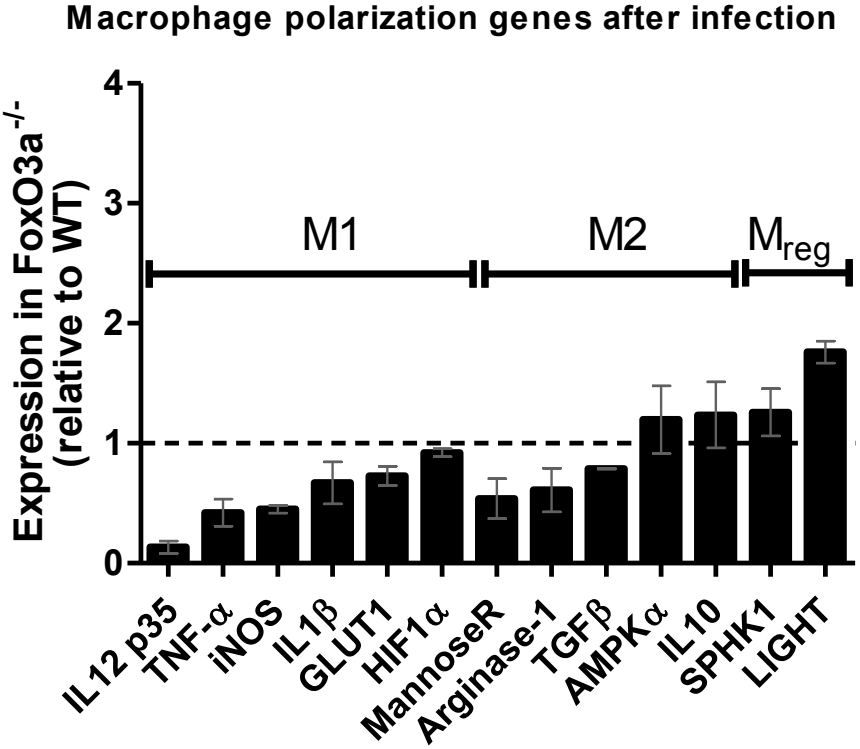
Macrophage polarization genes after infection
Expression in FoxO3a-/- (relative to WT)
0
1
2
3
4
M1
M2
Mreg
IL12 p35
TNF-α
iNOS
IL1β
GLUT1
HIF1α
MannoseR
Arginase-1
TGFβ
AMPKα
IL10
SPHK1
LIGHT

Figure 31. FoxO3a does not influence classical macrophage polarization

Bone marrow derived macrophages (BMDMs) were generated from WT and FoxO3a-deficient mice as described in the experimental methods. Cells were infected with ST at 10 MOI for 6h, then RNA was isolated and reverse transcription and subsequent qPCR were performed as indicated in the experimental methods.

Graphs display FoxO3a-deficient levels of various mRNAs relative to WT and normalized to β-actin, before and after infection. Data are pooled from at least 2 independent experiments and presented as mean ± SEM.

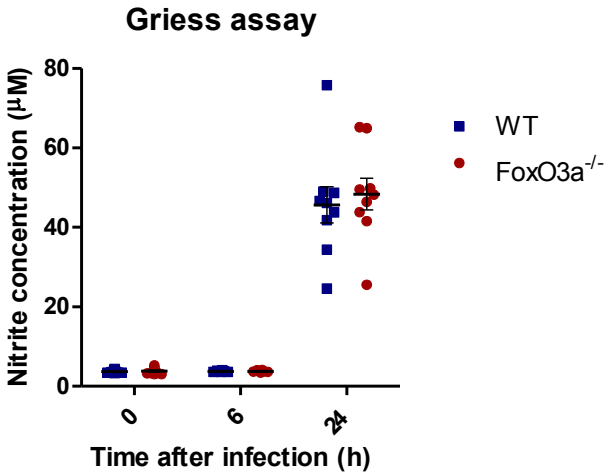
Griess assay
Nitrite concentration (μM)
80
60
40
20
0
0
6
24
Time after infection (h)
WT
FoxO3a-/-

Figure 32. FoxO3a signaling does not affect secretion of the M1 marker nitric oxide

Bone marrow derived macrophages (BMDMs) were generated from WT and FoxO3a-deficient mice as described in the experimental methods. Cells were infected with ST at 10 MOI for 6 and 24 hours (h). Cell supernatants were used for measurement of nitrite concentrations as a measure of nitric oxide concentrations by Griess assay, as described in the experimental methods.

Graphs display nitrite concentrations in cell supernatants in μM. Data are pooled from at least 2 independent experiments and presented as mean ± SEM. Statistical significance was calculated by unpaired two-tailed Student's t-test.

3.2.4. Glycolysis is required for expression of some cytokines during ST infection

Metabolism plays a key role in the response to infection, including cytokine production. For instance, cells are known to become more glycolytic when they are infected (Galván-Peña and O'Neill, 2014). Thus, since there was an impact of FoxO3a on anti and pro-inflammatory cytokine production, I investigated the effect of FoxO3a on metabolism. First, to determine if glycolysis plays a role in the effect of FoxO3a signaling on cytokine production, I inhibited glycolysis in WT and FoxO3a-deficient macrophages by treating the cells during ST infection with the glucose analog 2-deoxy-D-glucose (2-DG). Inhibiting glycolysis slightly decreased cell viability (Figure 33A) and reduced IL12, IL1β, and IL10 concentrations produced during infection (Figure 33B). There were still significant differences in the concentrations of IL12 and IL10 between WT and FoxO3a-deficient macrophages after 2-DG treatment, suggesting that FoxO3a does not regulate these cytokines through glycolysis. IL1β was lower in ST-infected FoxO3a-deficient BMDMs as compared with WT cells although the difference did not reach statistical significance in this case. When glycolysis was inhibited however, even though IL1β concentrations were reduced in both groups, there was a subtle but statistically significance increase in FoxO3a-deficient macrophages compared with WT cells. IL6 concentrations barely changed in either population after 2-DG treatment. TNF concentrations decreased in WT macrophages but remained unchanged in the absence of FoxO3a after inhibiting glycolysis, indicating that FoxO3a promotes TNF production through glycolysis.

3.2.5. FoxO3a regulates mitochondrial DNA amounts during ST infection

Next, the role of FoxO3a on mitochondrial metabolism during infection was analyzed.

The numbers of mitochondrial DNA copies were evaluated in infected macrophages relative to controls by qPCR. Total DNA was isolated, and relative mitochondrial DNA copy numbers were established using cytochrome c oxidase I (COI) copy numbers, normalized to 18S rRNA copy numbers. COI is encoded by the mitochondrial genome and was used to estimate the number of mitochondria in cells, whereas 18S rRNA is encoded by the nuclear genome. ST infection did not cause any change in mitochondrial DNA copy numbers in FoxO3a-deficient macrophages (Figure 34). However, in WT macrophages, there was an increase in mitochondrial DNA copy numbers after infection. These results highlight the role of FoxO3a in promoting an increase in mitochondrial DNA copy numbers during infection.

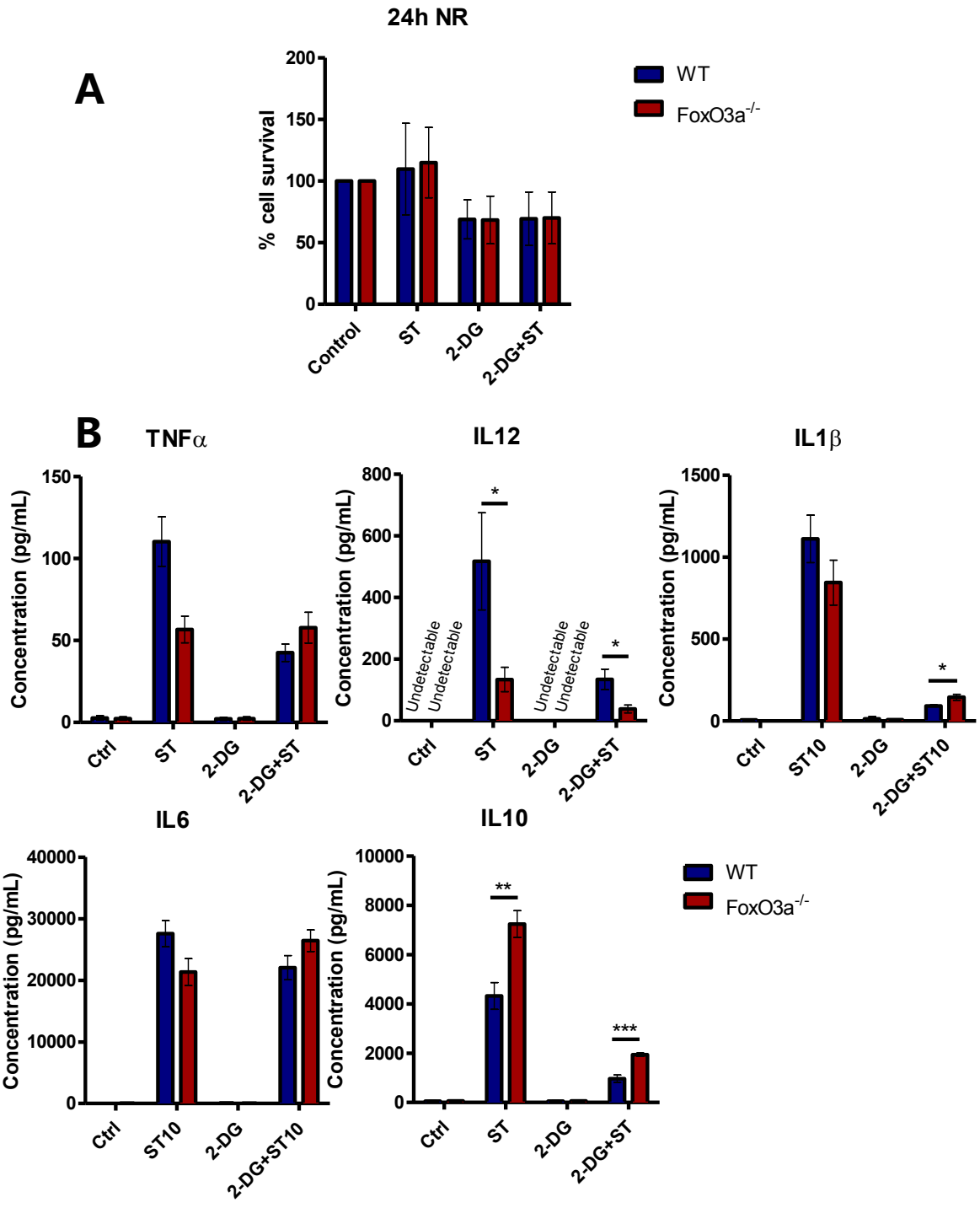
24h NR
A
% cell survival
200
150
100
50
0
Control
ST
2-DG
2-DG+ST
WT
FoxO3a-/-
B
TNFα
Concentration (pg/mL)
150
100
50
0
Ctrl
ST
2-DG
2-DG+ST
IL12
800
600
400
200
Undetectable
Undetectable
Undetectable
Undetectable
*
*
IL1β
1500
1000
500
*
Ctrl
ST10
2-DG
2-DG+ST10
IL6
40000
30000
20000
10000
Ctrl
ST10
2-DG
2-DG+ST10
IL10
10000
8000
6000
4000
2000
**
***
Ctrl
ST
2-DG
2-DG+ST

Figure 33. Glycolysis is required for expression of some cytokines

Bone marrow derived macrophages (BMDMs) were generated from WT and FoxO3a-deficient mice as described in the experimental methods. Cells were pre-treated with 2-deoxy-D-glucose (2-DG) (1mM) for 3h. Cells were then infected with ST at 10 MOI and treated with 2-DG for 24 hours. Cell viability was assessed by neutral red (NR) assay. Cell supernatants were used for measurement of cytokine concentrations by ELISA.

(A) Graph displays % cell survival. NR optical densities (ODs) were normalized to the unstimulated control (i.e. cells with R8 medium only). Data are pooled from 3 independent experiments performed in triplicate and presented as mean ± SEM.

(B) Graphs display cytokine concentrations determined by ELISA, in pg/ml. Cytokines measured are indicated in graph titles. Data are pooled from 2 independent experiments performed in triplicate and presented as mean ± SEM. Statistical significance was calculated by unpaired two-tailed Student's t-test: *$p<0.05$ **$p<0.001$, ***$p<0.0001$.

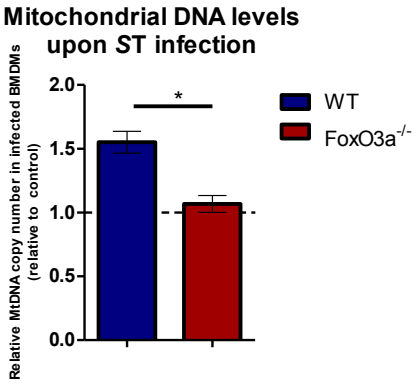
Mitochondrial DNA levels
upon ST infection
Relative MtDNA copy number in infected BMDMs
(relative to control)
2.0
1.5
1.0
0.5
0.0
*
WT
FoxO3a-/-

Figure 34. FoxO3a promotes an increase in mitochondrial DNA levels during ST infection

Bone marrow derived macrophages (BMDMs) were generated from WT and FoxO3a-deficient mice as described in the experimental methods. Cells were infected with ST at 10 MOI for 24 hours. DNA was extracted and qPCR was performed as described in the experimental methods. Relative mitochondrial DNA copy numbers were determined using cytochrome c oxidase I (COI) copy numbers normalized to 18S rRNA copy numbers.

Graph displays mitochondrial DNA (MtDNA) copy numbers in infected BMDMs relative to uninfected BMDMs. Data are pooled from 2 independent experiments and presented as mean ± SEM. Statistical significance was calculated by unpaired two-tailed Student's t-test: *$p<0.05$.

3.2.6. FoxO3a does not influence mitochondrial membrane potential in ST-infected macrophages

After investigating the impact of FoxO3a on mitochondrial copy number, I wanted to study its impact on mitochondrial function. I determined the impact of FoxO3a signaling on mitochondrial membrane potential during ST infection. Macrophages were infected with ST at various MOIs for 24h, then stained with tetramethylrhodamine ethyl ester (TMRE) for flow cytometry. TMRE is a cationic dye that accumulates in negatively charged, hyperpolarized active mitochondria in live cells. TMRE signal decreased with increasing MOI, indicating a reduction in mitochondrial membrane potential as cellular bacterial load increased (Figure 35A and B). TMRE signal appeared to be lower in uninfected FoxO3a-deficient macrophages but differences could no longer be observed between WT and FoxO3a-deficient cells after infection.

I repeated the same protocol using a simpler model with TLR4 activation using a 24h LPS treatment. The same trend could be noted as control FoxO3a-deficient BMDMs appeared to display a lower TMRE signal than WT BMDMs, but the difference could no longer be seen after LPS treatment (Figure 36A and B). Collectively, these results suggest that FoxO3a signaling might enhance mitochondrial membrane potential in uninfected cells but not during ST infection.

A

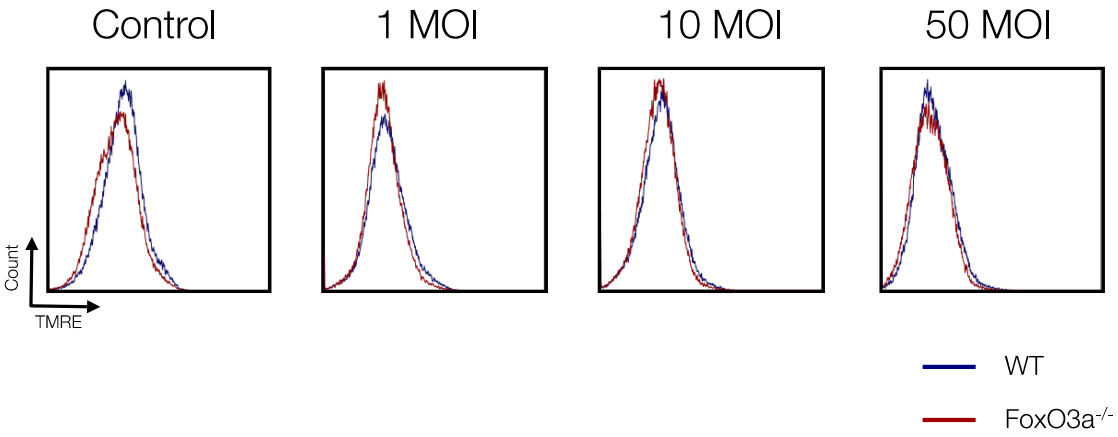
Control
1 MOI
10 MOI
50 MOI
Count
TMRE
WT
FoxO3a-/-

B

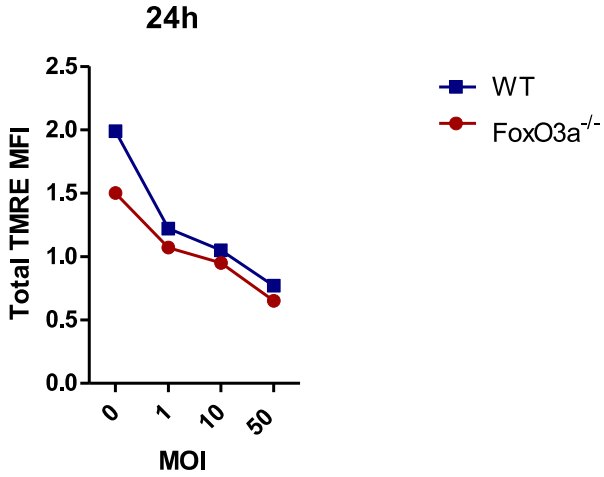
24h
Total TMRE MFI
2.5
2.0
1.5
1.0
0.5
0.0
0
1
10
50
MOI
WT
FoxO3a-/-

Figure 35. FoxO3a signaling mildly enhances mitochondrial membrane potential in untreated macrophages but not upon ST infection

Bone marrow derived macrophages (BMDMs) were generated from WT and FoxO3a-deficient mice as described in the experimental methods. BMDMs were infected with ST at various MOIs for 24 hours. Cells were then stained with TMRE as described in the experimental methods and acquired on a flow cytometer. Data were analyzed using Kaluza software (Version 1.2, Beckman Coulter).

(A) Representative TMRE histograms of infected cells.
(B) Graph displays total TMRE mean fluorescence intensity (MFI) of BMDMs infected with ST at various MOIs. Data are representative of 3 independent experiments.

A

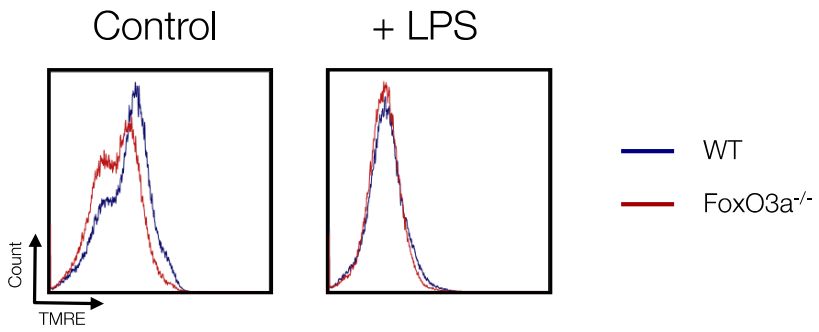
Control
+ LPS
Count
TMRE
WT
FoxO3a-/-

B

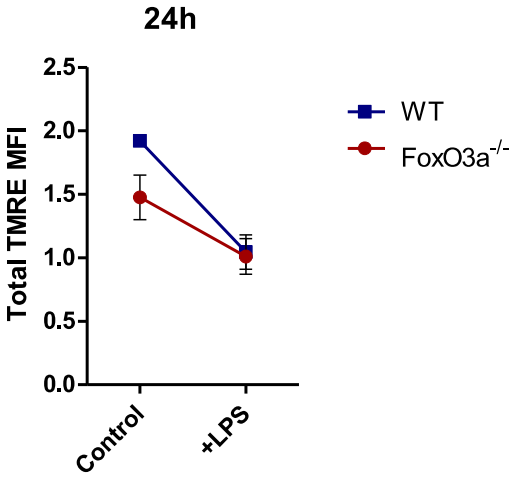
24h
Total TMRE MFI
2.5
2.0
1.5
1.0
0.5
0.0
Control
+LPS
WT
FoxO3a-/-

Figure 36. FoxO3a signaling mildly enhances mitochondrial membrane potential in untreated macrophages but not upon LPS treatment

Bone marrow derived macrophages (BMDMs) were generated from WT and FoxO3a-deficient mice as described in the experimental methods. BMDMs were treated with LPS (100 ng/ml) for 24h. Cells were then stained with TMRE as described in the experimental methods and acquired on a flow cytometer. Data were analyzed using Kaluza software (Version 1.2, Beckman Coulter).

(A) Representative TMRE histograms of LPS-treated cells.

(B) Graph displays total TMRE mean fluorescence intensity (MFI) of BMDMs treated with LPS. Data are pooled from 2 independent experiments.

3.2.7. FoxO3a signaling enhances mitochondrial respiration in ST-infected macrophages

I next studied the effect of FoxO3a on mitochondrial respiration during ST infection. WT and FoxO3a-deficient macrophages were infected with ST at 10 MOI for 24h, then oxygen consumption rates (OCR) were determined in the media using a Seahorse Bioscience XF24 Extracellular Flux Analyzer. Various inhibitors of mitochondrial respiration effectors were added as OCR was measured. First, basal OCR was measured, then oligomycin, carbonyl cyanide *m*-chlorophenyl hydrazone (CCCP), and Antimycin A were added at 14, 34, and 55 minutes, respectively. Oligomycin is an inhibitor of ATP synthase and thus allows determination of the oxygen consumption associated with ATP production. CCCP is an uncoupler that disrupts the mitochondrial membrane potential and allows a free movement of electrons through the electron transport chain. CCCP treatment reveals the maximal oxygen consumption capacity of a cell. Finally, antimycin A is a mitochondrial complex III inhibitor that completely shuts down mitochondrial respiration and thus allows determination of extra-mitochondrial respiration. There were no differences in OCR between WT and FoxO3a-deficient BMDMs before infection (Figure 37A). After ST infection however, the overall oxygen consumption of macrophages decreased in both groups and was disrupted as CCCP treatment was unable to increase the OCR (Figure 37B). Results also revealed that basal OCR and OCR after oligomycin treatment were lower in the absence of FoxO3a compared with WT macrophages during infection, although the differences did not reach statistical significance for basal OCR. No differences were noted in OCR after CCCP and antimycin A treatment. Together, these results reveal that FoxO3a promotes mitochondrial respiration in ST-infected macrophages.

A

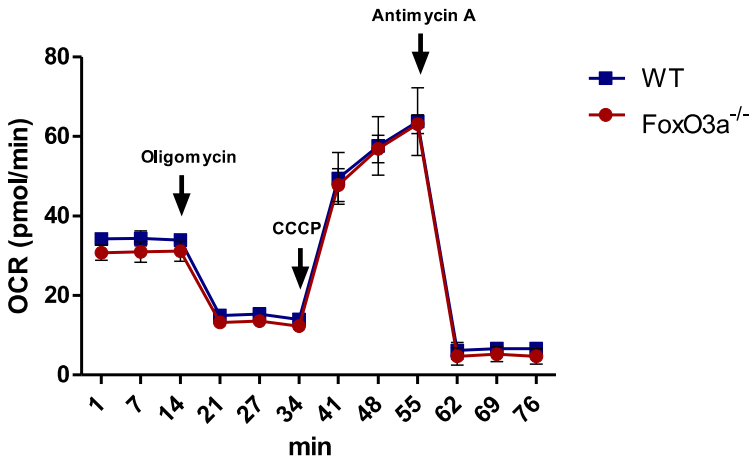
Control
Antimycin A
Oligomycin
CCCP
OCR (pmol/min)
80
60
40
20
0
1
7
14
21
27
34
41
48
55
62
69
76
min
WT
FoxO3a-/-

B

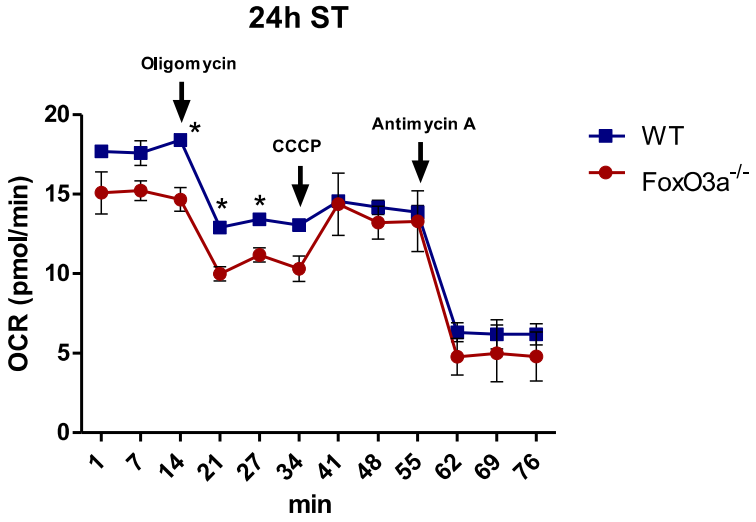
24h ST
Oligomycin
Antimycin A
CCCP
*
*
*
OCR (pmol/min)
20
15
10
5
0
1
7
14
21
27
34
41
48
55
62
69
76
min
WT
FoxO3a-/-

Figure 37. FoxO3a signaling enhances mitochondrial respiration in infected macrophages

Bone marrow derived macrophages (BMDMs) were generated from WT and FoxO3a-deficient mice as described in the experimental methods. BMDMs were infected with ST at 10 MOI for 24 hours. Mitochondrial respiration in BMDMs was then evaluated by measuring oxygen consumption rates (OCR) before and after sequential addition of specific inhibitors of mitochondrial respiration, as mentioned in the experimental methods.

Graphs show OCR of uninfected (A) and infected (B) BMDMs, before and after treatment with inhibitors of mitochondrial respiration. Data are pooled from 2 independent experiments and presented as mean ± SEM. Statistical significance was calculated by unpaired two-tailed Student's t-test: *$p<0.05$.

4. DISCUSSION

FoxO3a is a transcription factor that regulates genes involved in various important cellular processes including cell cycle, cell death, and metabolism. In particular, FoxO3a has been shown to regulate cell death in macrophages during HIV infection (Cui et al., 2008) and T cells during *Listeria monocytogenes* infection (Tzelepis et al., 2013). In various infection models, FoxO3a signaling has been shown to impact the T cell response without any impact on host survival (Tzelepis et al., 2013; Hedrick et al., 2012). Since the functions of FoxO3a might become more pertinent during conditions of chronic, cellular stress (Eijkelenboom and Burgering, 2013), I investigated the role of FoxO3a in the host response to invasive *Salmonella* infection, which induces a chronic infection that affects immune cell metabolism and death (Kelly and O'Neill, 2015; Keestra-Gounder et al., 2015). I hypothesized that FoxO3a might regulate inflammation during ST infection, which might be beneficial to the host. It is well known that immune cells such as neutrophils and macrophages are essential cell types of the innate immune system that are required for controlling *Salmonella* infection (LaRock et al., 2015). Since FoxO3a regulates cell cycle and cell death, my first objective was to determine the impact of FoxO3a on immune cell numbers both before and after *Salmonella* infection. I used WT C57BL/6 and FoxO3a-deficient mice for this purpose. FoxO3a-deficient mice were originally generated on a 129 background but were backcrossed more than 10 times to the C57BL/6 strain (Tzelepis et al., 2013). Both WT and FoxO3a-deficient mice were infected intravenously with ST-OVA, a transgenic strain of *S*T that injects OVA peptide into the cytosol of host cells while remaining inside the phagosome (Tzelepis et al., 2012). Relative to ST, ST-OVA infection is associated with the earlier onset of a potent $CD8^+$ T cell response that contributes to increased survival in susceptible C57BL/6 mice (Tzelepis et al., 2012). Using this model, I could thus study the impact of FoxO3a on innate and adaptive immune cell numbers during infection.

4.1. Impact of FoxO3a signaling on immune cell numbers

Since the model consisted of infecting mice systemically, and given the important role of the spleen in controlling blood borne bacteria (Delves et al., 2000) and as a protective niche for *Salmonella* (Dunlap et al., 1991), I decided to determine the impact of FoxO3a on the numbers of splenocytes. I observed that naïve FoxO3a-deficient mice displayed significantly increased numbers of spleen cells compared to WT mice. The same trend has been reported at least twice before, by Lin et al. (2004), as well as by Yalcin et al. (2010) even though the latter generated FoxO3a-deficient mice on a different background (FVB/n).

By dissecting individual splenocyte subsets, I noted that before infection, total T cell – but not B cell or NK cell – counts were increased in the absence of FoxO3a. Lin et al. (2004) also reported increased T cell numbers in FoxO3a-deficient spleens, with the ratio of $CD4^+$ to $CD8^+$ T cells and the number of B cells being unchanged. They indicated that $CD4^+$ T cells proliferated more readily upon stimulation in the absence of FoxO3a. However, the cause of the $CD8^+$ T cell increase remained to be identified. Another study by Dejean et al. (2009) did not observe any difference in T cell or B cell numbers between WT and FoxO3a-deficient mice; however, that study generated FoxO3a-deficient mice through two different methods on C57BL/6 and FVB backgrounds, while my work was performed using the same gene-trap model as that of Lin and colleagues. Consequently, the different approach in the generation of FoxO3a-deficient mice may explain the differential results.

After ST infection, there were no differences in total splenic T cell numbers, but FoxO3a-deficient mice displayed increased total bone marrow T cell numbers. According to Mazo et al. (2005), the major type of $CD8^+$ T cell in the bone marrow is a central memory T cell. Moreover, FoxO3a-deficient mice have enhanced numbers of splenic memory $CD8^+$ T cells

after *Listeria monocytogenes* infection (Tzelepis et al., 2013) and Lymphocytic Choriomeningitis Virus (LCMV) infection (Sullivan et al., 2012). Thus, it is possible that FoxO3a-deficient mice generate a higher proportion of memory T cells upon ST infection, which then home to the bone marrow. Because of the beneficial role of memory T cells during vaccination, it is possible that modulation of FoxO3a might impact vaccine development.

A study published in 2009 by Hinman et al. reported a decrease in bone marrow B cell numbers in FoxO3a-deficient mice compared with WT mice without any effect on splenic B cell counts. My results in uninfected mice confirm their findings. They also noted a subtle but reproducible decrease in $S1P_1$ mRNA levels in FoxO3a-deficient B cells. Since $S1P_1$ is a receptor for S1P – which participates in the migration of cells out of peripheral lymphoid organs and into the circulation – they suggested that FoxO3a-deficient mice displayed reduced numbers of bone marrow-homing B cells because of defective egress of those cells from peripheral lymphoid organs (Hinman et al., 2009).

After ST infection however, I did not observe any difference in bone marrow B cell counts between WT and FoxO3a-deficient mice. The same observation was made for B cells in the spleen and blood, indicating that ST infection normalizes any differences in B cell numbers, observed between naïve WT and FoxO3a-deficient mice.

The effect of FoxO3a signaling on splenocytes was much more uniform in myeloid cells as all cell numbers – including dendritic cells, neutrophils, monocytes, and macrophages – were significantly increased in the absence of FoxO3a, and all differences were abrogated by ST infection. The same trend was observed in the blood as well. Similar findings were described by Dejean et al. (2009) in the naïve spleen, as well as by Yalcin et al. (2010). Furthermore, in this

last report, the authors suggested that the increased blood and spleen myeloid counts were caused by an enhanced myeloid progenitor compartment in the bone marrow, spleen, and blood of FoxO3a-deficient mice. Specifically, they demonstrated using flow cytometry that bone marrow Lin^{-} $Sca\text{-}1^{-}$ $c\text{-}kit^{+}$ (LSK) $IL7R^{-}$ cells were increased in the absence of FoxO3a. However, these cells encompass CMPs and their derivatives that include megakaryocyte and erythrocyte progenitors (MEPs). Thus, the differences observed could originate from MEP numbers. Yalcin and colleagues also confirmed their previous result by using an *in vitro* CFU assay of myeloid progenitor growth to show that myeloid progenitor colonies were increased in the bone marrow (Yalcin et al., 2010). My results did not corroborate their findings, as I did not observe any differences in CMP, GMP or MEP numbers by flow cytometry, nor an increase in myeloid progenitor colony numbers by *in vitro* CFU assay. However, they used erythropoietin (EPO) in their methylcellulose medium for the CFU assay whereas I did not. Since EPO promotes differentiation of erythroid cells, the differential growth of progenitors they observed could again stem from increased erythroid progenitors. Miyamoto et al. (2007) also performed a CFU assay with a methylcellulose medium that contained EPO and did not find differences in erythroid or granulocyte-monocyte (CFU-GM) progenitor colony numbers between WT and FoxO3a-deficient mice. Thus, the cause of the increased myeloid cell numbers in the blood and spleen in my model remains to be identified. Possible causes include enhanced proliferation or reduced cell death given the role of FoxO3a as a negative regulator of cell cycle and a positive regulator of cell death in some cell types (Greer and Brunet, 2005). Indeed, a recent report stated that MYFKO:$ldlR^{-/-}$ mice (a knock-out of LDL receptor and myeloid-specific knock-out of FoxO1, 3, and 4) displayed splenomegaly with a concomitant expansion of monocytes in the spleen and blood and of neutrophils in the blood in comparison to $ldlR^{-/-}$ mice (which just lack the LDL receptor). This expansion appeared to be caused by increased cycling of GMPs.

Absolute GMP numbers appeared to be similar in both strains (Tsuchiya et al., 2013). Although I have used mice in which only the FoxO3a gene was deleted, my results were similar to Tsuchiya and colleagues'. Thus, it is conceivable that there could also be increased cycling of myeloid progenitors in FoxO3a-deficient mice, which would account for the increase in myeloid cell numbers in the spleen. Moreover, I have observed that upon M-CSF treatment of bone marrow cells to generate macrophages from myeloid precursors, there were more FoxO3a-deficient macrophages compared with WT cells on day 6 and 12 after treatment (Figure 24). This indicates that there is a possible role of FoxO3a signaling in controlling myeloid progenitor proliferation or death. However, it is not clear why myeloid cell numbers were not increased in the bone marrow, an anatomical site where they are generated. The increase in splenic and blood myeloid counts could also be explained by enhanced egress of myeloid cells from the bone marrow to the spleen. Lastly, another reason that could explain the myeloid cell expansion is enhanced extra-medullary hematopoiesis, especially as Yalcin and colleagues reported an increase in FoxO3a-deficient myeloid progenitor CFU of splenic origin *in vitro* (Yalcin et al., 2010).

After infection, the numbers of bone marrow monocytes were higher in the absence of FoxO3a, and this was associated with a concomitant increase in bone marrow CMP but not GMP. Spleen monocyte numbers remained unaffected. Therefore, it is possible that more monocytes were produced in the bone marrow in response to infection, but had impaired egress, which has to be verified. It is also possible that these cells migrated to the spleen and were efficiently eliminated in response to *Salmonella* infection.

4.2. Impact of FoxO3a on macrophage function and death

Macrophages act both as scavengers of *Salmonella* and as a niche for replication of *Salmonella* (Mastroeni et al., 2009). The molecular pathways that govern host–pathogen interactions between the bacteria and macrophages are still not fully understood. Given the role of FoxO3a in various important processes during infection such as cell death or cell cycle, my second objective was to determine the impact of FoxO3a signaling on macrophage function and death during ST infection. For this purpose, I have used bone-marrow-derived macrophages (BMDMs) throughout my experiments. These macrophages were generated by treating bone marrow cells with the cytokine M-CSF, which induces differentiation of myeloid progenitors into macrophages (Zhang et al., 2008). This technique is practical as it yields at least 30 million of $CD11b^+$ $F4/80^+$ macrophages per mouse. My results indicated that FoxO3a has no impact on macrophage cell death before or upon ST infection. However, the transcription factor was found to positively regulate inflammation by up-regulating pro-inflammatory cytokine production.

4.2.1. Impact of FoxO3a signaling on macrophage cell death

Salmonella can induce different types of cell death in macrophages as a virulence mechanism (Hu and Zhao, 2012). These include apoptosis, necroptosis, pyroptosis, or autophagic cell death (Hu and Zhao, 2012). The first three types have already been described earlier in this thesis, and autophagy can cause a form of cell death that involves destruction of cellular contents in vesicles called autophagosomes and that associate with lysosomes (Hu and Zhao, 2012). Similarly to apoptosis, it is a non-inflammatory form of cell death. I have studied the impact of FoxO3a on some of these types of cell death in BMDMs. First of all, I induced necroptosis in macrophages by treating them with LPS while inhibiting caspases with the pan-

caspase inhibitor zVAD (McComb et al., 2014). Data linking FoxO transcription factors and necroptosis are scarce, and my results revealed that FoxO3a does not impact necroptotic cell death in BMDMs.

FoxO3a is known to positively regulate apoptosis in a cell-type- and context-dependent manner (Greer and Brunet, 2005). For instance, Haoues and colleagues (2014) demonstrated using human and murine macrophages that FoxO3a could induce caspase-independent apoptosis in BCG-infected macrophages. Another study reported that FoxO1 and FoxO3a signaling contributed to apoptosis induced in peritoneal macrophages during endoplasmic reticulum (ER) stress (Senokuchi et al., 2008). Many intracellular bacteria, such as *Listeria monocytogenes* or *Mycobacterium tuberculosis* can cause ER-stress-induced apoptosis in host cells (Celli and Tsolis, 2015). Thus, I evaluated the effect of FoxO3a on ER-stress-induced cell death in BMDMs as induced by brefeldin A. Unlike Senokuchi and colleagues (2008), I did not note any effect of FoxO3a on ER-stress-induced cell death. This difference could arise from the fact that ER-stress was induced in different ways in both cases. More specifically, I induced ER-stress using brefeldin A, whereas Senokuchi et al. (2008) have used free-cholesterol loading for that purpose. Brefeldin A disrupts ER-Golgi apparatus protein transport leading to ER stress (Klausner et al., 1992), while free cholesterol induces ER stress through disruption of ER calcium stores (Feng et al., 2003). Unlike the studies mentioned above, I have not verified that brefeldin-A-induced cell death was indeed apoptosis so this remains to be confirmed.

In my experiments, overall cell death after ST infection as determined by neutral red assay was not different between both groups of BMDMs. The main form of cell death induced during ST infection in macrophages is caspase-1 dependent pyroptosis (Brennan and Cookson,

2000). Caspase-1 is known to cleave the pro-inflammatory cytokines IL1β and IL18, which results in their activation and release along with other intracellular contents during pyroptosis. Since I observed similar cell death in WT and FoxO3a-deficient macrophages, I expected to measure the same concentrations of these cytokines in cell supernatants after ST infection. Unexpectedly, FoxO3a-deficient macrophages secreted significantly reduced amounts of IL1β. These BMDMs also had reduced levels of IL1β transcripts as compared to WT BMDMs. This result suggests that FoxO3a signaling does not impact inflammasome-induced processing of pre-IL1β to its active form. Thus, the reduced expression of IL1β in FoxO3a-deficient cells can be attributed to mechanisms involved in gene transcription such as NFκB or MAPK signaling. A study published in 2009 by Su and colleagues reported that FoxO1 also promoted IL1β production in murine RAW264.7 macrophages upon LPS treatment. These results are not surprising, as it is known that although FoxO factors have distinct roles, they can also be redundant (Eijkelenboom and Burgering, 2013). In their paper, Su et al. (2009) indicated that FoxO1 induced IL1β production in an NFκB-dependent manner. Whether FoxO3a regulates IL1β the same way is still not known.

4.2.2. Impact of FoxO3a signaling on macrophage function

Pro-inflammatory cytokine production by host cells is essential for the control of pathogens during infection whereas anti-inflammatory cytokines can be detrimental (Mosser and Edwards, 2008). For example, during *Salmonella* infection, macrophages produce IL12, which induces IFNγ secretion by NK cells and T cells. This in turn promotes pathogen clearance through increased activation of phagocytes with enhanced secretion of antimicrobial compounds (Gilchrist et al., 2015). Other important pro-inflammatory cytokines during ST

infection include TNFα, IL1β, and IL6 (de Jong et al., 2012). I have measured the expression of these cytokines in the supernatant of ST-infected BMDMs. My results revealed that FoxO3a-deficient macrophages had significantly reduced levels of all the aforementioned pro-inflammatory cytokines. Conversely, concentration of the anti-inflammatory cytokine IL10 was significantly higher in the absence of FoxO3a. Similar trends in cytokine concentrations were obtained upon TLR4 engagement following LPS treatment.

IL10 mediates its anti-inflammatory effect in a variety of ways, including through down-regulation of pro-inflammatory cytokines and chemokines in myeloid cells at the transcriptional and post-transcriptional level (Moore et al., 2001). As explained earlier, FoxO1 was already found to promote IL1β production in macrophages after LPS treatment (Su et al., 2009). Although they reported no impact of FoxO1 on TNFα, IL12, or IL6, this previous report found that FoxO1 also negatively regulated IL10 production in the same cells. However, they have not explained the mechanism behind that inhibition. A previous study by McNab et al. (2014) established that type I IFN enhanced IL10 production in murine BMDMs during *Mycobacterium tuberculosis* infection. Therefore, I tested whether type I IFN was also higher in FoxO3a-deficient macrophages using infection with ST. This was indeed the case, indicating that FoxO3a could inhibit IL10 during ST infection in a type I IFN-dependent manner. Accordingly, another study demonstrated that FoxO3a could inhibit IFNβ in human monocyte-derived dendritic cells, possibly through modulation of NFκB and IRF transcription factors (Luron et al., 2012). In addition, a recent report mentioned that FoxO3a knockdown in murine peritoneal macrophages promotes type I IFN secretion in an IRF7-dependent manner during vesicular stomatitis virus (VSV) infection (Chen et al., 2016).

It has been reported previously that IL10 can inhibit IL12 subunit p40 (McNab et al., 2014) and IL12p70 (Rahim et al., 2005) protein levels in macrophages. Thus, I wanted to

determine if FoxO3a promoted IL12 production through inhibition of IL10. Neutralization of IL10 in FoxO3a-deficient macrophages with an anti-IL10 antibody did not rescue the impairment in IL12 expression in BMDMs, suggesting that FoxO3a does not regulate IL12 through increased IL10 expression.

Transcriptional analysis by qRT-PCR revealed that FoxO3a-deficient macrophages also had lower levels of IL12, TNFα, and IL1β transcripts after infection. Whether FoxO3a increases the transcription of these cytokines or promotes mRNA stability remains to be addressed. Taken together, these results suggest that FoxO3a can be modulated to promote inflammation for the control of intracellular bacteria such as ST. A study by Dejean et al. (2009) stated that FoxO3a-deficient dendritic cells (DCs) produced higher amounts of IL6 and TNFα than WT DCs upon LCMV infection. Perhaps the contrast between their results and mine is related to the different cell types studied or the different nature of the pathogens used for infection. Another report by Lee et al. (2013) suggested that FoxO3a nuclear localization in human monocytes inhibited pro-inflammatory cytokines upon LPS stimulation. This difference could be due to the different model organisms used and indicates that data extrapolation to humans must be exercised with caution.

Next, I wanted to determine if FoxO3a signaling promoted pro-inflammatory cytokine production and inhibited anti-inflammatory cytokines by modulating macrophage polarization. As explained earlier, extracellular signals such as bacterial products – including LPS – and cytokines – including IL4 – can induce macrophage differentiation towards pro- or anti-inflammatory phenotypes, called M1 and M2 respectively, or towards different phenotypes that share characteristics of both to different degrees (Mosser and Edwards, 2008). That way, macrophages can respond to extracellular stimuli by either increasing their microbicidal activity

as M1 macrophages or promote wound healing and tissue repair as M2 macrophages (Mosser and Edwards, 2008). Differentiation towards a context-appropriate phenotype during specific environmental conditions is essential. For example, M2 macrophages are not suitable to control ST as they have reduced ability to control intracellular replication of *Salmonella* compared with M1 macrophages (Lathrop et al., 2015). My results suggested that FoxO3a had no impact on macrophage polarization towards M1 or M2 phenotypes, as markers for both M1 and M2 macrophages (Kelly and O'Neill, 2015; Mosser and Edwards, 2008) were down regulated in FoxO3a-deficient macrophages after ST infection.

Nitric oxide (NO) has antimicrobial properties and is produced from arginine by the enzyme inducible nitric oxide synthase (iNOS), an M1 macrophage marker (Mosser and Edwards, 2008). As expected, the concentration of NO increased after infection in both WT and FoxO3a-deficient BMDMs. Nevertheless, in accord with the fact that FoxO3a does not influence macrophage polarization towards M1 or M2 phenotypes, I did not observe any difference in NO production between both groups.

Interestingly, compared with WT macrophages, FoxO3a-deficient macrophages appeared to express slightly higher levels of two regulatory macrophage (M_{reg}) markers, namely LIGHT and sphingosine kinase-1. Regulatory macrophages are cells that downregulate inflammation without affecting wound healing and thus can be detrimental during infection or for vaccine efficacy as these states require potent inflammatory responses (Mosser and Edwards, 2008). M_{regs} are usually induced by FcγR ligation associated with a pro-inflammatory stimulus such as LPS signaling (Edwards et al., 2006). My data suggest that FoxO3a could play a role in preventing macrophage polarization towards the M_{reg} phenotype. Confirmation of this role for FoxO3a would mean that its activity could be increased to promote vaccine efficacy for instance, and decreased in infected individuals with fibrosis, as regulatory macrophages do not

promote extracellular matrix generation. More work needs to be done to decipher whether FoxO3a signaling indeed impacts the development of M_{reg} cells.

Macrophage polarization is associated with modulation of metabolism. In fact, M1 macrophages display enhanced glycolysis for a quick source of energy whereas M2 macrophages tend to resort to oxidative phosphorylation for a slower but sustained energy supply in the form of ATP (O'Neill et al., 2016). In fact, during inflammation, the increase in glycolysis in M1 macrophages promotes pro-inflammatory cytokine production (O'Neill et al., 2016). Thus, I wanted to determine if the higher amounts of pro-inflammatory cytokines produced in WT BMDMs in comparison to FoxO3a-deficient BMDMs were the result of an alteration of metabolism by FoxO3a signaling. To do that, I evaluated the impact of glycolysis on cytokine production during ST infection in WT and FoxO3a-deficient macrophages by inhibiting glycolysis with the glucose analog 2-DG. Treatment with 2-DG resulted in reduced cell survival during infection, indicating the importance of glycolysis for macrophage survival during ST infection. I did not note any difference in survival between WT and FoxO3a-deficient BMDMs, which indicates that FoxO3a did not impact 2-DG-induced cell death. Most cytokines, including IL12, IL1β, and IL10, were decreased upon 2-DG treatment. This could either confirm that glycolysis is required for cytokine production during infection, or these results could simply be due to the reduction in cell survival observed upon 2-DG treatment. However, the differences in IL12 and IL10 concentrations between WT and FoxO3a-deficient BMDMs were not abrogated by inhibiting glycolysis, indicating that FoxO3a does not regulate these cytokines through glycolysis. There was a subtle increase in IL1β production in FoxO3a-deficient macrophages compared with WT cells after inhibition of glycolysis, which might suggest that FoxO3a limits IL1β production when glycolysis is inhibited during infection. However, since

there were no differences in cell death between both groups, it is unlikely that the reduction in IL1β was associated with reduced pyroptosis. IL6 concentrations remained unchanged after 2-DG treatment. A previous paper reported that during infection of BMDMs with the bacterium *Bordetella pertussis*, inhibition of glycolysis with 2-DG reduced IL1β but did not affect IL6 at the transcriptional level (Tannahill et al., 2013). These findings are similar to my data with ST. However, in that paper, they also found that TNFα transcription and protein levels were unaffected by 2-DG in these settings whereas my results indicated that TNF concentration was reduced in WT cells when glycolysis was inhibited. These differences might be due to the difference in the bacteria used. Interestingly, while TNFα was reduced in infected BMDMs from WT mice, the TNFα levels remained unchanged in FoxO3a-deficient BMDMs following 2-DG treatment. These data suggest that during ST infection, FoxO3a up-regulates TNFα through glycolysis suggesting that increasing the glycolytic capacity of a cell could increase its production of TNFα through FoxO3a-signaling. It has been shown before that FoxO3a is a negative regulator of glycolysis in IL3-dependent hematopoietic FL5.12 liver cells (Khatri et al., 2010). A recent report published by the Sad laboratory indicated that FoxO3a signaling had no effect on glycolysis during ST infection, as determined by L-lactate production, an end product of glycolysis (Joseph et al., 2016).

As mentioned above, M2 macrophages rely on oxidative phosphorylation for energy (O'Neill et al., 2016). Oxidative phosphorylation consists of serial redox reactions that produce ATP through the electron transport chain (ETC), which is a group of proteins located in the inner mitochondrial membrane. Hence, mitochondrial biogenesis can contribute to increasing oxidative phosphorylation (O'Neill et al., 2016). Thus, I evaluated the impact of FoxO3a on the number of mitochondria during ST infection by measuring mitochondrial DNA (MtDNA) copy

numbers. Although WT macrophages displayed an increase in MtDNA copy numbers after infection, these numbers did not change in FoxO3a-deficient macrophages even though these cells were more anti-inflammatory as indicated by their cytokine production profiles. Unlike my results, a study by Ferber and colleagues (2012) found that FoxO3a signaling reduced MtDNA copy numbers and negatively regulated mitochondrial respiration in a human epithelial cell line. Many factors could explain the differences between my results and the report by Ferber et al. (2012), such as the different cell types from different species that were used. Overall, my results suggest that FoxO3a signaling promotes mitochondrial biogenesis or prevents degradation of mitochondria during ST infection.

I also assessed mitochondrial function in BMDMs by evaluating the oxygen consumption rate (OCR), as well as the mitochondrial membrane potential. Compared with uninfected cells, the basal OCR and the mitochondrial membrane potential were reduced after ST infection of macrophages, which was expected since infected cells are known to upregulate glycolysis to the detriment of mitochondrial respiration (O'Neill et al., 2016). I observed that in contrast to WT cells, the basal OCR was slightly reduced in FoxO3a-deficient cell following ST infection. These results were consistent with the MtDNA copy number data that was also lower in FoxO3a-deficient BMDMs after infection. ATP-associated OCR, which is defined as basal OCR minus OCR after ATP synthase inhibition by oligomycin (Reily et al., 2013) did not appear to be affected by FoxO3a. This finding was confirmed by assessing the mitochondrial membrane potential, which is a more direct measure of ATP-associated mitochondrial function (Perry et al., 2011) and was similar between WT and FoxO3a-deficient BMDMs upon ST infection or LPS treatment. These data suggest that even though FoxO3a signaling appears to up-regulate the number of mitochondria and promote oxygen consumption after infection, it

does not affect mitochondrial membrane potential and possibly ATP production although this last possibility remains to be confirmed by direct measures of ATP production. The impact of the increased mitochondrial biogenesis and oxygen consumption in cells with a functional FoxO3a protein after infection also remains to be understood. Rimmelé et al. (2015) noted decreased oxygen consumption in FoxO3a-deficient HSCs – which I also observed in macrophages but only after ST infection –, as well as a reduction in ATP production in these cells. Rimmelé and colleagues also found that mitochondrial membrane potential was increased in these cells, which they suggest was a compensatory mechanism to palliate the reduction in ATP. I have found that the reduced oxygen consumption after infection in FoxO3a-deficient BMDMs was not associated with any change in mitochondrial membrane potential, which indicates that there might be less ATP produced in these cells although this remains to be confirmed.

Interestingly, mitochondrial membrane potential appeared to be lower in FoxO3a-deficient macrophages before infection, even though oxygen consumption was similar between both groups at this point. These results suggest that despite normal oxygen consumption, FoxO3a might promote mitochondrial activity in uninfected macrophages. The mechanism of that increased mitochondrial activity by FoxO3a signaling also remains to be unveiled.

5. CONCLUSION

The work presented in this thesis reveals that FoxO3a plays a role in the promotion of inflammation. First, my results consolidated previous findings indicating that FoxO3a negatively regulates splenic and circulating myeloid cell numbers (Dejean et al., 2009; Yalcin et al., 2010). FoxO3a had a less consistent role in the regulation of lymphoid cell numbers. No differences were observed in terms of bone marrow myeloid cell numbers or myeloid progenitor cell numbers. A few possibilities that could explain the lower spleen and blood myeloid cell counts in WT mice would be that FoxO3a controls cell cycling or regulates egress from the bone marrow for example. The mechanism behind that phenomenon remains to be uncovered. My results also revealed that after ST infection, spleen and blood cell numbers were similar between WT and FoxO3a-deficient mice. Thus, FoxO3a did not appear to play a role in the regulation of peripheral myeloid cell numbers during ST infection.

Although FoxO3a was not found to play a role in the regulation of myeloid cell numbers during infection, it was found to profoundly affect macrophage function, specifically the expression of pro/anti-inflammatory cytokines by macrophages. Even though there was no impact of FoxO3a on ST-induced cell death, FoxO3a signaling was found to promote pro-inflammatory cytokine production upon infection – namely TNFα, IL12, and IL1β at the transcriptional level – as well as IL6, while inhibiting the anti-inflammatory cytokine IL10. Since type I IFN was also lower in WT cells, it is possible that FoxO3a regulated IL10 through these cytokines although this remains to be confirmed. As mentioned earlier, a recent report from the Sad laboratory has demonstrated that FoxO3a-deficient mice are more susceptible to ST infection than WT mice (Joseph et al., 2016). It is unclear whether FoxO3a-mediated survival of the host during ST infection is mediated by specific cytokines. *In vitro* infection data indicated

that inhibition of IL10 did not revert the reduced IL12 production in FoxO3a-deficient macrophages to WT levels, but current research in our laboratory will investigate how inhibition of IL10 *in vivo* in FoxO3a-deficient mice impacts survival during ST infection. Together, these results indicate that up-regulation of FoxO3a activity might have beneficial effects on host survival during ST infection and possibly other intracellular bacterial infections. Identifying the upstream regulators of FoxO3a signaling during infection would also provide us with precise targets and ways to increase FoxO3a activity in order to promote inflammation. FoxO3a affected cytokine profiles but not classical (M1) or alternative (M2) macrophage polarization. Nevertheless, it seemed to prevent expression of regulatory macrophage (M_{reg}) markers, which indicates FoxO3a signaling might have a role in controlling differentiation towards this phenotype. M_{reg} macrophages are known to downregulate inflammation and thus are supposed to have an adverse effect on vaccine efficacy, which requires potent inflammatory responses (Mosser and Edwards, 2008). Thus, perhaps preventing this phenotype by increasing FoxO3a activity could be used during ST infection or vaccination to improve the host response. The data presented in this thesis also unveil a role of glycolysis in the generation of FoxO3a-dependent TNFα and in the production of other cytokines including IL12, IL1β, and IL10. This means that modulating glycolysis during infection could be used for instance to prevent septic shock which is associated with aberrant cytokine signaling (Coburn et al., 2007). Finally, FoxO3a was found to increase mitochondrial membrane potential before infection. After infection, the transcription factor seemed to increase the number of mitochondria as estimated by the number of mitochondrial DNA copy numbers, as well as to promote oxygen consumption in macrophages. These findings reveal novel roles of FoxO3a in macrophage metabolism. Understanding how FoxO3a regulates metabolism and the downstream effects of this regulation are important. Since

mitochondria are a source of sustained ATP production, FoxO3a could promote cellular activity through its effect on these organelles.

Collectively, these results highlight the importance of FoxO3a signaling on macrophage inflammation during bacterial infection. Through the regulation of different cellular processes (Figure 38), FoxO3a promotes the inflammatory response in macrophages and thus appears to be an ideal target to enhance vaccine or therapeutic efficacy against intracellular bacteria such as ST.

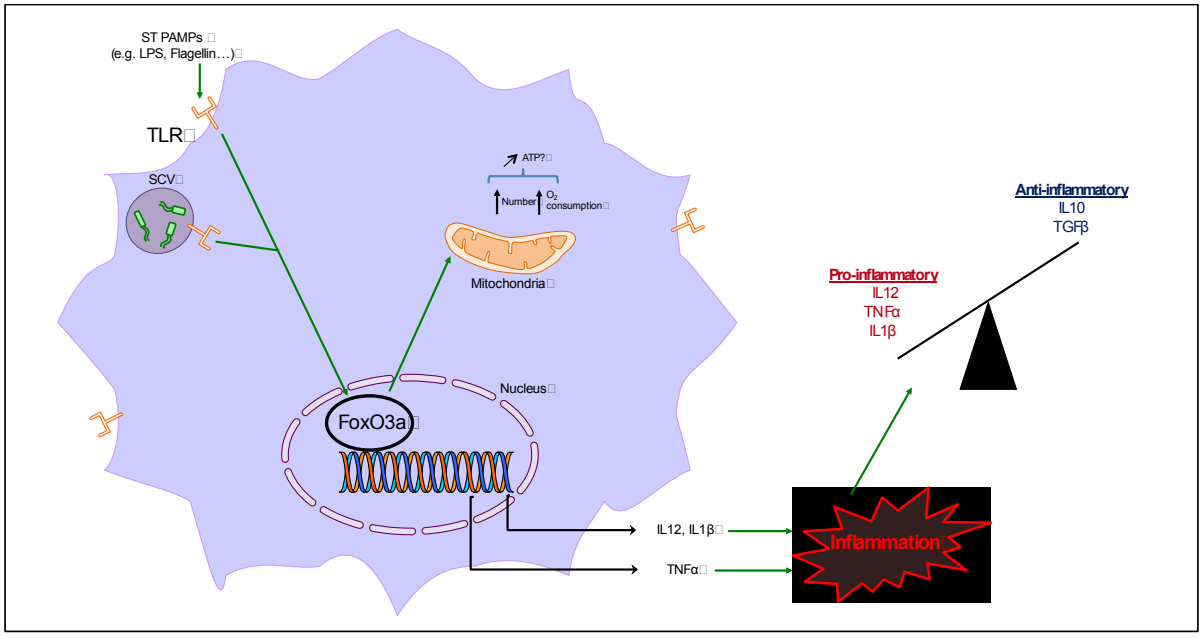
ST PAMPs
(e.g. LPS, Flagellin…)
TLR
SCV
ATP?
Number
O2 consumption
Mitochondria
Nucleus
FoxO3a
IL12, IL1β
TNFα
Inflammation
Anti-inflammatory
IL10
TGFβ
Pro-inflammatory
IL12
TNFα
IL1β

Figure 38. Model of the role of FoxO3a in inflammation in BMDMs
Salmonella infection causes enhanced pro-inflammatory cytokine transcription through FoxO3a signaling. At the same time, IL10 is inhibited, possibly through type I IFN. FoxO3a signaling also promotes an increase in the number of mitochondria, as well as an increase in oxygen consumption, which might together upregulate ATP production.

6. REFERENCES

1. Abbas, A.K., and Janeway, C.A. (2000). Immunology: improving on nature in the twenty-first century. Cell *100*, 129–138.

2. Alpuche-Aranda, C.M., Racoosin, E.L., Swanson, J.A., and Miller, S.I. (1994). Salmonella stimulate macrophage macropinocytosis and persist within spacious phagosomes. J. Exp. Med. *179*, 601–608.

3. Alpuche-Aranda, C.M., Swanson, J.A., Loomis, W.P., and Miller, S.I. (1992). Salmonella typhimurium activates virulence gene transcription within acidified macrophage phagosomes. Proc. Natl. Acad. Sci. *89*, 10079–10083.

4. Blander, J.M. (2014). A long-awaited merger of the pathways mediating host defence and programmed cell death. Nat Rev Immunol *14*, 601–618.

5. Boyce, M. (2005). A Selective Inhibitor of eIF2 Dephosphorylation Protects Cells from ER Stress. Science *307*, 935–939.

6. Brennan, M.A., and Cookson, B.T. (2000). Salmonella induces macrophage death by caspase-1-dependent necrosis. Mol. Microbiol. *38*, 31–40.

7. Broz, P., and Monack, D.M. (2011). Molecular mechanisms of inflammasome activation during microbial infections. Immunol. Rev. *243*, 174–190.

8. Buckle, G.C., Walker, C.L.F., and Black, R.E. (2012). Typhoid fever and paratyphoid fever: Systematic review to estimate global morbidity and mortality for 2010. J. Glob. Health *2*, 10401.

9. Castrillon, D.H., Miao, L., Kollipara, R., Horner, J.W., and DePinho, R.A. (2003). Suppression of ovarian follicle activation in mice by the transcription factor Foxo3a. Science *301*, 215–218.

10. Celli, J., and Tsolis, R.M. (2015). Bacteria, the endoplasmic reticulum and the unfolded protein response: friends or foes? Nat. Rev. Microbiol. *13*, 71–82.

11. Chen, L., Song, Y., He, L., Wan, X., Lai, L., Dai, F., Liu, Y., and Wang, Q. (2016). MicroRNA-223 promotes type I interferon production in antiviral innate immunity by targeting forkhead box protein O3 (FOXO3). J. Biol. Chem. *291*, 14706–14716.

12. Clementi, E., Brown, G.C., Feelisch, M., and Moncada, S. (1998). Persistent inhibition of cell respiration by nitric oxide: crucial role of S-nitrosylation of mitochondrial complex I and protective action of glutathione. Proc. Natl. Acad. Sci. U. S. A. *95*, 7631–7636.

13. Coburn, B., Grassl, G.A., and Finlay, B. (2007). Salmonella, the host and disease: a brief review. Immunol. Cell Biol. *85*, 112–118.

14. Cui, M., Huang, Y., Zhao, Y., and Zheng, J. (2008). Transcription Factor FOXO3a Mediates Apoptosis in HIV-1-Infected Macrophages. J. Immunol. *180*, 898–906.

15. Delves, P.J., and Roitt, I.M. (2000). The immune system. First of two parts. N. Engl. J. Med. *343*, 37–49.

16. Dunlap, N.E., Benjamin, W.H., McCall, R.D., Tilden, A.B., and Briles, D.E. (1991). A "safe site" for Salmonella typhimurium is within splenic cells during the early phase of infection in mice. Microb. Pathog. *10*, 297–310.

17. Eckmann, L., Kagnoff, M.F., and Fierer, J. (1993). Epithelial cells secrete the chemokine interleukin-8 in response to bacterial entry. Infect. Immun. *61*, 4569–4574.

18. Edwards, J.P., Zhang, X., Frauwirth, K.A., and Mosser, D.M. (2006). Biochemical and functional characterization of three activated macrophage populations. J. Leukoc. Biol. *80*, 1298–1307.

19. Eijkelenboom, A., and Burgering, B.M.T. (2013). FOXOs: signalling integrators for homeostasis maintenance. Nat. Rev. Mol. Cell Biol. *14*, 83–97.

20. Feasey, N.A., Dougan, G., Kingsley, R.A., Heyderman, R.S., and Gordon, M.A. (2012). Invasive non-typhoidal salmonella disease: An emerging and neglected tropical disease in Africa. Lancet *379*, 2489–2499.

21. Feng, B., Yao, P.M., Li, Y., Devlin, C.M., Zhang, D., Harding, H.P., Sweeney, M., Rong, J.X., Kuriakose, G., Fisher, E. a, et al. (2003). The endoplasmic reticulum is the site of cholesterol-induced cytotoxicity in macrophages. Nat. Cell Biol. *5*, 781–792.

22. Ferber, E.C., Peck, B., Delpuech, O., Bell, G.P., East, P., and Schulze, A. (2012). FOXO3a regulates reactive oxygen metabolism by inhibiting mitochondrial gene expression. Cell Death Differ. *19*, 968–979.

23. Furuyama, T., Nakazawa, T., Nakano, I., and Mori, N. (2000). Identification of the differential distribution patterns of mRNAs and consensus binding sequences for mouse DAF-16 homologues. Biochem. J. *349*, 629–634.

24. Galluzzi, L., López-Soto, A., Kumar, S., and Kroemer, G. (2016). Caspases Connect Cell-Death Signaling to Organismal Homeostasis. Immunity *44*, 221–231.

25. Galván-Peña, S., and O'Neill, L.A.J. (2014). Metabolic reprograming in macrophage polarization. Front. Immunol. *5*, 1–6.

26. Gilchrist, J.J., MacLennan, C. a., and Hill, A.V.S. (2015). Genetic susceptibility to invasive Salmonella disease. Nat. Rev. Immunol. *15*, 452–463.

27. Greer, E.L., and Brunet, A. (2005). FOXO transcription factors at the interface between longevity and tumor suppression. Oncogene *24*, 7410–7425.

28. Hansen-Wester, I., and Hensel, M. (2001). Salmonella pathogenicity islands encoding type III secretion systems. Microbes Infect. *3*, 549–559.

29. Haoues, M., Refai, A., Mallavialle, A., Barbouche, M.R., Laabidi, N., Deckert, M., and Essafi, M. (2014). Forkhead box O3 (FOXO3) transcription factor mediates apoptosis in BCG-infected macrophages. Cell. Microbiol. *16*, 1378–1390.

30. Haraga, A., Ohlson, M.B., and Miller, S.I. (2008). Salmonellae interplay with host cells. Nat. Rev. Microbiol. *6*, 53–66.

31. Hedrick, S.M., Michelini, R.H., Doedens, A.L., Goldrath, A.W., and Stone, E.L. (2012). FOXO transcription factors throughout T cell biology. Nat. Rev. Immunol. *12*, 649–662.

32. Hinman, R.M., Nichols, W.A., Diaz, T.M., Gallardo, T.D., Castrillon, D.H., and Satterthwaite, A.B. (2009). Foxo3-/- mice demonstrate reduced numbers of pre-B and recirculating B cells but normal splenic B cell sub-population distribution. Int. Immunol. *21*, 831–842.

33. van der Horst, A., and Burgering, B.M.T. (2007). Stressing the role of FoxO proteins in lifespan and disease. Nat. Rev. Mol. Cell Biol. *8*, 440–450.

34. Hu, Z.-Q., and Zhao, W.-H. (2013). Type 1 interferon-associated necroptosis: a novel mechanism for Salmonella enterica Typhimurium to induce macrophage death. Cell. Mol. Immunol. *10*, 10–12.

35. Infantino, V., Convertini, P., Cucci, L., Panaro, M.A., Di Noia, M.A., Calvello, R., Palmieri, F., and Iacobazzi, V. (2011). The mitochondrial citrate carrier: a new player in inflammation. Biochem. J. *438*, 433–436.

36. Jansen, A.M., Hall, L.J., Clare, S., Goulding, D., Holt, K.E., Grant, A.J., Mastroeni, P., Dougan, G., and Kingsley, R.A. (2011). A Salmonella Typhimurium-Typhi Genomic Chimera: A Model to Study Vi Polysaccharide Capsule Function In Vivo. PLoS Pathog. *7*, e1002131.

37. Jensen, K.S., Binderup, T., Jensen, K.T., Therkelsen, I., Borup, R., Nilsson, E., Multhaupt, H., Bouchard, C., Quistorff, B., Kjaer, A., et al. (2011). FoxO3A promotes metabolic adaptation to hypoxia by antagonizing Myc function. EMBO J. *30*, 4554–4570.

38. de Jong, H.K., Parry, C.M., van der Poll, T., and Wiersinga, W.J. (2012). Host-Pathogen Interaction in Invasive Salmonellosis. PLoS Pathog. *8*, 1–9.

39. Joseph, J., Ametepe, E.S., Haribabu, N., Agbayani, G., Krishnan, L., Blais, A., and Sad, S. (2016). Inhibition of ROS and upregulation of inflammatory cytokines by FoxO3a promotes survival against Salmonella typhimurium. Nat. Commun. *7*, 12748.

40. Jürgens, G., and Weigel, D. (1988). Terminal versus segmental development in the Drosophila embryo: the role of the homeotic gene fork head. Roux's Arch. Dev. Biol. *197*, 345–354.

41. Kayagaki, N., Wong, M.T., Stowe, I.B., Ramani, S.R., Gonzalez, L.C., Akashi-Takamura, S., Miyake, K., Zhang, J., Lee, W.P., Muszynski, A., et al. (2013). Noncanonical Inflammasome Activation by Intracellular LPS Independent of TLR4. Science *341*, 1246–1249.

42. Keestra-Gounder, A.M., Tsolis, R.M., and Bäumler, A.J. (2015). Now you see me, now you don't: the interaction of Salmonella with innate immune receptors. Nat. Rev. Microbiol. *13*, 206–216.

43. Kelly, B., and O'Neill, L.A. (2015). Metabolic reprogramming in macrophages and dendritic cells in innate immunity. Cell Res. *25*, 771–784.

44. Khatri, S., Yepiskoposyan, H., Gallo, C.A., Tandon, P., and Plas, D.R. (2010). FOXO3a regulates glycolysis via transcriptional control of tumor suppressor TSC1. J. Biol. Chem. *285*, 15960–15965.

45. Klausner, R.D., Donaldson, J.G., and Lippincott-Schwartz, J. (1992). Brefeldin A: Insights into the control of membrane traffic and organelle structure. J. Cell Biol. *116*, 1071–1080.

46. Kondo, M., Weissman, I.L., Akashi, K., Akashi, K., Weissman, I.L., Akashi, K., Harada, M., Shibuya, T., Fukagawa, K., Kimura, N., et al. (1997). Identification of clonogenic common lymphoid progenitors in mouse bone marrow. Cell *91*, 661–672.

47. Kornblau, S.M., Singh, N., Qiu, Y., Chen, W., Zhang, N., and Coombes, K.R. (2010). Highly phosphorylated FOXO3A is an adverse prognostic factor in acute myeloid leukemia. Clin. Cancer Res. *16*, 1865–1874.

48. LaRock, D.L., Chaudhary, A., and Miller, S.I. (2015). Salmonellae interactions with host processes. Nat. Rev. Microbiol. *13*, 191–205.

49. Lathrop, S.K., Binder, K.A., Starr, T., Cooper, K.G., Chong, A., Carmody, A.B., and Steele-Mortimer, O. (2015). Replication of Salmonella enterica serovar Typhimurium in human monocyte-derived macrophages. Infect. Immun. *83*, 2661–2671.

50. Lee, J.C., Espéli, M., Anderson, C.A., Linterman, M.A., Pocock, J.M., Williams, N.J., Roberts, R., Viatte, S., Fu, B., Peshu, N., et al. (2013). Human SNP links differential outcomes in inflammatory and infectious disease to a FOXO3-regulated pathway. Cell *155*, 57–69.

51. Lim, C.-Y., and Zoncu, R. (2016). The lysosome as a command-and-control center for cellular metabolism. J. Cell Biol. *214*, 653–664.

52. Lin, L., Hron, J.D., Peng, S.L., Andrews, B.S., Eisenberg, R.A., Theofilopoulos, A.N., Izui, S., Wilson, C.B., McConahey, P.J., Murphy, E.D., et al. (2004). Regulation of NF-κB, Th Activation, and Autoinflammation by the Forkhead Transcription Factor Foxo3a. Immunity *21*, 203–213.

53. Luron, L., Saliba, D., Blazek, K., Lanfrancotti, A., and Udalova, I.A. (2012). FOXO3 as a new IKK-ε-controlled check-point of regulation of IFN-β expression. Eur. J. Immunol. *42*, 1030–1037.

54. Mammucari, C., Milan, G., Romanello, V., Masiero, E., Rudolf, R., Del Piccolo, P., Burden, S.J., Di Lisi, R., Sandri, C., Zhao, J., et al. (2007). FoxO3 Controls Autophagy in Skeletal Muscle In Vivo. Cell Metab. *6*, 458–471.

55. Marinkovic, D., Zhang, X., Yalcin, S., Luciano, J.P., Brugnara, C., Huber, T., and Ghaffari, S. (2007). Foxo3 is required for the regulation of oxidative stress in erythropoiesis. J. Clin. Invest. *117*, 2133–2144.

56. Martínez-Gac, L., Marqués, M., García, Z., Campanero, M.R., and Carrera, A.C. (2004). Control of cyclin G2 mRNA expression by forkhead transcription factors: novel mechanism for cell cycle control by phosphoinositide 3-kinase and forkhead. Mol. Cell. Biol. *24*, 2181–2189.

57. Mastroeni, P., Grant, A., Restif, O., and Maskell, D. (2009). A dynamic view of the spread and intracellular distribution of Salmonella enterica. Nat. Rev. Microbiol. *7*, 73–80.

58. Mazo, I.B., Honczarenko, M., Leung, H., Cavanagh, L.L., Bonasio, R., Weninger, W., Engelke, K., Xia, L., McEver, R.P., Koni, P.A., et al. (2005). Bone marrow is a major reservoir and site of recruitment for central memory CD8 + T cells. Immunity *22*, 259–270.

59. McClelland, M., Sanderson, K.E., Clifton, S.W., Latreille, P., Porwollik, S., Sabo, A., Meyer, R., Bieri, T., Ozersky, P., McLellan, M., et al. (2004). Comparison of genome degradation in Paratyphi A and Typhi, human-restricted serovars of Salmonella enterica that cause typhoid. Nat. Genet. *36*, 1268–1274.

60. McComb, S., Cessford, E., Alturki, N. a., Joseph, J., Shutinoski, B., Startek, J.B., Gamero, a. M., Mossman, K.L., and Sad, S. (2014). Type-I interferon signaling through ISGF3 complex is required for sustained Rip3 activation and necroptosis in macrophages. Proc Natl Acad Sci U S A *111*, E3206–E3213.

61. McNab, F.W., Ewbank, J., Howes, A., Moreira-Teixeira, L., Martirosyan, A., Ghilardi, N., Saraiva, M., and O'Garra, A. (2014). Type I IFN induces IL-10 production in an IL-27-independent manner and blocks responsiveness to IFN-γ for production of IL-12 and bacterial killing in Mycobacterium tuberculosis-infected macrophages. J. Immunol. *193*, 3600–3612.

62. Michelucci, A., Cordes, T., Ghelfi, J., Pailot, A., Reiling, N., Goldmann, O., Binz, T., Wegner, A., Tallam, A., Rausell, A., et al. (2013). Immune-responsive gene 1 protein links metabolism to immunity by catalyzing itaconic acid production. Proc. Natl. Acad. Sci. U. S. A. *110*, 7820–7825.

63. Miyamoto, K., Araki, K.Y., Naka, K., Arai, F., Takubo, K., Yamazaki, S., Matsuoka, S., Miyamoto, T., Ito, K., Ohmura, M., et al. (2007). Foxo3a is essential for maintenance of the hematopoietic stem cell pool. Cell Stem Cell *1*, 101–112.

64. Moore, K.W., de Waal Malefyt, R., Coffman, R.L., and O'Garra, A. (2001). Interleukin -10 and the Interleukin -10 Receptor. Annu. Rev. Immunol. *19*, 683–765.

65. Morris, B.J., Willcox, D.C., Donlon, T.A., and Willcox, B.J. (2015). FOXO3: A Major Gene for Human Longevity - A Mini-Review. Gerontology *61*, 515–525.

66. Mosser, D.M., and Edwards, J.P. (2008). Exploring the full spectrum of macrophage activation. Nat. Rev. Immunol. *8*, 958–969.

67. O'Neill, L.A.J., Kishton, R.J., and Rathmell, J. (2016). A guide to immunometabolism for immunologists. Nat. Rev. Immunol. *16*, 553–565.

68. Parkin, J., and Cohen, B. (2001). An overview of the immune system. Lancet *357*, 1777–1789.

69. Perry, S., Norman, J., Barbieri, J., Brown, E., and Gelbard, H. (2011). Mitochondrial membrane potential probes and the proton gradient: a practical usage guide. Biotechniques *50*, 98–115.

70. Petvises, S., and O'Neill, H.C. (2012). Hematopoiesis leading to a diversity of dendritic antigen-presenting cell types. Immunol. Cell Biol. *90*, 372–378.

71. PJ Delves, and Roitt, I. (2000). Advances in Immunology: The immune system - Second of two parts. N. Engl. J. Med. *343*, 108–117.

72. Rahim, S.S., Khan, N., Boddupalli, C.S., Hasnain, S.E., and Mukhopadhyay, S. (2005). Interleukin-10 (IL-10) mediated suppression of IL-12 production in RAW 264.7 cells involves c-rel transcription factor. Immunology *114*, 313–321.

73. Reily, C., Mitchell, T., Chacko, B.K., Benavides, G.A., Murphy, M.P., and Darley-Usmar, V.M. (2013). Mitochondrially targeted compounds and their impact on cellular bioenergetics. Redox Biol. *1*, 86–93.

74. Richter-Dahlfors, a, Buchan, a M., and Finlay, B.B. (1997). Murine salmonellosis studied by confocal microscopy: Salmonella typhimurium resides intracellularly inside macrophages and exerts a cytotoxic effect on phagocytes in vivo. J. Exp. Med. *186*, 569–580.

75. Rimmelé, P., Liang, R., Bigarella, C.L., Kocabas, F., Xie, J., Serasinghe, M.N., Chipuk, J., Sadek, H., Zhang, C.C., and Ghaffari, S. (2015). Mitochondrial metabolism in hematopoietic stem cells requires functional FOXO3. EMBO Rep. *16*, 1164–1176.

76. Rosenbauer, F., and Tenen, D.G. (2007). Transcription factors in myeloid development: balancing differentiation with transformation. Nat. Rev. Immunol. *7*, 105–117.

77. Santos, R.L., Zhang, S., Tsolis, R.M., Kingsley, R.A., Garry Adams, L., and Bäumler, A.J. (2001). Animal models of Salmonella infections: enteritis versus typhoid fever. Microbes Infect. *3*, 1335–1344.

78. Senokuchi, T., Liang, C.P., Seimon, T.A., Han, S., Matsumoto, M., Banks, A.S., Paik, J.H., Depinho, R.A., Accili, D., Tabas, I., et al. (2008). Forkhead transcription factors (FoxOs) promote apoptosis of insulin-resistant macrophages during cholesterol-induced endoplasmic reticulum stress. Diabetes *57*, 2967–2976.

79. Su, D., Coudriet, G.M., Hyun Kim, D., Lu, Y., Perdomo, G., Qu, S., Slusher, S., Tse, H.M., Piganelli, J., Giannoukakis, N., et al. (2009). FoxO1 Links Insulin Resistance to Proinflammatory Cytokine IL-1 Production in Macrophages. Diabetes *58*, 2624–2633.

80. Sullivan, J.A., Kim, E.H., Plisch, E.H., Peng, S.L., and Suresh, M. (2012). FOXO3 regulates CD8 T cell memory by T cell-intrinsic mechanisms. PLoS Pathog. *8*, 32–43.

81. Tannahill, G.M., Curtis, A.M., Adamik, J., Palsson-McDermott, E.M., McGettrick, A.F., Goel, G., Frezza, C., Bernard, N.J., Kelly, B., Foley, N.H., et al. (2013). Succinate is an inflammatory signal that induces IL-1β through HIF-1α. Nature *496*, 238–242.

82. Togher, S., Larange, A., Schoenberger, S.P., and Feau, S. (2015). FoxO3 is a negative regulator of primary CD8+ T-cell expansion but not of memory formation. Immunol. Cell Biol. *93*, 120–125.

83. Tran, H., Brunet, A., Grenier, J.M., Datta, S.R., Fornace, A.J., DiStefano, P.S., Chiang, L.W., and Greenberg, M.E. (2002). DNA Repair Pathway Stimulated by the Forkhead Transcription Factor FOXO3a Through the Gadd45 Protein. Science *296*, 530–534.

84. Tsuchiya, K., Westerterp, M., Murphy, A.J., Subramanian, V., Ferrante, A.W., Tall, A.R., Accili, D., and Accili, D. (2013). Expanded granulocyte/monocyte compartment in myeloid-specific triple FoxO knockout increases oxidative stress and accelerates atherosclerosis in mice. Circ. Res. *112*, 992–1003.

85. Tzelepis, F., Alcon, V., Dudani, R., Gurnani, K., Zafer, A., Everson, E.S., Young, K.G., Rüssmann, H., Krishnan, L., and Sad, S. (2012). Modulation of Antigenic Location Converts Chronic into Acute Infection by Forcing CD8+ T Cell Recognition. Cell Rep. *2*, 1710–1721.

86. Tzelepis, F., Joseph, J., Haddad, E.K., Maclean, S., Dudani, R., Agenes, F., Peng, S.L., Sekaly, R.-P., and Sad, S. (2013). Intrinsic role of FoxO3a in the development of CD8+ T cell memory. J. Immunol. *190*, 1066–1075.

87. Ushach, I., and Zlotnik, A. (2016). Biological role of granulocyte macrophage colony-stimulating factor (GM-CSF) and macrophage colony-stimulating factor (M-CSF) on cells of the myeloid lineage. J. Leukoc. Biol. *100*, 1–9.

88. Wang, S., Dale, G.L., Song, P., Viollet, B., and Zou, M.H. (2010). AMPKα1 deletion shortens erythrocyte life span in mice: Role of oxidative stress. J. Biol. Chem. *285*, 19976–19985.

89. Weiss, D.S., Raupach, B., Takeda, K., Akira, S., and Zychlinsky, A. (2004). Toll-Like Receptors Are Temporally Involved in Host Defense. J. Immunol. *172*, 4463–4469.

90. Yalcin, S., Marinkovic, D., Mungamuri, S.K., Zhang, X., Tong, W., Sellers, R., and Ghaffari, S. (2010). ROS-mediated amplification of AKT/mTOR signalling pathway leads to myeloproliferative syndrome in Foxo3(-/-) mice. EMBO J. *29*, 4118–4131.

91. Zhang, X., Goncalves, R., and Mosser, D.M. (2008). The Isolation and Characterization of Murine Macrophages. In Current Protocols in Immunology, (Hoboken, NJ, USA: John Wiley and Sons, Inc.), p. Unit 14.1.

92. Zhao, J., Brault, J.J., Schild, A., Cao, P., Sandri, M., Schiaffino, S., Lecker, S.H., and Goldberg, A.L. (2007). FoxO3 Coordinately Activates Protein Degradation by the Autophagic/Lysosomal and Proteasomal Pathways in Atrophying Muscle Cells. Cell Metab. *6*, 472–483.

93. Zhu, J., and Emerson, S.G. (2002). Hematopoietic cytokines, transcription factors and lineage commitment. Oncogene *21*, 3295–3313.

CURRICULUM VITAE

Emmanuelle Ametepe

EDUCATION

Master of Science in Microbiology and Immunology, **2014 - Present**
University of Ottawa, ON.

- Thesis: FoxO3a signaling promotes the inflammatory response during *Salmonella* Typhimurium infection
- Supervisor: Dr. Subash Sad
- Planned date of end of studies: January 2017

Bachelor in science with honors in biomedical science, **2011- 2014**
Magna cum laude
University of Ottawa, ON.

- Thesis: Cardiac CT Assessment of LV Mass in Mid-Diastole: Is it Accurate and Does it Predict Mortality?
- Supervisor: Dr. Benjamin Chow, University of Ottawa Heart Institute, 2014.

General French scientific baccalaureate, **2011**
Option European section, Summa cum laude,
Lycée français Bonaparte of Doha, Qatar

HONORARY DISTINCTIONS

Admission scholarship, University of Ottawa, ON **2011- 2016**
Undergraduate Dean's honor list, University of Ottawa, ON **2011- 2014**
1st place cash prize (100 CAD), **2016**
BMI Seminar day, University of Ottawa, ON
One-minute thesis prize, **2016**
Canadian Society for Immunology conference, Ottawa, ON

PUBLICATIONS

Joseph, J., **Ametepe, E. S.**, Haribabu, N., Agbayani, G., Krishnan, L., Blais, A., and Sad, S. (2016). Inhibition of ROS and upregulation of inflammatory cytokines by FoxO3a promotes survival against *Salmonella* Typhimurium. *Nature Communications, 7*.

SKILLS AND EXPERIENCE

Organization skills and administration

- Completed an extra mandatory course during my Master's degree. With strict planning and organization, all laboratory trainings and courses listed in the Certification section below (from WHMIS), one master's degree course and an additional immunology course were completed while doing laboratory work, all within the first four months of my Master's degree.

- Learned how to use multiple new softwares (GraphPad Prism, Kaluza and SoftMax Pro) efficiently, for data analysis.

- Improved my presentation skills significantly. Performed multiple experiments every week, while preparing a concise presentation for my colleagues and supervisor during weekly laboratory meetings as training, and to receive feedback on my research.

- Used shared equipment in a manner that is respectful to others. Many pieces of equipment were shared, most notably the flow cytometer that had to be reserved for a precise amount of time. Bookings and experiments were executed in a timely manner.

- Participated in teaching new students laboratory rules and techniques. Taught newcomers laboratory etiquette, tips and techniques.

Communication and social skills

- Gave presentations as part of courses, laboratory meetings, Faculty presentations and a conference. I have won the first cash Prize during the BMI Seminar day in 2016, as well as a prize in the one-minute thesis contest that took place during the Canadian Society for Immunology conference that same year.

- Successfully pursued a Master's degree in a language other that my first language. I can now read, write and speak fluently in English, as well as in French and Spanish. I also have a basic knowledge of written Arabic.

- Successfully worked with individuals who have various opinions, cultures, religions and languages. This was done during the two years spent in the laboratory during my Master's degree, as well as during my stay in Qatar for my high school studies.

Leadership

- Co-lead a Bible study of 5-6 students weekly, from October 2013 to April 2014; suggested and planned weekly activities with a team of around 20 individuals for groups

of 50-100 students. This was done during my undergraduate studies as a member of the University of Ottawa Intervarsity Christian Fellowship.

- From 2015, aided as an assistant in teaching Bible fundamentals to young children (4 to 6 year olds) during Sunday school at Church.

- Taught laboratory techniques to a volunteer undergraduate student for 2 months in May and June 2016. By the end of his contract, the student was able to successfully complete experiments without supervision.

LABORATORY SKILLS

- Laboratory mouse handling (infected and non-infected mice)
- Cardiac puncture, Saphenous bleed, Oral infection of laboratory mice
- Cell culture and *in vitro* infection
- Work with pathogenic bacteria in a BSL-2 laboratory
- Various biochemical tests (ELISA, Griess assay etc.)
- Flow cytometry
- PCR, qRT-PCR

CERTIFICATIONS

TEF Canada, C2 level **2016**
TCPS2: CORE – Course on Research Ethics **2014**
Workplace Hazardous Materials Information System (WHMIS) – for laboratory workers **2014**
Worker Health and Safety Awareness **2014**
Accessibility Standards for Customer Service **2014**
Respect in the Workplace **2014**
Violence Prevention **2014**
Principles of Biosafety **2014**
Autoclave Safety **2014**
Working together: The Code and the AODA **2016**

INTERESTS

Literature, travel and sprint.